(54)

JPO, 1999

Ocean turbulence III: two–point closure model Momentum, heat and salt vertical diffusivities in the presence of shear

V.M. Canuto[1,2], M. S. Dubovikov[1], A. Howard[1] and Y. Cheng[1]

[1]NASA Goddard Institute for Space Studies

2880 Broadway, N.Y., N.Y., 10025

[2]Dept. Applied Physics, Columbia University, NY, NY, 10027

Abstract

In papers I and II we have presented the results of the most updated 1–point closure model for the turbulent vertical diffusivities of momentum, heat and salt, $K_{m,h,s}$. In this paper, In this paper, we derive the analytic expressions for $K_{m,h,s}$ using a new 2–point closure model that has recently been developed and successfully tested against some ~80 turbulence statistics for different flows. *The new model has no free parameters.* The expressions for $K_{m,h,s}$ are analytical functions of two stability parameters: the Turner number R_ρ (salinity gradient/temperature gradient) and the Richardson number Ri (temperature gradient/shear). The turbulent kinetic energy K and its rate of dissipation may be taken local or non–local (K–ϵ model).

Contrary to all previous models that to describe turbulent mixing below the mixed layer (ML) have adopted three adjustable "background diffusivities" for momentum, heat and salt, we propose a model that avoids such adjustable diffusivities. *We assume that below the ML,* $K_{m,h,s}$ *have the same functional dependence on Ri and* R_ρ *derived from the turbulence model.* However, in order to compute Ri below the ML, we use data of vertical shear due to wave–breaking measured by Gargett et al. (1981). The procedure frees the model from adjustable background diffusivities and indeed we use the same model throughout the entire vertical extent of the ocean.

Using the new $K_{m,h,s}$, we run an O–GCM and present a variety of results that we compare with Levitus and the KPP model.

Since the traditional 1–point (used in papers I and II) and the new 2–point closure models used here represent different modeling philosophies and procedures, testing them in an O–GCM is indispensable. The basic motivation is to show that the new 2–point closure model gives results that are overall superior to the 1–point closure in spite of the fact that the latter rely on several adjustable parameters while the new 2–point closure has none.

After the extensive comparisons presented in papers I and II, we conclude that the new model presented here is overall superior for it not only is parameter free but also

because is part of a more general turbulence model that has been previously successfully tested on a wide variety of other types of turbulent flows.

I.Introduction

a) O–GCM dynamic equations. Turbulent Diffusivities

The dynamic equations for the large scale mean velocity, temperature and salinity, U_i, T and S, are given by (Semtner; 1995; Semtner and Chervin, 1992; Anderson and Willebrand, 1992)

$$\frac{D}{Dt}U_i + \frac{\partial}{\partial x_j}\tau_{ij} = -\frac{\partial P}{\partial x_i} + ... \qquad (1a)$$

$$\frac{DT}{Dt} + \frac{\partial}{\partial x_i}h_i = \frac{\partial}{\partial x_i}(\chi\frac{\partial T}{\partial x_i}) + ... \qquad (1b)$$

$$\frac{DS}{Dt} + \frac{\partial}{\partial x_i}s_i = \frac{\partial}{\partial x_i}(\kappa\frac{\partial S}{\partial x_i}) + ... \qquad (1c)$$

where $D/Dt \equiv \partial/\partial t + U_j\partial/\partial x_j$, χ and κ are the temperature and salt kinematic diffusivities. Eqs.(1a–c) depend on turbulence via the the Reynolds stresses $\tau_{ij}=\overline{u_iu_j}$ and the heat and salt fluxes $h_i=\overline{u_i\theta}$, $s_i=\overline{u_i\sigma}$, where u_i, θ and σ represent the turbulent (fluctuating) components of the velocity, temperature and salinity fields. The dots represent external forces, rotation, etc. The vertical turbulent diffusivities $K_{m,h,s}$ (cm^2s^{-1}) enter via the relations:

$$\overline{uw} = -K_m\frac{\partial U}{\partial z}, \quad \overline{w\theta} = -K_h\frac{\partial T}{\partial z}, \quad \overline{w\sigma} = -K_s\frac{\partial S}{\partial z} \qquad (1d)$$

Historically, a value of $K_h=1$ was suggested by Munk (1966). Bryan (1991) and Colin de Verdiere (1988) later showed that the polar heat transport scales like $K_h^{2/3}$ and that in order to reproduce its observed value (~1Petawatt), O–GCM require K_h~2 (Holland, 1989; Mellor, 1989; Cummings et., 1990). Chen et al. (1994) concluded that an improved mixed layer ameliorates the large scale equatorial circulation as well as the annual cycles of the SST (sea surface temperatures) while on a global scale McWilliams (1996) has recently stressed that O–GCMs are sensitive, among other things, to the vertical diffusivities. From high resolution profiles and tracer experiments (Moum 1989; Gargett, 1989; Ledwell et al. 1993; McPhee and Martison 1994; Toole et al. 1994; Polzin et al. 1997), it was concluded that in the ocean mixed layer K_h can be as large as $(1–2)10^2$, while in the thermocline

K_h~(0.11–0.6) with perhaps the tendency to vary as N^{-1}, where N is the Brunt–Vaisala frequency (Gargett and Holloway 1984; Gargett et al., 1989; Gargett 1984, 1993; Matear and Wong, 1997). Thus, diffusivities are not constant with depth and different processes contribute to the K's at different depths resulting in different values.

b) general constraints on the K's

Since the dimensions of the diffusivities are $(\text{length})^2(\text{time})^{-1}$, to construct the diffusivities K's one needs two independent variables. Over the years, three expressions have been adopted:

1) Richardson law: $\quad \text{Diffusivity} \sim \ell^{4/3}\epsilon^{1/3}$ (1e)

2) Prandtl law: $\quad \text{Diffusivity} \sim K^{\frac{1}{2}}\ell$ (1f)

3) Turbulence modeling: $\quad \text{Diffusivity} \sim \frac{K^2}{\epsilon}$ (1g)

where ℓ is a typical length scale, K is the turbulent kinetic energy and ϵ is the rate of dissipation of K. Richardson law (a precursor of Kolmogorov law) emphasizes the diffusive nature of large eddies while Prandtl law is reminiscent of kinetic theory of gases and mean free path arguments. Both expressions entail a length scale ℓ which is usually difficult to quantify, especially in the case of stable stratification (Cheng and Canuto, 1994), whereas (1g) depends on K and ϵ for which we shall derive two differential equations thus avoiding the need of an ℓ. On that basis alone, (1g) is preferable to both (1e–f). Even so, (1g) is still not satisfactory. In fact, consider the case of stable stratification when shear is the source of turbulence. In the absence of salt, the turbulent Prandtl number,

$$\sigma_T = \frac{K_m}{K_h} \tag{1h}$$

is known to increase with stratification represented by the Richardson number Ri,

$$\sigma_T = \sigma_T(\text{Ri}), \qquad \frac{d}{d\text{Ri}}\,\sigma_T(\text{Ri}) > 0 \tag{1i}$$

(Webster, 1964; Istweire and Helland, 1989; Schumann, 1991; Wang et al., 1996). If we limit the functional dependence of the K's to the forms (1e–g), we obtain σ_T=constant

which violates the second of (1i). For example, the model of Pacanoswki and Philander does not satisfy (1i) since it yields a constant σ_T. The recent model for $K_{m,h}$ of D'Alessio et al. (1998) does not satisfy (1i) either. In addition, the function S_m must satisfy the well known asymptotic limits of Ri→0 (shear driven flows)

$$\text{Ri}\to 0: \qquad 2S_m \approx 0.1 \tag{1j}$$

as studies of shear flow indicate (Launder et al., 1975).

Finally, the model must provide a correct value of the critical Richardson numbe: Ri_{cr} above which turbulence can no longer be sustained by shear. While linear stability analysis implies that turbulence exists only for

$$\text{Ri} < \text{Ri}_{cr}, \qquad \text{Ri}_{cr} = 1/4 \tag{1k}$$

even early laboratory data by Taylor (cited in Monin and Yaglom, 1971, Vol.I, pages 502–503) show that considerable turbulent exchange exists up to Ri~10. More recently, Martin (1985), Smart (1988) and Kundu et al. (1991) have found considerable mixing in the ocean up to Ri~1, a result also validated by the LES results of Wang et al. (1996). This means that a model for stably stratified turbulence must allow turbulence past $\text{Ri}_{cr}=1/4$. The original MY model (Mellor and Yamada, 1982) does not satisfy this criterion since it yields $\text{Ri}_{cr}=0.19$ nor do any of the subsequent models that have not significantly improved the physical content of the MY model. This brief discussion about $\sigma_T(\text{Ri})$ and Ri_{cr} suffices to show that there are some basic data that any model must satisfy before being considered a candidate for ocean turbulence.

The general functional form of the *turbulent diffusivities* for momentum, heat and salt $K_{m,h,s}$ are of the form:

$$K_{m,h,s} = 2\,\frac{K^2}{\epsilon} S_{m,h,s} \tag{2a}$$

where K and ϵ are the turbulent kinetic energy and its rate of dissipation which in principle are given by two dynamic equations (the K–ϵ model). The *dimensionless structure functions* $S_{m,h,s}$ must differ from one another so that:

$$K_m \neq K_h \neq K_s \tag{2b}$$

In general we can write:

$$S_{m,h,s} = S_{m,h,s}(\nabla U,\ \alpha_T \nabla T,\ \alpha_s \nabla S) \tag{2c}$$

where α_T and α_s are the volume expansion coefficients $\alpha_T = -\rho^{-1}\partial\rho/\partial T$ and $\alpha_s = \rho^{-1}\partial\rho/\partial S$ and where the shear ∇U can be generated either by external sources like in the mixed layer ML or by internal wave–breaking processes below the ML. If one introduces the Turner number R_ρ and the Richardson number Ri:

$$R_\rho = g\alpha_s \frac{\partial S}{\partial z}\,(g\alpha_T \frac{\partial T}{\partial z})^{-1}, \qquad Ri = N_h^2/N_u^2 \tag{2d}$$

where

$$N_h^2 = g\alpha_T \frac{\partial T}{\partial z}, \qquad N_u^2 = 2(\Sigma_{ij}\Sigma_{ij})$$
$$N^2 = -\frac{g}{\rho}\frac{\partial \rho}{\partial z} = g\alpha_T \frac{\partial T}{\partial z} - g\alpha_s \frac{\partial S}{\partial z} = N_h^2(1-R_\rho) \tag{2e}$$

we can rewrite (2c) more concisely as

$$S_{m,h,s} = S_{m,h,s}(R_\rho,\ Ri) \tag{2f}$$

(Clearly, we could have also defined Ri in terms of N^2 rather than just the thermal gradient. We have chosen the latter for reasons of presentation of the results). One must distinguish the following four cases:

SF (*salt fingers, salty–warm over fresh–cold*):

$$\frac{\partial S}{\partial z} > 0, \quad \frac{\partial T}{\partial z} > 0,$$
$$R_\rho > 0, \quad Ri > 0$$
$$R_\rho < 1 \text{ Stable}, \ N^2 > 0, \quad R_\rho > 1 \text{ Unstable}, \ N^2 < 0 \tag{3a}$$

DC (*diffusive convection, fresh–cold over salty–warm*):

$$\frac{\partial S}{\partial z} < 0, \quad \frac{\partial T}{\partial z} < 0,$$
$$R_\rho > 0, \ Ri < 0$$
$$R_\rho < 1 \text{ Unstable}, \ N^2 < 0, \quad R_\rho > 1 \text{ Stable}, \ N^2 > 0 \tag{3b}$$

DS (*doubly stable, fresh–warm over salty–cold*)

$$\frac{\partial S}{\partial z} < 0, \quad \frac{\partial T}{\partial z} > 0,$$
$$R_\rho < 0, \ Ri > 0, \ N^2 > 0, \ \text{Stable} \tag{3c}$$

DU (*doubly unstable, salty–cold over fresh–warm*):

$$\frac{\partial S}{\partial z}>0, \quad \frac{\partial T}{\partial z}<0,$$

$$R_\rho<0, \quad Ri<0, \quad N^2<0, \quad \text{Unstable} \tag{3d}$$

The stability/instability is predicated on the Brunt–Vaisala frequency N with $N^2>0$ (stable) and $N^2<0$ (unstable).

The general problem is to construct (2f) so as to encompass all four cases (3a–d). First, there is ample evidence from laboratory and oceanic field data that show that K_h is different from K_s. In the SF case, the ratio $K_s/K_h>1$ (Hamilton et al., 1989) while in the DC case, $K_h/K_s>1$ (Kelley, 1984). Schmitt (1981) has also shown that the observed T–S relationship is not consistent with $K_h=K_s$. For a discussion and review of the importance of these processes and their extent in different parts of the ocean, see Turner (1967, 1973, 1985), Schmitt (1994) and Zhang et al. (1998). In spite of this evidence, almost all O–GCM still assume

$$K_s=K_h \tag{3e}$$

Recently, attempts have been made to overcome (3e) but the task is not easy. The main difficulty is that in the absence of a model capable of encompassing all four cases, SF, DC, DS and DU, the only alternative is to employ laboratory and ocean data to build the functional form of the diffusivities to be used in an O–GCM. This is the approach employed by Large et al. (1994), Zhang et al. (1998, ZSH) and Merryfield et al. (1999, MHG) who used relations by Schmitt (1981) and Kelley (1984, 1990), among others.

There is, however, an internal limitation to such a procedure since the available data refer to SF and DC but not to DS and DU which are also important (Duffy and Caldera, 1999). Thus, away from the regions where SF and DC are active, the above authors take

$$K_{m,h,s}(DS, DU) =0 \tag{3f}$$

or, more precisely, they use a background diffusivity which is chosen primarily on grounds of numerical stability but whose physical origin must be an internal–wave breaking phenomenon. This is clearly not a satisfactory situation especially in view of the fact that

Since the studies by ZHS and MHG have shown the importance of double diffusion, the above procedure is certainly better than (3e) but still not fully satisfactory. The goal of this paper is to consider the same problem but with a different methodology.

We develop *a turbulence model to compute the three diffusivities for momentum, heat and salt* to encompass the four processes SF, DC, DS and DU in the presence of an arbitrary shear. The inclusion of shear is quite relevant since is known to hamper the SF mechanism (Linden, 1971, 1974a, b; Kunze, 1990) and yet, the above procedures do not account for shear since they expressed K_h and K_s in terms of only one stability parameter R_ρ, rather than R_ρ and the Richardson number Ri.

The model comes in three forms: 1) K and ϵ are solutions of two dynamical equations, the so called K–ϵ model whose main but not unique advantage is to avoid the introduction of any mixing length, 2) only one of them satisfies a differential equation while the other is taken to be the local limit of its dynamic equation and 3) both K and ϵ are taken as the local limit of their respective dynamic equations. As we shall show, in model 3) all the relations are algebraic and one must solve a cubic equation. All the numerical results correspond to case 3).

c) *How to compute the diffusivities K's*

Since from the first O–GCM it clearly emerged that several key ocean features, e.g., polar heat transport, meridian circulation, T–S relationship (temperature–salinity), etc., depend sensitively on the vertical turbulent diffusivities of momentum K_m, heat K_h and salt K_s (F.O. Bryan, 1987; K.Bryan, 1991) even though until recently all codes employed the approximation $K_s=K_h$. The need to reliably compute such diffusivities has been dealt in the past with three quite distinct approaches.

d) *descriptive–diagnostic method*

One can adopt a descriptive–diagnostic approach whereby the O–GCM are used to

show that in order to obtain overall agreement with the data, the diffusivities K's must lie in a restricted range of values. Such a diagnostic, a posteriori approach is however inadequate in climate studies where the predictive power of the model is the key feature on which the reliability of the model results is predicated.

e) *turbulence models.* These models are based on the Navier–Stokes equations and thus, at least in principle, have a built–in degree of generality, resiliency and predictive power. In particular, one–point closure turbulence models have the longest tradition (Chou, 1940, 1945) and, naturally, they were the first tools used to construct the turbulence variables needed in O–GCM. The pioneering work in this field is that of Mellor and Yamada (1982, MY; Mellor, 1989) who applied the 1980 state–of–the–art turbulence modeling to geophysical problems. However, almost 20 years later, most of the work in ocean turbulence still employs essentially the same 1980 state of the art turbulence modeling (Rosati and Miyakoda 1988; Galperin et al.1989; Gaspar et al. 1990; Blanke and Delecluse 1992; Baum and Caponi, 1992; Ma et al. 1994; Kantha and Clayson 1994; Burchard and Baumert 1995; D'Alessio et al., 1998). This means that the basic difficulties that plagued the original MY model are still present. They can be identified with the closure of the pressure correlations terms, and the need to express the non–local third order moments (TOM) in terms of lower order moments. The pressure–correlations bring about adjustable constants which the model is unable to predict and the TOM are treated with the down gradient approximation which Moeng and Wyngaard (1989) have convincingly shown to be seriously inadequate (see paper I for details).

f) *Non–turbulence models.* On the grounds that the above uncertainties have not been satisfactorily resolved, Large et al. (1994) have suggested an alternative model (called KPP), not based on any turbulence model.

g) *New turbulence models.* It is generally agreed that, potentially, turbulence models have far greater generality, resiliency and predictability power that any ad–hoc–model. In papers I and II, we offered the most updated 1–point closure models that one can construct today. Here, we offer a new *2–point closure model* that has been assessed over some ~80m turbulent statistics pertaining to large variety of flows. We derive the expressions for K_m, K_h and K_s and run the O–GCM with the new K's. The new model has no adjustable parameters.

II. New turbulence model

The turbulence model to be employed here (Canuto et al., 1996–1999, cited as CD) was tested on about 100 turbulent statistics belonging to a wide variety of flows: pure shear flows, Rayleigh–Benard convection, rotating turbulence, 2D turbulence, rotating convection, freely decaying turbulence, stably stratified turbulence, etc. In all cases, the model reproduces the data quite accurately and thus the model can be considered validated. In addition, t*he model has no adjustable parameters.* Since this is the first application of this new turbulence model to ocean turbulence, it is necessary to begin by presenting the physical foundations of the model.

Recent advances in phenomena related to turbulence (e.g., critical phenomena) have provided us with new tools and new perspectives on how to tackle the problem of turbulence. Like in many other fields, one begins with the case of homogeneous–isotropic turbulence for which an exact solution of the NSE found by Wyld (1961). The solution for the energy spectrum E(k) can be shown to be equivalent to the solution of a stochastic Langevin–type dynamic equation for the turbulent velocity fields $\mathbf{u}(\mathbf{k})$ of the form

$$\frac{\partial}{\partial t} u_i(\mathbf{k}) = f_i^{ext}(\mathbf{k}) + f_i^{t}(\mathbf{k}) - \nu_d(k) k^2 u_i(\mathbf{k}) \qquad (4a)$$

where $E(k) \sim k^2 u(\mathbf{k}) u(\mathbf{k})$. Eq.(4a) has an appealing physical interpretation: external forces are represented by the first term whose specific form is obtained from the NSE for arbitrary flows (shear, convection, rotation, etc). The second term is a random turbulent force

representing the action of the large eddies on a given eddy **k** even when the external forces are no longer operative (for example in the Kolmogorov region) and finally, the last term represents the dynamical viscosity felt by an eddy **k** due to all smaller eddies. Though derived for homogeneous and isotropic turbulence, Eq.(4a) seems to capture the main ingredients that one needs to build the canonical picture of a supply, transfer and enhanced dissipation of energy that is at the base of Kolmogorov original picture of turbulent dynamics. The challenge is to give an explicit expression to all the terms and prove that in spite of its "idealized" origin, Eq.(4a) is valid quite in general and capable of reproducing real flows. It must be stressed that we are not the first to suggest a Langevin–type equation as a starting point to describe turbulence. Several previous models were in fact recast in terms of a Langevin–type equations but, to the best of our knowledge, this is the first case in which Eq.(4a) has been shown to be a viable, successful, operational tool to treat real turbulent flows. To construct the explicit form of the dynamical viscosity, CD first generalized the well developed and well tested renormalization group method (RNG) to derive the following expression for $\nu_d(k)$

$$\nu_d(k) = \nu_t(k) + \nu = (\nu^2 + \frac{2}{5}\int_k^\infty E(p)p^{-2}dp)^{\frac{1}{2}} \qquad (4b)$$

where ν is the kinematic viscosity and $\nu_t(k)$ is the so–called turbulent viscosity. This expression tells two things: first, the integration from k to ∞ means that $\nu_d(k)$ is contributed by all eddies smaller than k, as indeed expected on physical grounds and that while the Langevin equation is linear in the velocity fields, its "coefficients" like $\nu_d(k)$ are non linear since they depend on E(k). Thus, while in the NSE the coefficients are numbers and the velocity fields enter non–linearly (giving rise to closure problems), in the Langevin equation the situation is reversed. This a key point that allows us to derive a closed system of equations for the second–order moments like Reynolds stresses, etc. Next, we consider the first term in (4a). It represents the external forces driving turbulence, is a linear function of the turbulent fields and its form can be derived directly from the NSE. In the

present paper we consider the turbulent fields of velocity, temperature and salinity u_i, θ and σ in which case f^{ext} is the sum of three terms

$$f_i^{ext} = f_i^u + f_i^\theta + f_i^\sigma \tag{4c}$$

where

$$f_i^u = - U^{\perp}_{i,j} u_j(k) + k_j U_{j,m} [\frac{\partial}{\partial k_m} u_i(k)]^{\perp} \tag{4d}$$

$$f_i^\theta = - \alpha_T P_{ij}(\mathbf{k})\, g_j \theta(\mathbf{k}) \tag{4e}$$

$$f_i^S = \alpha_S P_{ij}(\mathbf{k})\, g_j \sigma(\mathbf{k}) \tag{4f}$$

Here, $U_{i,j}$ is the mean velocity gradient, and the α's are the expansion coefficients (T and S_a are mean temperature and salinity)

$$\alpha_T = - \rho^{-1} \frac{\partial \rho}{\partial T}, \qquad \alpha_S = \rho^{-1} \frac{\partial \rho}{\partial S_a} \tag{4g}$$

which must be computed using the equation of state for seawater. The superscript $\perp$ in (4d) means that only transverse components are allowed, that is, for any tensor $\mathbf{A}$,

$$A^{\perp}_{ij} \equiv P_{i\ell}(\mathbf{k}) A_{\ell m} P_{mj}(\mathbf{k}) \tag{4h}$$

where $P_{ij} = \delta_{ij} - k_i k_j k^{-2}$ is the projection operator. Analogously, for the θ and σ fields, we have the Langevin equations:

$$\frac{\partial}{\partial t} \theta(\mathbf{k},t) = f^t_\theta(\mathbf{k},t) - \chi_d(k,t) k^2 \theta(\mathbf{k},t) + f^S_\theta(\mathbf{k},t) \tag{5a}$$

$$\frac{\partial}{\partial t} \sigma(\mathbf{k},t) = f^t_\sigma(\mathbf{k},t) - \kappa_d(k,t) k^2 \sigma(\mathbf{k},t) + f^S_\sigma(\mathbf{k},t) \tag{5b}$$

with

$$\chi_d(k) = \chi + \chi_t(k), \qquad \kappa_d(k) = \kappa + \kappa_t(k) \tag{6}$$

where χ and κ are the heat and salt kinematic diffusivities. The stirring forces are:

$$f^t_\theta(\mathbf{k},t) = - \beta^\theta_i u_i(\mathbf{k}), \qquad f^t_\sigma(\mathbf{k},t) = - \beta^\sigma_i u_i(\mathbf{k}) \tag{7a,b}$$

where the β's are the gradients of the mean temperature T and the mean salinity S_a,

$$\beta^\theta_i = \frac{\partial T}{\partial x_i}, \qquad \beta^\sigma_i = \frac{\partial S_a}{\partial x_i} \tag{7c}$$

As Eqs.(1a–c) show, what one needs in practice the Reynolds stress τ_{ij} which are the integral over all wavenumbers $\mathbf{k}$ of the two–point Reynolds stresses

$$R_{ij}(\mathbf{k}) \delta(\mathbf{k}+\mathbf{k}') = \langle u_i(\mathbf{k},t) u_j(\mathbf{k}',t) \rangle_S \tag{8a}$$

$$\tau_{ij} = \tag{8b}$$

where s means symmetrization with respect to $\mathbf{k}$ and $\mathbf{k}'$ and i,j. The other required second–order moments are the temperature and salinity fluxes:

$$j_i^{\theta}(\mathbf{k})\delta(\mathbf{k}+\mathbf{k}') = <u_i(\mathbf{k},t)\theta(\mathbf{k}',t)>_s \tag{9a}$$

$$j_i^{\sigma}(\mathbf{k})\delta(\mathbf{k}+\mathbf{k}') = <u_i(\mathbf{k},t)\sigma(\mathbf{k}',t)>_s \tag{9b}$$

As it will be shown, these variables entail other turbulence variables, and precisely, the variances of both the temperature and salt fields,

$$e_{\theta}(\mathbf{k})\delta(\mathbf{k}+\mathbf{k}') = \tfrac{1}{2}<\theta(\mathbf{k})\theta(\mathbf{k}')> \tag{10a}$$

$$e_{\sigma}(\mathbf{k})\delta(\mathbf{k}+\mathbf{k}') = \tfrac{1}{2}<\sigma(\mathbf{k})\sigma(\mathbf{k}')>= \tag{10b}$$

as well as the temperature–salinity correlation

$$e_{\theta\sigma}(\mathbf{k})\delta(\mathbf{k}+\mathbf{k}') = <\theta(\mathbf{k})\sigma(\mathbf{k}')> \tag{10c}$$

The spectra of energy, temperature and salt fields E(k), $E_{\theta,\sigma}(k)$ are obtained by integrating over the directions of the vector $\mathbf{k}$ (times a factor k^2) the density functions in the left hand sides of Eqs.(8)–(10), namely:

$$E(k) = \tfrac{1}{2}k^2 \int R_{ii}(\mathbf{k})d\mathbf{n}_k \tag{11a}$$

$$E_{\theta,\sigma}(k) = k^2 \int e_{\theta,\sigma}(\mathbf{k})d\mathbf{n}_k \tag{11b}$$

The dynamic equations for the second–order moments (8)–(10) are derived by multiplying the stochastic dynamic equations (4a) and (5a,b) by $u_i(k')$, $\theta(k')$ and $\sigma(k')$ and then averaging. The key difficulty is represented by the correlation of the first terms in (4a) and (5a,b) with the turbulent fields which physically represent the work performed by the turbulent forces $f^t(k)$. To compute these terms, we adopted two assumptions which are in agreement with the general understanding of turbulent processes: 1) energy generated at the largest scales is transferred locally to high k regions in a manner analogous to the flow of gas in a pipe, a model that applies to temperature and salinity as well, 2) as turbulent energy is transferred to smaller scales, the correlation functions of different fields, as well as correlation functions between different components of the velocity fields, decreases with increasing k even faster than the energy spectrum itself. The first assumption leads to a

representation of the energy flux $\Pi(k)$ of the form:

$$\Pi(k) = r(k)E(k) \tag{12}$$

where $r(k)$ is the rapidity with which energy is propagated among different eddies. Eq.(12) can be viewed as the analog of $j=\rho v$ with $j\rightarrow\Pi(k)$, $\rho\rightarrow E(k)$ and $v\rightarrow r(k)$. The energy flux $\Pi(k)$ is related to the energy transfer function $T(k)$ by:

$$T(k) = -\frac{\partial}{\partial k}\Pi(k), \quad \int T(k)dk=0 \tag{13a}$$

$$T(k) = -r(k)\frac{\partial}{\partial k}E(k) - [\frac{\partial}{\partial k}r(k)]E(k) \tag{13b}$$

On the other hand, the function $T(k)$ can be obtained by multiplying (4a) by $u_i(k')$ and separating the work of the non–linear interactions entering the first two terms in (4a).

$$T(k) = A^t(k) - 2\nu_t(k)\, k^2E(k) \tag{14}$$

where the work of the force f^t is defined by

$$A_t(k) = k^2\int d\mathbf{n}_k\, dk'<u_i(\mathbf{k}',t)f_i^t(\mathbf{k},t)> \tag{15}$$

Comparing (13b) and (14), we obtain:

$$A_t(k) = -r(k)\frac{\partial}{\partial k}E(k), \qquad \tfrac{1}{2}r(k) = \int_0^k \nu_t(p)p^2dp \tag{16}$$

For the fields θ and σ, assumption 1) leads to relations analogous to Eqs.(15)–(16), namely:

$$<\theta(\mathbf{k}')f_\theta^t(\mathbf{k})>_s = (4\pi k^2)^{-1}A_\theta\delta(\mathbf{k}+\mathbf{k}') \tag{17}$$

$$<\sigma(\mathbf{k}')f_\sigma^t(\mathbf{k})>_s = (4\pi k^2)^{-1}A_\sigma\delta(\mathbf{k}+\mathbf{k}') \tag{18}$$

where the expressions for the functions $A_{\theta,\sigma}(k)$ are analogous to Eq.(16), namely,

$$A_{\theta,\sigma}(k) = -r_{\theta,\sigma}(k)\frac{\partial}{\partial k}E_{\theta,\sigma}(k) \tag{19}$$

$$\tfrac{1}{2}r_\theta(k) = \int_0^k \chi_t(p)p^2dp \tag{20}$$

$$\tfrac{1}{2}r_\sigma(k) = \int_0^k \kappa_t(p)p^2dp \tag{21}$$

The functions χ_d,κ_d satisfy the differential equation (F stands for χ_d and/or κ_d)

$$\frac{dF}{d\nu_d} = \frac{10}{3}\nu_d(\nu_d+F)^{-1} \tag{22}$$

In the present paper, we shall be mostly interested in situations where

$$\nu_d>\nu, \quad \chi_d>\chi, \quad \kappa_d>\kappa \tag{23}$$

and thus it follows from Eq.(22) that

$$(\chi_d, \kappa_d) = \sigma_t^{-1}\nu_d(k) \tag{24}$$

where the turbulent Prandtl number σ_t=0.72 and $\nu_d(k)$ is given by Eq.(4b). As for assumption 2) above, it leads to the following relations:

$$\begin{aligned} <f_i^t(\mathbf{k},t)u_j(\mathbf{k}',t)> &= -(8\pi k^2)^{-1}A_t(k)P_{ij}(\mathbf{k})\delta(\mathbf{k}+\mathbf{k}') \\ <u_i(\mathbf{k}')\theta(\mathbf{k}')f^t_{\theta,\sigma}(\mathbf{k})> &= 0 \\ <\theta(\mathbf{k}')f^t_{i,\sigma}(\mathbf{k})> &= 0 \\ <\sigma(\mathbf{k}')f^t_{i,\theta}(\mathbf{k})> &= 0 \end{aligned} \tag{25a}$$

Finally, the dynamic equations for E(k) is:

$$\frac{\partial}{\partial t}E(k) = A_{ext}(k) + A_t(k) - 2k^2\nu_d(k)E(k) \tag{25b}$$

The information we have derived concerning the terms in the basic equations (4a) and (5a,b) is sufficient to allow us to derive a closed system of equations for the second–order moments (8)–(10).

III. Dynamic Equations for the Second–Order Moments

Multiplying the stochastic equations (4a) and (5a,b) by the fields u_i, θ and σ, it is straightforward to derive the following dynamic equations for the second–order correlation functions:

$$\begin{aligned} \tfrac{1}{2}\frac{\partial}{\partial t}R_{ij}(\mathbf{k}) &= (8\pi k^2)^{-1}A_t(k)P_{ij}(\mathbf{k}) - [S^{\perp}_{im}R_{mj}(\mathbf{k})]_s - \\ &- \tfrac{1}{2}[\mathbf{V}^{\perp}, \mathbf{R}(\mathbf{k})]_{ij} + \tfrac{1}{2}[\hat{D}\mathbf{R}(\mathbf{k})]^{\perp}_{ij} - k^2\nu_d(k)R_{ij}(\mathbf{k}) \\ &- \alpha_T[g^{\perp}_i j^{\theta}_j(k)]_s + \alpha_s[g^{\perp}_i j^{\sigma}_j(k)]_s \end{aligned} \tag{26}$$

$$\begin{aligned} \tfrac{1}{2}\frac{\partial}{\partial t}j^{\theta}_i(\mathbf{k}) &= -S^{\perp}_{im}j^{\theta}_m(\mathbf{k}) - V^{\perp}_{im}j^{\theta}_m(\mathbf{k}) + [\hat{D}\mathbf{j}^{\theta}(\mathbf{k})]^{\perp}_i \\ &- k^2[\nu_d(k)+\chi_d(k)]j^{\theta}_i(\mathbf{k}) - \beta^{\theta}_m R_{im}(\mathbf{k}) \\ &[-2\alpha_T e_{\theta}(\mathbf{k}) + \alpha_s e_{\sigma\theta}(\mathbf{k})]g_j P_{ij}(\mathbf{k}) \end{aligned} \tag{27}$$

$$\frac{\partial}{\partial t}e_{\theta}(\mathbf{k}) = (4\pi k^2)^{-1}A_{\theta}(k) - \beta^{\theta}_i j^{\theta}_i(\mathbf{k}) - 2k^2\chi_d(k)e^{\theta}(\mathbf{k}) \tag{28}$$

$$\frac{\partial}{\partial t}e_{\theta\sigma}(\mathbf{k}) = -\beta^{\theta}_i j^{\sigma}_i(\mathbf{k}) - \beta^{\sigma}_i j^{\theta}_i(\mathbf{k}) - 2k^2[\chi_d(k)+\kappa_d(k)]e_{\theta\sigma}(\mathbf{k}) \tag{29}$$

In addition there are two equations which can be obtained from Eqs.(27) and (28) with the substitutions:

$$j_i^{\theta} \to j_i^{\sigma},\ \beta_i^{\theta} \to \beta_i^{\sigma},\ \alpha_T \to -\alpha_S,\ e_{\theta} \to e_{\sigma},\ A_{\theta} \to A_{\sigma},\ \chi_d \to \kappa_d \tag{30}$$

In Eqs.(26)–(27) we have introduced the tensors

$$U_{i,j}=S_{ij}+V_{ij},\ \ 2S_{ij}=U_{i,j}+U_{j,i},\ \ 2V_{ij}=U_{i,j}-U_{j,i} \tag{31}$$

where S_{ij} and V_{ij} are the mean shear and vorticity and $\hat{D}$ is the operator

$$\hat{D} = k_j(S_{j\ell}+ V_{j\ell})\frac{\partial}{\partial k_{\ell}} \tag{32}$$

Eqs.(26)–(29) must be solved together with the incompressibility condition

$$k_i R_{ij}(\mathbf{k})=k_j R_{ij}(\mathbf{k})=k_i j_i^{\theta,\sigma}=0 \tag{33}$$

This suggests that one may solve the above equations in spherical coordinates where one can write (for any j)

$$\mathbf{j}(\mathbf{k}) = j_{\phi}(\mathbf{k})\mathbf{e}_{\phi} + j_{\theta}(\mathbf{k})\mathbf{e}_{\theta} \tag{34}$$

where $\mathbf{e}_{\phi,\theta}$ are the basic units vectors. Due to condition (33), the only non–zero components of R_{ij} lie in the plane perpendicular to $\mathbf{k}$ so that their number is three and the general decomposition has the form:

$$R_{ij}(\mathbf{k}) = e(\mathbf{k})P_{ij}(\mathbf{k}) + a(\mathbf{k})\rho_{ij}(\mathbf{k}) + b(\mathbf{k})\eta_{ij}(\mathbf{k}) \tag{35}$$

where $e(\mathbf{k})$ is the energy density in $\mathbf{k}$–space while the orthogonal tensors $\boldsymbol{\rho}$ and $\boldsymbol{\eta}$ should be chosen so as to avoid singularities in the functions $a(\mathbf{k})$ and $b(\mathbf{k})$ which invariably arise when the tensors $\boldsymbol{\rho}$ and $\boldsymbol{\eta}$ depend on ϕ as $\theta \to 0$. This point and the details of the decomposition are fully discussed in Sec.III of Canuto and Dubovikov (1996b). In the 3D case, the final equations for the scalar functions $e(\mathbf{k})$, $a(\mathbf{k})$, $b(\mathbf{k})$ etc are quite cumbersome. Thus, we shall consider only the case of direct physical interest: the mean fields U_i, T, and salt depend only on the coordinate where there is a non–zero gravity. The final result is:

$$\frac{\partial}{\partial t}e(\mathbf{k}) = (4\pi k^2)^{-1}A_t(\mathbf{k}) - 2k^2\nu_d(\mathbf{k})e(\mathbf{k}) + \mathbf{M}_0 e(\mathbf{k}) + \mathbf{M}_a a(\mathbf{k}) + \mathbf{M}_b b(\mathbf{k}) - \\ - \lambda_{\phi}^{\theta} j_{\phi}^{\theta}(\mathbf{k}) - \lambda_{\theta}^{\theta} j_{\theta}^{\theta}(\mathbf{k}) + \lambda_{\phi}^{\sigma} j_{\phi}^{\sigma}(\mathbf{k}) + \lambda_{\theta}^{\sigma} j_{\theta}^{\sigma}(\mathbf{k}) \tag{36}$$

$$\frac{\partial}{\partial t}a(\mathbf{k}) = -2k^2\nu_d(k)a(\mathbf{k}) + \mathbf{M}_0 a(\mathbf{k}) + \mathbf{M}_a e(\mathbf{k}) + \mathbf{M}_{ab} b(\mathbf{k}) - \\ + \delta_1 j_\phi^\theta(\mathbf{k}) + \delta_2 j_\theta^\theta(\mathbf{k}) + \delta_3 j_\phi^\sigma(\mathbf{k}) + \delta_4 j_\theta^\sigma(\mathbf{k}) \tag{37a}$$

with

$$\delta_1 \equiv \lambda_\phi^\theta \cos 2\phi + \lambda_\theta^\theta \sin 2\phi, \quad \delta_2 \equiv -\lambda_\theta^\theta \cos 2\phi + \lambda_\phi^\theta \sin 2\phi$$
$$\delta_3 = -\lambda_\phi^\sigma \cos 2\phi - \lambda_\theta^\sigma \sin 2\phi, \quad \delta_4 = \lambda_\theta^\sigma \cos 2\phi - \lambda_\phi^\sigma \sin 2\phi \tag{37b}$$

$$\frac{\partial}{\partial t}b(\mathbf{k}) = -2k^2\nu_d(k)b(\mathbf{k}) + \mathbf{M}_0 b(k) + \mathbf{M}_b e(\mathbf{k}) - \mathbf{M}_{ab} a(\mathbf{k}) - \\ + \gamma_1 j_\phi^\theta(\mathbf{k}) + \gamma_2 j_\theta^\theta(\mathbf{k}) + \gamma_3 j_\phi^\sigma(\mathbf{k}) + \gamma_4 j_\theta^\sigma(\mathbf{k}) \tag{38a}$$

with

$$\gamma_1 \equiv \lambda_\phi^\theta \sin 2\phi - \lambda_\theta^\theta \cos 2\phi, \quad \gamma_2 \equiv -\lambda_\theta^\theta \sin 2\phi - \lambda_\phi^\theta \cos 2\phi$$
$$\gamma_3 = -\lambda_\phi^\sigma \sin 2\phi + \lambda_\theta^\sigma \cos 2\phi, \ \gamma_4 = \lambda_\theta^\sigma \sin 2\phi + \lambda_\phi^\sigma \cos 2\phi \tag{38b}$$

$$\frac{\partial}{\partial t}j_\theta^\theta(\mathbf{k}) = -2k^2 p\nu_d(k) j_\theta^\theta(\mathbf{k}) + \mathbf{M}_\theta j_\theta^\theta - Sz(1-\sin 2\phi) j_\phi^\theta - \beta_\theta^\theta e(\mathbf{k}) - \\ - 2\lambda_\theta^\theta e_\theta(\mathbf{k}) + \lambda_\theta^\sigma e_{\sigma\theta}(\mathbf{k}) + \epsilon_1 a(\mathbf{k}) + \epsilon_2 b(\mathbf{k}) \tag{39a}$$
$$\epsilon_1 = \beta_\phi^\theta \sin 2\phi - \beta_\theta^\theta \cos 2\phi\ , \quad \epsilon_2 = -\beta_\theta^\theta \sin 2\phi - \beta_\phi^\theta \cos 2\phi \tag{39b}$$

$$\frac{\partial}{\partial t}j_\phi^\theta(\mathbf{k}) = -2k^2 p\nu_d(k) j_\phi^\theta(\mathbf{k}) + \mathbf{M}_\phi j_\phi^\theta + Sz j_\theta^\theta - \beta_\phi^\theta e(\mathbf{k}) - \\ - 2\lambda_\phi^\theta e_\theta(\mathbf{k}) + \lambda_\phi^\sigma e_{\sigma\theta}(\mathbf{k}) + \eta_1 a(\mathbf{k}) + \eta_2 b(\mathbf{k}) \tag{40a}$$
$$\eta_1 = \beta_\phi^\theta \cos 2\phi + \beta_\theta^\theta \sin 2\phi\ , \quad \eta_2 = -\beta_\theta^\theta \cos 2\phi + \beta_\phi^\theta \sin 2\phi \tag{40b}$$

$$\frac{\partial}{\partial t}e_\theta(\mathbf{k}) = (4\pi k^2)^{-1} A_\theta(k) - 2k^2\sigma_t^{-1}\nu_d(k) e_\theta(\mathbf{k}) \\ - \beta_\phi^\theta j_\phi^\theta(k) - \beta_\theta^\theta j_\theta^\theta(k) \tag{41}$$

$$\frac{\partial}{\partial t}e_{\sigma\theta}(\mathbf{k}) = -2k^2\sigma_t^{-1}\nu_d e_{\sigma\theta}(\mathbf{k}) - \beta_\phi^\theta j_\phi^\sigma(k) - \\ - \beta_\theta^\theta j_\theta^\sigma(k) - \beta_\phi^\sigma j_\phi^\theta(k) - \beta_\theta^\sigma j_\theta^\theta(k) \tag{42}$$

We have defined the following variables ($z=\cos\theta$):

$$\hat{M}_0 = \tfrac{1}{2}S(1-z^2)\cos 2\phi + \hat{D} \tag{43}$$

$$-4S^{-1}\hat{M}_a = (1+z)^2 + (1-z)^2\cos 4\phi$$

$$-4S^{-1}\hat{M}_b = (1-z)^2\sin 4\phi$$

$$S^{-1}\hat{M}_{ab} = (1-z)(1-\sin 2\phi) - z$$

$$\hat{M}_\theta = -\tfrac{1}{2}Sz^2\cos 2\phi + \hat{D}, \qquad \hat{M}_\phi = \tfrac{1}{2}S\cos 2\phi + \hat{D} \tag{44a}$$

$$2S^{-1}\hat{D} = \cos 2\phi\,(1-z^2)\,(k\partial_k - z\partial_z) + (1-\sin 2\phi)\partial_\phi$$

$$p = \tfrac{1}{2}(1+\sigma_t^{-1}) = 1.2 \tag{44b}$$

$$\beta_\phi^{\theta,\sigma} = -2^{-\frac{1}{2}}(\sin\phi - \cos\phi)\beta^{\theta,\sigma}$$

$$\beta_\theta^{\theta,\sigma} = 2^{-\frac{1}{2}}z(\cos\phi + \sin\phi)\beta^{\theta,\sigma} \tag{44c}$$

$$\lambda_\theta^{\theta,\sigma} = -2^{-\frac{1}{2}}z(\sin\phi + \cos\phi)g\alpha_{T,s}$$

$$\lambda_\phi^{\theta,\sigma} = 2^{-\frac{1}{2}}(\sin\phi - \cos\phi)g\alpha_{T,s} \tag{44d}$$

Finally, the equations for

$$j_\theta^\sigma(\mathbf{k}), \quad j_\phi^\sigma(\mathbf{k}), \quad e_\sigma(\mathbf{k}) \tag{44e}$$

are obtained from Eqs.(40)–(41) via the substitution (30). In the above and subsequent equations,

$$S = (2S_{ij}S_{ij})^{\frac{1}{2}}, \quad N^2 = g\alpha_T\frac{\partial T}{\partial z}, \quad Ri = \frac{N^2}{S^2} \tag{44f}$$

S, N and Ri are the mean shear,the Brunt–Vaisala frequency and the Richardson number.

IV. Spectra of the Second–Order Moments

The above equations do not contain free parameters and can be solved numerically once the initial density functions are known. Concrete examples were discussed in Canuto and Dubovikov (1996c) for different types of shear driven flows for which we can compare the model results against DNS/LES and laboratory data. The model reproduces such data quite well. The case of buoyancy driven flows was also studied (Canuto and Dubovikov, 1997a) and in that case too, the model results were in good agreement with a variety of data. This performance of the model gives us confidence that the extension discussed here is based on solid foundations. Our final goal is to express the one–point second order

moments like the Reynolds stresses, the temperature and salinity fluxes in terms of the gradients of the large scale fields. Since a numerical solution of the above dynamic equations would not be of practical use, especially if the results are to be used in an O–GCM, an analytical model is needed which by necessity requires that we make some approximations. We shall employ the same philosophy that was employed earlier when we treated shear and buoyancy driven flows. The gist of the method is as follows. In the inertial ranges, Eqs.(36)–(42) can be solved perturbatively since we have the small parameters

$$S(k^2\nu_t)^{-1}, \quad g\alpha_T\beta^{\theta}(k^2\chi_t)^{-2}, \quad g\alpha_S\beta^{\sigma}(k^2\kappa_t)^{-2} \tag{45}$$

Once the inertial spectra are obtained, we extrapolate them all the way back to the infrared cut–off k_0 below which we assume that $E(k)=0$. Upon integrating the resulting spectra over all k's, we obtain the desired one–point correlation functions. In the case of shear–driven flows, the results obtained with this method differ less than 15% from those obtained by numerically solving the full equations (Canuto et al., 1999c). *We shall carry out the procedure without salinity* which we shall incorporate in the next paper. To calculate the spectra, we first need to integrate the **k**–space densities, Eqs.(8)–(10), over all directions of **k**. In turn, the densities are expressed in terms of the variables in Eq.(36)–(42) as described in detail in Canuto and Dubovikov (1998b). Furthermore, we shall consider first the stationary case. To the zeroth–order in the smallness parameters (45), the only non–zero results are the isotropic components of the energy densities $\bar{e}(k)$, $\bar{e}_{\theta}(k)$ and $\bar{e}_{\sigma}(k)$ which are obtained by retaining only the first two terms in Eqs.(36) and (41) and in the equation for e_{σ} which is obtained from (41) and the substitution (30). The results are:

$$4\pi k^2\bar{e}(k) = E(k) = Ko\epsilon^{2/3}k^{-5/3} \tag{46}$$

$$4\pi k^2\bar{e}_{\theta}(k) = E_{\theta}(k) = Ba\epsilon_{\theta}\epsilon^{-1/3}k^{-5/3} \tag{47a}$$

$$4\pi k^2\bar{e}_{\sigma}(k) = E_{\sigma}(k) = Ba\epsilon_{\sigma}\epsilon^{-1/3}k^{-5/3} \tag{47b}$$

with

$$Ko = \frac{5}{3}, \qquad Ba = \sigma_t Ko \tag{48}$$

where Ba is the Batchelor constant and the ϵ's represent the rate of dissipation of the total kinetic and potential energies for the temperature and salinity fields. To compute the first order terms in the smallness parameters (45), we must consider the first and third terms in (37a), (38a), the first, fourth and fifth terms in (39a), (40a) and in the corresponding equation for j_σ, whereas in (36) the second and third terms should be taken into account provided that only the component $\tilde{e}\equiv e-\bar{e}$ is retained in the second term since the $\bar{e}$–part has already been used in the zeroth–order. The results of the above procedure, as well as further intermediate steps, are presented for the simplified case in the absence of salinity, whereas the final results will include salinity.

Reynolds stress spectrum

$$\mathbf{R}(k) = \frac{2}{3}\mathbf{I}E(k) + C_\sigma(k)\boldsymbol{\sigma} + C_\Sigma\boldsymbol{\Sigma} + C_t(k)\mathbf{t} + C_\lambda(k)\boldsymbol{\lambda} \tag{49a}$$

where the basis tensors are:

$$\boldsymbol{\sigma} = S^{-1}\mathbf{S}, \quad \boldsymbol{\Sigma} = S^{-2}\mathbf{S}^2 - \frac{1}{6}\mathbf{I}$$
$$\mathbf{t} = S^{-2}[\mathbf{V},\mathbf{S}], \quad \boldsymbol{\lambda} = g^{-2}g_i g_j - \frac{1}{3}\mathbf{I} \tag{49b}$$

The coefficients C's are given by (superscripts indicate the perturbative order at which they were obtained and $\beta\equiv\beta^\theta$)):

$$C_\sigma^1(k) = -\frac{20}{27}S\epsilon^{1/3}k^{-7/3} \tag{50a}$$
$$C_\sigma^3(k) = 0.92(1 - \sigma_t\epsilon_\theta\epsilon^{-1}\alpha_T g\beta^{-1})N^2S\epsilon^{-1/3}k^{-11/3} \tag{50b}$$
$$C_t^2(k) = \frac{28}{27}S^2k^{-3} \tag{50c}$$
$$C_t^4(k) = -1.08\,(1 - \sigma_t\epsilon_\theta\epsilon^{-1}\alpha_T g\beta^{-1})N^2S^2\epsilon^{-2/3}k^{-13/3} \tag{50d}$$
$$C_\Sigma^2(k) = -3.3S^2k^{-3} \tag{50e}$$
$$C_\lambda^2(k) = -1.3N^2(1 - 1.44\epsilon_\theta\epsilon^{-1}\alpha_T g\beta^{-1})k^{-3} \tag{50f}$$

where the Brunt–Vaisala frequency N is: (50g)

$$N^2 = g\alpha_T\frac{\partial T}{\partial z} \tag{50h}$$

Heat flux spectrum:

$$\mathbf{J}(\mathbf{k}) = J_g(k)\mathbf{g}_0 + J_u\mathbf{U}_0 \tag{51a}$$
$$\mathbf{g}_0 = g^{-1}\mathbf{g}, \quad \mathbf{U}_0 = U^{-1}\mathbf{U} \tag{51b}$$

$$J_g^1(k) = 0.93\beta\,(1 - 1.44\epsilon_\theta\epsilon^{-1}\alpha_T g\beta^{-1})\epsilon^{1/3}k^{-7/3} \tag{52c}$$

$$J_u(k) = \frac{10}{27}p^{-1}\beta[1 + \frac{17}{20}\,p^{-1}(1 - 1.44\epsilon_\theta\epsilon^{-1}\alpha_T g\beta^{-1})]Sk^{-3} \tag{52a}$$

V. One–point Reynolds stresses and temperature flux

The case of the Reynolds stresses in the presence of shear was discussed in detail in Canuto and Dubovikov (1999c) and we shall not repeat it here. The final result for the one–point Reynolds stress, arrived at by integrating (49a) over wavenumbers from the infrared cutoff to infinity, is:

$$\tau_{ij} = \overline{u_i u_j} - \frac{2}{3}K\delta_{ij} \tag{53a}$$

$$\tau_{ij} = C_\sigma\sigma + C_t t + C_\lambda\lambda \tag{53b}$$

where the basis tensors were defined in Eqs.(49b). The coefficients C's are :

$$C_\sigma = -\frac{5}{9}S\epsilon^{1/3}k_0^{-4/3}\sigma_m \tag{54a}$$

$$C_t = \frac{14}{27}\,S^2k_0^{-2}\sigma_m \tag{54b}$$

$$C_\lambda = -\,0.65N^2k_0^{-2}(1 - 1.44\epsilon_\theta\epsilon^{-1}\alpha_T g\beta^{-1}) \tag{54c}$$

$$\sigma_m = 1 - 0.62(1 - 0.72\epsilon_\theta\epsilon^{-1}\alpha_T g\beta^{-1})N^2\epsilon^{-2/3}k_0^{-4/3} \tag{54d}$$

Upon integration of the thermal spectra (51) and (52), we obtain the two components:

$$J_g = 0.7\beta\epsilon^{1/3}k_0^{-4/3}(1 - 1.44\epsilon_\theta\epsilon^{-1}\alpha_T g\beta^{-1}) \tag{55a}$$

$$J_u = 0.156\,\beta Sk_0^{-2}[1 + 1.43(1 - 1.44\epsilon_\theta\epsilon^{-1}\alpha_T g\beta^{-1})] \tag{55b}$$

We recall that k_0 is obtained via the relations:

$$K = \int_{k_0}^{\infty} E(k)\,dk = \frac{5}{2}\,\epsilon^{2/3}k_0^{-2/3} \tag{55c}$$

$$k_0 = (\frac{5}{2})^{3/2}\epsilon K^{-3/2} \tag{55d}$$

Some modifications are however required. As stated earlier, the above results correspond to the stationary case and thus, they imply that production=dissipation, that is,

$$P=\epsilon,\;\; P_\theta=\epsilon_\theta \tag{56}$$

where P and P_θ represent the rate production of turbulent kinetic energy and of temperature variance (that is, potential energy). To introduce the P/ϵ dependence into the

equations, we must somehow keep the left hand side of Eq.(36). In carrying out the perturbative approach, we obtain the following differential equation for the functions e,a,b to the first order in the smallness parameter (45):

$$\frac{\partial}{\partial t} f_1(\mathbf{k}) = \epsilon^{1/3} k^{2/3} [f_1^0(\mathbf{k}) - f_1(\mathbf{k})] \tag{57}$$

where f_1^0 is the first order term representing any of the functions e,a,b in the stationary limit. The same equation holds true for the first order of the spectrum $C_\sigma(k)$. To integrate (57) over k for the component $C_\sigma^1(k)$, we assume that its form is the same as in the stationary limit, that is, $k^{-7/3}$. Then, from (57) we obtain:

$$\tfrac{1}{2} \epsilon^{-1/3} k_0^{-2/3} \frac{\partial}{\partial t} C_\sigma^1(k) = C_\sigma^0 - C_\sigma^1(k) \tag{58a}$$

Following a practice widely used in treating the Reynolds stresses, we shall assume that

$$\frac{\partial}{\partial t} C_\sigma^1(k) = C_\sigma \dot{K} K^{-1} = C_\sigma K^{-1} (P - \epsilon) \tag{58b}$$

Thus, Eq.(58a) gives finally

$$C_\sigma^1(k) = F_1 C_\sigma^0(k) \tag{58c}$$

$$F^{-1} = 1 + \tfrac{1}{5}(P/\epsilon - 1) \tag{58d}$$

Proceeding in an analogous fashion, we obtain

$$J_g = J_g^0 \hat{F}_1 \tag{59a}$$

$$\hat{F}_1 = 1 + 0.084 \, [P/\epsilon - 1 + \sigma_t^{-1} (P_\theta / \epsilon_\theta - 1)] \tag{59b}$$

We can continue the analysis of the P/ϵ dependence to the next order of perturbation, as it was described in detail in Canuto and Dubovikov (1999c). The results will be presented below but before we must discuss another correction to C_σ^1 which is due to the fact that an unmodified extension of the initial expression for the first–order function $\tilde{e}_1(k)$ up to k_0 results in a violation of the positiveness of the energy density $e(\mathbf{k})$ in the region $k_0 < k < k_1$ where

$$k_1 = \frac{8}{15} x k_0^{2/3}, \qquad x = \frac{KS}{\epsilon} \tag{60a}$$

Such a violation can be prevented by multiplying the function $\tilde{e}_2(\mathbf{k})$ by $(k/k_1)^{2/3}$ in the region $k_0 < k < k_1$. This leads to the following correction factor to $C_\sigma^1(k)$

$$F_c = \frac{9}{5} - 3x^{-1}(1 - \frac{15}{16}x^{-1}) \quad \text{for } x>15/8$$

$$F_c=1, \text{ for } x<15/8 \tag{60b}$$

Next, we substitute the variables k_0 from Eq.(55d) and adopt $P_\theta=\epsilon_\theta$ to obtain

$$\epsilon_\theta= \beta J_g \tag{60c}$$

Substituting (55a), we obtain a linear equation in ϵ_θ/ϵ whose solution is

$$\frac{\epsilon_\theta}{\epsilon} = \frac{11}{100}\beta^2 N^{-2}x^2 Ri(1 + 0.16x^2 Ri)^{-1} \tag{61}$$

The last modification we have to carry out accounts for corrections of higher orders in $(N^2)^n$ to the function σ_m, Eq.(54d) where we took into account only the first correction and thus σ_m has the form

$$\sigma_m= 1-\xi \tag{62a}$$

Since $\sigma_m>0$. a consistent way to extrapolate (62a) to the regions where $\xi\sim1$ in the spirit of Pade' approximations, we write

$$1-\xi \rightarrow (1+\xi)^{-1} \tag{62b}$$

VI. Reynolds stresses, temperature and salinity fluxes

After performing the modifications indicated above, we obtain the following results:

Reynolds Stresses:

$$\tau_{ij}= \overline{u_i u_j} - \frac{2}{3}K\delta_{ij} \tag{63a}$$

$$\tau_{ij} = C_\sigma \sigma + C_t t + C_\lambda \lambda \tag{63b}$$

where the basis tensors are defined in Eqs.(49b) and:

$$C_\sigma = -4\frac{K^2}{\epsilon} S S_m \tag{63c}$$

$$C_t = 4\gamma_3 \frac{K^2}{\epsilon} \tau S^2 S_m \tag{63d}$$

$$C_\lambda = -8\, 3^{-\frac{1}{2}}\gamma_4 \frac{K^2}{\epsilon} \tau N^2 S_h \tag{63e}$$

$$\tau = 2K\epsilon^{-1} \tag{63f}$$

In particular:

$$\overline{uw} = -K_m \frac{\partial U}{\partial z}, \qquad \overline{vw} = -K_m \frac{\partial V}{\partial z} \tag{63g}$$

$$K_m = 2\frac{K^2}{\epsilon}S_m \tag{63h}$$

Vertical Heat Flux J_θ:

$$J_\theta = \overline{w\theta} = = -K_h\frac{\partial T}{\partial z} \tag{64a}$$

$$K_h = 2\frac{K^2}{\epsilon}S_h \tag{64b}$$

Vertical Salt Flux J_σ:

$$J_\sigma = \overline{w\sigma} = = -K_\sigma\frac{\partial S}{\partial z} \tag{65a}$$

$$K_\sigma = 2\frac{K^2}{\epsilon}S_\sigma \tag{65b}$$

Dimensionless Structure Function for Momentum:

$$S_m = \frac{1}{25}F_1\tilde{F}_c\sigma_m \tag{66a}$$

where

$$\tilde{F}_c = \frac{5}{9}F_c = 1-\frac{5}{3}x^{-1}+\frac{25}{16}x^{-2} \quad \text{for } x\geq 15/8$$
$$\tilde{F}_c = \frac{5}{9}, \quad \text{for } x\leq 15/8 \tag{66b}$$

where the dimensionless variable x is given by

$$x = \frac{KS}{\epsilon} \tag{66c}$$

The other dimensionless functions are:

$$\sigma_m^{-1} = 1 + (\eta_\theta+\eta_\sigma)F_c^{-1} \tag{66d}$$

$$10^2\eta_\theta = 5\tilde{F}_2F_3x^2Ri[1+\frac{1}{12}\tilde{F}_1F_1^{-1}(5+7F_2\tilde{F}_2^{-1})(1-0.16x^2\tilde{F}_1R_\rho Ri)\psi_1] \tag{66e}$$

$$10^2\eta_\sigma = -5\tilde{F}_2F_3x^2R_\rho Ri[1+\frac{1}{12}\tilde{F}_1F_1^{-1}(5+7F_2\tilde{F}_2^{-1})(1+0.16x^2\tilde{F}_1Ri)\psi_1] \tag{66f}$$

$$\psi_1^{-1} = 1 + 0.16\,\tilde{F}_1x^2(1-R_\rho)Ri - 0.013\,\tilde{F}_1^2x^4R_\rho Ri^2\phi \tag{66g}$$

$$\phi^{-1} = 1+ 0.08\,x^2(1-R_\rho)Ri \tag{66h}$$

$$R_\rho = (g\alpha_S\frac{\partial S}{\partial z})(g\alpha_T\frac{\partial T}{\partial z})^{-1} \tag{66i}$$

Furthermore:

$$\tilde{S}_m = \frac{1}{36}\tilde{\sigma}_m, \qquad \tilde{\sigma}_m^{-1} = 1+\tilde{\eta}_\theta+\tilde{\eta}_\sigma \tag{67a}$$

$$10^2\tilde{\eta}_\theta = 4\tilde{F}_3F_4x^2Ri[1+\frac{1}{12}\tilde{F}_2F_2^{-1}(5+7F_3\tilde{F}_3^{-1})(1-0.16x^2\tilde{F}_2R_\rho Ri)\psi_2] \tag{67b}$$

$$10^2\tilde{\eta}_\sigma = -4\tilde{F}_3 F_4 x^2 Ri R_\rho [1+\frac{1}{12}\tilde{F}_2 F_2^{-1}(5+7F_3\tilde{F}_3^{-1})(1+0.16x^2\tilde{F}_2 Ri)\psi_2] \quad (67c)$$

$$\psi_2^{-1} = 1 + 0.16\tilde{F}_2 x^2(1-R_\rho)Ri - 0.013\,\tilde{F}_2^2 x^4 R_\rho Ri^2\phi \quad (67d)$$

The functions γ's and F_n are given by:

$$\gamma_3 = 0.12F_1F_2, \qquad \gamma_4 = 0.095F_2 \quad (68a)$$

$$F_n^{-1} = 1 + \frac{2}{5}n(1+n)^{-1}(\frac{P}{\epsilon}-1) \quad (68b)$$

$$\tilde{F}_n^{-1} = 1 + \frac{1}{6}n(1+n)^{-1}(\frac{P}{\epsilon}-1) \quad (68c)$$

Dimensionless Structure Function for Temperature and Salinity:

$$S_h = 0.056\tilde{F}_1^2(\tilde{F}_1^{-1} - 0.08x^2\phi Ri R_\rho)\psi_1 \quad (68d)$$

$$S_\sigma = 0.056\tilde{F}_1^2(\tilde{F}_1^{-1} + 0.08x^2\phi Ri)\psi_1 \quad (68e)$$

VII. Local and Non–Local Models

The above expressions require the knowledge of both the turbulent kinetic energy K and of its rate of dissipation ϵ. In principle, K and ϵ satisfy the non–local dynamic equations:

$$\frac{\partial K}{\partial t} + \frac{\partial}{\partial z}F(K) = -\tau_{ij}S_{ij} + g\alpha_T J_\theta - g\alpha_S J_\sigma - \epsilon \quad (69a)$$

$$\frac{\partial \epsilon}{\partial t} + \frac{\partial}{\partial z}F(\epsilon) = [-c_3\tau_{ij}S_{ij} + c_1(g\alpha_T J_\theta - g\alpha_S J_\sigma)]\epsilon K^{-1} - c_2\epsilon^2 K^{-1} \quad (69b)$$

The values of the coefficients $c_{1,2,3}$ have been discussed at length by Burchard and Baumert (1995). F(K) and F(ϵ) denote the fluxes of K and ϵ and they are third–order moments. The most complete expressions for these third–order moments (TOM) are those given by Canuto et al. (1994) which were successfully tested in the PBL (planetary boundary layer) against results from LES (large eddy simulation). Use of these TOM, together with the above model for the diffusivities, would represent a very complete treatment of ocean mixed layer turbulence. It is the K–ϵ model widely used in engineering turbulent flows.

Here, we present numerical results for the local limits of (69a,b) which we can write as

$$-\tau_{ij}S_{ij} + g\alpha J_\theta = \epsilon \quad (69c)$$

$$\epsilon = K^{3/2}\Lambda^{-1} \quad (69d)$$

where Λ is a mixing length. The first equation has the simple physical interpretation of production=dissipation, while (69d) is a statement of Kolmogorov law. Using the above expressions for τ_{ij} and J_θ, Eq.(69c) becomes the equation for the dimensionless variable x defined in Eq.(66c). We obtain:

$$x^2 = \tfrac{1}{2}(S_m - RiS_h)^{-1} \tag{69e}$$

where both $S_{m,h}$ depend on x. The Richardson number Ri is defined in Eq.(44f). For a given Ri, x is thus uniquely determined, x=x(Ri) and so are the structure functions

$$S_{m,h} = S_{m,h}(Ri) \tag{69f}$$

If we use the other local relation (69d), we finally obtain

$$K_{m,h} = 2\Lambda^2 S x^{-1} S_{m,h} \tag{69g}$$

which yields the turbulent diffusivities *in units* of $\Lambda^2 S$. Finally, we note in the production=dissipation local case, there is further simplification:

$$F_{1,2,3,4} = \hat{F}_{1,2,3} = 1 \tag{69h}$$

We must stress, however, that the use of a local model is not required by the turbulence model we have presented being made here only for reasons of simplicity. The length scale Λ is determined using the Deardorff–Blackadar formula:

$$\Lambda = 2^{-3/2} B_1 \ell, \qquad B_1 = 24.7,$$

$$\ell = \min(\tfrac{1}{2}\frac{q}{N}, \ell_1) \tag{69i}$$

$$\ell_1 = \kappa z \ell_0 (\ell_0 + \kappa z)^{-1}, \qquad \ell_0 = 0.17H \tag{69j}$$

where $\frac{1}{2}q^2 = K$ is the turbulent kinetic energy, N is the Brunt–Vaisala frequency, $\kappa = 0.4$ is the von Karman constant and H is the mixed layer depth. When used within the NCAR CSM Ocean Model, H is determined as the depth where the buoyancy difference

$$g[\rho(H) - \rho(\text{surface})]\rho(H)^{-1} = 3\ 10^{-4} ms^{-2} \tag{69k}$$

VIII. Ocean GCM

We tested the new vertical diffusivities in a global ocean general circulation model, O–GCM. We used the NCAR CSM Ocean Model produced by the University Corporation

for Research. National Center for Atmospheric Research, Climate and Global Dynamics Division. They developed their model by modifying the MOM 1.1 GFDL code as described in the NCAR CSM Ocean Model Technical Note, "The NCAR CSM Ocean Model", by the NCAR Oceanography section. We employed the stand–alone 3^0x3^0 configuration of the model detailed in their technical note with the default parameter values. It has 3.6^0 spacing in longitude and a variable spacing in latitude increasing from 1.8^0 at the equator to 3.4^0 at 17^0 N, S and then decreasing back to 1.8^0 for 60^0 N, S and poleward. There are 25 levels of increasing thickness in the vertical, with the surface level 6 meters thick. The option for the GM mesoscale eddy parameterization was enabled. Bulk forcing with a seasonal cycle plus a 1/2 year timescale restoring condition on the salinity is used, except under sea–ice where there is strong restoring. This configuration corresponds to the case B–K described in Large et al. (1997). It should be noted, however, that for determination of the length scale in our turbulence model we used the program's definition for mixed layer depth (a buoyancy difference from the surface of 3 $10^{-4}ms^{-2}$), which is different from that graphed as a diagnostic in Fig.5 of Large et al.(1997). We initialized our runs with annually averaged Levitus data and ran for 126 momentum years. As in Large et al. (1997) a 3504sec timestep for momentum is used, while for the first 96 momentum years the tracers are accelerated by a factor increasing from 10 at the surface to 100 for the deep ocean. We then set all timesteps equal for the remaining 30 years as they did.

First, we ran the NCAR program as is, with the option for the KPP mixing enabled, producing the KPP data presented in the figures below. Then, in place of the KPP module, we inserted a module which uses our new model for the diffusivities for momentum and heat with the salt diffusivity set equal to that of heat. To save computing time, we constructed tables of the dimensionless functions $S_{m,h}$ and of the dimensionless variable y (obtained from solving Eq.69e),

$$y = \tfrac{1}{2}\frac{S^2\ell^2}{K} \equiv \tfrac{1}{2}x^2(\frac{\ell}{\Lambda})^2 \qquad (70a)$$

vs. Ri. Then, for each point in space and time these were interpolated to the local Ri. To construct the diffusivities $K_{m,h}$(model), we used the results (63h) and (64b) which can be rewritten in terms of (70a) as

$$K_{m,h}/\ell^2 S = \tfrac{1}{2} B_1 y^{-\frac{1}{2}} S_{m,h} \tag{70b}$$

IX. Below the Mixed Layer

Below the ocean mixed layer, the external wind–generated shear is too small to generate turbulent mixing and yet, even in regions where both the temperature and the salinity gradients are stably stratified, it is usual to assume "background diffusivities" for viscosity, heat and salt diffusivity which are believed to be caused by internal wave breaking (Large et al., 1997). It would be preferable not to do so but rather model the physical processes causing this background mixing. Our main assumption is that the turbulence model has given us the correct functional dependence of the $K_{m,h,s}$ on Ri and R_ρ and that such diffusivities can thus be used below the ML. Since all the arguments discussed below, are valid for any of the three K's, we shall use only the generic symbol K and write succinctly

$$K = K(Ri, R_\rho) \tag{71a}$$

The key problem is how to define and thus compute Ri. Here, we shall make us of the measured data (Gargett et al., 1981) on the vertical shear generated by the wave breaking phenomenon. By integrating over all wavenumbers one can compute the shear due to internal waves, S_{wb}. One can then form a corresponding Ri_{wb} as follows:

$$Ri_{wb} = N^2/S_{wb}^2 \tag{71b}$$

where

$$N^2 = -g\rho^{-1}\frac{\partial \rho}{\partial z} \tag{71c}$$

Gargett et. al. (1981, sec. 5) confirmed earlier arguments by Munk (1966) that $Ri_{wb} \sim 1$. To those argument, we would like to add the following consideration. As the value of Ri_{cr}, above which there is no longer turbulent mixing, computed from our model is O(1), if Ri_{wb}

were >>1, there would be no turbulence generated by the internal waves at all. On the other hand if Ri_{wb} were <<1, there would be a very strong turbulence producing a viscosity sufficient to damp out the waves themselves. The wave–generated turbulence is thus self–limiting. Since the turbulence model gives a precise value for Ri_{cr}, while the above argument only tells us that Ri_{wb}~O(1), we shall write:

$$Ri_{wb}=cRi_{cr} \tag{71d}$$

where c is a constant reasonably close to unity. We have found that c=0.88 gives a diffusivity close that measured by Ledwell et al. (1993). Since in the local model, the K's are also proportional to the length scale Λ or ℓ, see Eq.(69i,j). Below the mixed layer, we thus need an analogous ℓ_{wb}. We shall use the same formal expressions (69i,j) but with different $\ell_0(wb)$ which we compute as follows. Assuming a Kolmogorov spectrum at wavenumbers upward of a breakpoint k_0 and integrating, we obtain:

$$\ell_0(wb) = (3Ko)^{3/2}(B_1 k_0)^{-1} \tag{71e}$$

where Ko=1.6 is the Kolmogorov constant. We identify k_0 with the best value of Gargett et al. (1981) for the break in slope of the observed spectrum of internal waves, namely

$$k_0 = \frac{1}{10}\,2\pi \text{ radians/meter} \tag{71f}$$

Thus, $\ell_0(wb)$ is known and so is ℓ_{wb}. Similarly, y_{wb} is obtained by solving the production=dissipation, Eq.(69c). Thus, the complete wave–breaking expressions for the three diffusivities are:

$$K_{m,h,s}(wb) = \tfrac{1}{2}B_1 \ell^2(wb) S_{wb} y_{wb}^{-\frac{1}{2}} S_{m,h,s}(Ri_{wb}, R_\rho) \tag{72a}$$

We add together the diffusivities calculated using the shear resolved in the ocean model and the background diffusivities, ensuring continuity in the transition between regions where external excited shear dominates and those where the internal wave shear does. We thus take the total diffusivities to be:

$$K_{m,h,s} = K_{m,h,s}(Ri,R_\rho) + K_{m,h,s}(wb, R_\rho) \tag{72b}$$

In the statically unstable case (Ri< 0), we set $K_{m,h,s}(wb)=0$. The very large mixing due to convective instability makes the background irrelevant in this situation in any case.

X. O–GCM results

In Fig.1 we present the dimensionless structure functions $S_{m,h}$ vs.Ri. They are given by Eqs.(66a) and (68d). The graphs correspond to the case without salinity. In Fig.2 we present the ratio K_m/K_h (again for the case without salinity) versus the LES data (dots) of Wang et al. (1996). In Figs.3–8 we present various diffusivities and their ratios for the full case with salinity and shear. The latter is represented by Ri, defined as the ratio of N^2, Eq.(50h) and the shear squared. The numbers on the curves represent the Turner number R_ρ, defined in Eq.(66i). The nomenclature SF, DC, DS and DU was introduced and discussed in the Introduction.

In Figs.9–20 we present the results of the O–GCM which comprise both global temperature and salinity profiles as well as for the case of different ocean basins. In Figs.21–29 we present the diffusivities in different ocean basins. Particularly interesting is the case of the Canary Islands since one can compare the model results with the value of $0.11\pm0.02 cm^2 s^{-1}$ measured by Ledwell et al. (1993). In each case, we compare our results with Levitus data as well as with the results we have obtained by running the same code with the KPP model which is available only for the case $K_s=K_h$.

Finally, in Fig.30 we present the polar heat transport.

XI. Discussion

It seems natural to require that the reliability of a model used to describe a given phenomenon should precede rather than follow the application of the model. Stated somewhat differently, a model should be judged on more than its performance in a given instance. Regrettably, the 1–point closure models used thus far to treat vertical mixing and following the Mellor–Yamada seminal work, have suffered and still do, from the presence of several adjustable parameters which have not allowed a clear appraisal of their performance before their use in the ocean context. In that respect, the new 2–point model presented here is quite different for it is being used only after it has exhibited a pedigree based on its

performance on a wide variety of turbulent flows. Its credibility, manageability and resiliency makes the best candidate for the computation of the vertical diffusivities.

The work is however not complete. In fact, it is known that double–diffusion phenomena change a smooth gradient into one that exhibit a step–like structure. As of today no theory that we know of is capable of encompassing such phenomenon. It is a challenge that we shall undertake in future work.

Figure caption

Fig.1 The momentum diffusivity K_m vs. Ri for different values of the Turner number R_ρ The label DC and SF are defined in the Introduction.

Fig.2 Same as in Fig.1 for the DU and DS cases.

Fig.3. Heat diffusivity vs. Ri for different R_ρ for the DC and SF cases.

Fig.4 Same as in Fig.3 for the DU and DS cases.

Fig.5 Salt diffusivity K_s vs. Ri for the SF and DC cases

Fig.6 Same as in Fig.5 for the DU and DS cases

Fig.7 The turbulent Prandtl number K_m/K_h vs. Ri for different R_ρ. The heavy line corresponds to the case of laboratory (see paper I, Figs. 3–4). Cases DC and SF.

Fig.8. The ratio of K_m/K_h vs. Ri for different R_ρ. Cases DU and DS.

Fig.9 The ratio of K_m/K_s vs. Ri for different R_ρ. DC and SF cases.

Fig.10 The ratio of K_m/K_s vs. Ri for different R_ρ. DU and DS cases.

Fig.11 The ratio of K_h/K_s vs. Ri for different R_ρ. DC and SF cases.

Fig.12 The ratio of K_h/K_s vs. Ri for different R_ρ. DU and DS cases.

Fig.13 The efficiency ratio Γ (paper II, Eq.59f) vs. Ri for different R_ρ. DC and SF cases

Fig.14 The global ocean temperature using the O–GCM discussed in VIII–IX with the new diffusivities. The Levitus (1994) data are the solid line. We have also run the O–GCM code with the KPP model ($K_s=K_h$) and the results are indicated by diamonds. The results with our new 1–point closure model with $K_s=K_h$ (paper II) are shown by squares while the present model results with $K_s \neq K_h$ are indicated by asterisks.

Fig.15. Global salinity

Fig.16. Artic ocean temperature

Fig.17. Artic ocean salinity

Fig.18. Atlantic ocean temperature

Fig.19. Artic ocean salinity

Fig.20. Pacific ocean temperature

Fig.21. Pacific ocean salinity

Fig.22. Indian ocean temperature

Fig.23.Indian ocean salinity

Fig.24. Southern ocean temperature

Fig.25. Southern ocean salinity

Fig.26. The four diffusivities $K_{m,h,s,\rho}$ (cm^2s^{-1}) for the Papa station

Fig.27 The four diffusivities $K_{m,h,s,\rho}$ (cm^2s^{-1}) for the Artic ocean

Fig.28 The four diffusivities $K_{m,h,s,\rho}$ (cm^2s^{-1}) for the Canary Islands.

Fig.29 Same as in Fig.26 but for the first 1km

Fig.30. Same as in Fig.27 for the first 1km

Fig.31 Same as in Fig.28 for the first 1km. Ledwell et al. (1993) value of 0.11 ± 0.02 cm^2s^{-1} (see, however, the discussion in the main text)

Fig.32. Same as in Fig.26 for the first 40m

Fig.28 Same as in Fig.22 for the first 40m

Fig.29 Same as in Fig.23 for the first 60m.

Fig.30 Polar heat transport vs. latitude for three different models.

References

Anderson, D.K.T. and and J. Willebrandt, 1992: Recent advances in modelling the ocean circulation and its effects on climate, *Rep. Prog. Phys.*, **55**, 1–37

Baum, E. and E.A. Caponi, 1992: Modeling the effects of buoyancy on the evolution of geophysical boundary layer. *J.Geophys. Res.*, **97**, 15513–15527

Blanke, B. and P. Delecluse, 1993: Variability of the tropical atlantic ocean simulated by the general circulation model with two different mixed layer physics, *J. Phys. Oceanogr.*. **23**, 1363–1388

Bryan, F.O., 1987: Parameter sensitivity of primitive equation ocean ciculation models. *J.Phys. Oceanogr.*, **17**, 970–985

Bryan, K. 1991: Poleward heat transposrt in the ocean. A review of a hierarachy of models of increasing resolution, *Tellus*, **43AB**, 104–115

Burchard, H. and H. Baumert, 1995: On the performance of a mixed layer model based on the K–ϵ turbulence closure. *J.Geophys. Res.*, **100**, 8523–8540

Canuto, V.M., F. Minotti, C. Ronchi, M. Ypma, and O. Zeman, 1994: Second–order closure PBL model with new third–order moments: comparison with LES data. *J. Atmos. Sci.*, **51**, 1605–1618

Canuto, V.M. and M.S. Dubovikov, 1996a: A dynamical model for turbulence: I. General formalism. *Phys. Fluids*, **8**, 571–586

Canuto, V.M. and M.S. Dubovikov, 1996b: A dynamical model for turbulence: II Shear driven flows, *Phys. Fluids*, **8**, 587–598

Canuto, V.M, M.S. Dubovikov, Y. Cheng and A. Dienstfrey, 1996c: A dynamical model for turbulence: III, Numerical results, *Phys. Fluids*, **8**, 599–613,

Canuto, V.M., M.S. Dubovikov and A. Dienstfrey, 1997a: A dynamical model for turbulence: IV. Buoyancy–driven flows". *Phys. Fluids*, **9**, 2118–2131,

Canuto, V.M. and M.S. Dubovikov, 1997b: A dynamical model for turbulence. V The effect

of rotation", *Phys. Fluids*, **9**, 2132–2140,

Canuto, V.M., M.S. Dubovikov and D.J. Wielaard, 1997c: A dynamical model for turbulence. VI. Two–dimensional turbulence. *Phys. Fluids*, **9**, 2141–2147,

Canuto, V.M. and M.S. Dubovikov, 1999A: A dynamical model for turbulence VII. The five invariants for shear driven flows". *Phys. Fluids*, **11**, 659–664

Canuto, V.M., M.S. Dubovikov and G.Yu, 1999b: A dynamical model for turbulence VIII. IR and UV Reynolds stress spectra for shear driven flows. *Phys. Fluids*, **11**, 656–677

Canuto, V.M., M.S. Dubovikov and G.Yu, 1999c: A dynamical model for turbulence IX. The Reynolds stresses for shear driven flows. *Phys. Fluids*, **11**, 678–694

Chen, A.J. Busalacchi and L.M. Rothstein, 1994: The roles of vertical mixing, solar radiation and wind stresses in model simulation of the sea surface temperature seasonal cycle in the tropical pacific ocean. *J. Phys. Oceanogr.* **99**, 20345–20359

Cheng, Y. and V.M. Canuto, 1994: Stably stratified turbulence: a new model for the energy dissipation length scale, *J. Atmos. Sci.*, **51**, 2384–2396

Chou, P.Y, 1940: On an extension of Reynolds method of finding apparent stresses and the nature of turbulence, *Chinese J. Phys.*, **4**(1), 1–33

Chou, P.Y., 1945: On velocity correlations and the solutions of the equations of the turbulent fluctautions, *Quart. Applied Math.*, **3**(1), 38–54

Colin de Verdiere, A., 1988: Buoyancy driven planetary flows, *J. Mar. Res.* **46**, 215–265

Cummings, P.F., G. Holloway and A.E. Gargett, 1990: Sensitivity of the GFDL ocean circulation model to a parameterization of vertical diffusion, *J. Phys. Oceanogr.*, **20**, 817–830

D'Alessio, S.J.D., K. Abdella and N.A. McFarlane, 1998: A new second–order turbulence scheme for modeling the ocean mixed layer, *J.Phys. Oceanogr.*, **28**, 1624–1641

Galperin, B., A. Rosati, L.H.Kantha and G.L. Mellor, 1989: Modeling rotating stratified turbulent flows with application to ocean mixed layers, *J. of Phys. Ocean.* **19**, 901–916.

Gargett, A. E. 1984: Vertical eddy diffusivity in the ocean interior, *J. Mar. Res.*, **42**,

359–393

Gargett, A. E. 1989: Ocean turbulence, *Ann. Rev. Fluid Mech.*, **21**, 419–451

Gargett, A.E., 1993: Parameterizing the effects of small–scale mixing in large–scale numerical models, in *Modeling Oceanic Climate Interactions,* Eds. J. Willebrand and D.L.T. Anderson, NATO ASI Series, Vol I11, 185–204, Springer–Verlag, New York

Gargett, A.E. and G. Holloway, 1984: Dissipation and diffusion by internal wave breaking, *J. Mar. Res.*, **42,** 15–27

Gargett, A. E., P.F. Cummins and G. Holloway, 1989: Effects of variable vertical diffusivity in the GFDL model, in *Parameterization of Small Scale Processes,* Proc. Hawaiian Winter Workshop, Univ. of Hawaii, Jan 17–20, 11–20

Gaspar, P., Gregoris, Y. and Lefevre, J.M., 1990: A simple eddy kinetic energy model for simulations of the oceanic vertical mixing: test at station Papua and long–term upper ocean study site, *J. Geophys. Res.*, **95,** 16179–16193

Holland, W.R., 1989: Experience with various parameterizations of sub–grid scale dissipation and diffusion in numerical models of ocean circulation, in *Parameterization of Small Scale Processes,* Proc. Hawaiian Winter Workshop, Univ. of Hawaii, Jan 17–20, 1–11

Itsweire, E. C. and K.N. Helland, 1989: Spectra and energy transfer in stably stratified turbulence, *J. Fluid Mech.* **207**, 419–452

Khanta, L. and C.A. Clayson, 1994: An improved mixed layer model for geophysical applications, *J. Geophys. Res.* **99**, C12, 25235–25266

Kundu, P.K. and R.C. Beardsley, 1991: Evidence of a critical Richardson number in moored measurements during the upwelling season off northen California, *J.Geophys. Res.*, **96,** 4855–4868

Large, W.G., McWilliams, J.C. and Doney, S.C., 1994: Oceanic vertical mixing: a review and a model with non–local boundary layer parameterization, *Rev. of Geophys.*, **32**, 4, 363–403

Large, W.G., G. Danabasoglu, S.C. Doney and J.C. McWilliams, 1997: Sensitivity to surface forcing and boundary layer mixing in a global ocean model: annual mean climatology, *J. Phys. Ocean.*, **47**, 2418–2447

Launder, B. E., G. J. Reece and W. Rodi, 1975: Progress in the development of a Reynolds stress turbulent closure, *J. Fluid Mech.* **68**, 537–566

Ledwell, J.R., A.J. Watson and C. Law, 1993: Evidence for slow mixing across pycoline from open–ocean tracer experiment, *Nature*, **364**, 701–703

Ma, C.C., C.R. Mechoso, A. Arakawa and J.D. Ferrara, 1994: Sensitivity of a coupled ocean–atmosphere model to physical parameterizations, *J. Phys. Oceanogr.*, **7**, 1883–1896

Martin, P. J., 1985, Simulation of the Mixed Layer at OWS November and Papa with several models, *J. Geophys. Res.*., Vol. 90, C1, 903–916

Matear, R.J. and C.S. Wong, 1997: Estimation of vertical mixing in the upper ocean at Station P from chlorofluorocarbons, *J. Marine Res.*, **55**, 507–521

McPhee. M.G., and D.G. Martison, 1994: Turbulent mixing under drifting pack of ice in the Weddell Sea, *Science*, **263,** 218–221

McWilliams, J.C., 1996: Modeling the ocean general circulation. *Ann. Rev. Fluid Mech.* **28**, 215–248

Mellor, G.L, 1989: Retrospect on oceanic boundary layer modeling and second moment closure, *Parameterization of Small Scale Processes,* Proc. Hawaiian Winter Workshop, Univ. of Hawaii, Jan 17–20, 251–272

Mellor, G. L. and T.Yamada, 1982: Development of a turbulence closure model for geophysical fluid problems, *Rev. of Geophys. and Space Physics*, **20,** 85–875

Moum, J.N., 1989: Measuring turbulent fluxes in the ocean. The quest for K_ρ, in *Parameterization of Small Scale Processes,* Proc. Hawaiian Winter Workshop, Univ. of Hawaii, Jan 17–20, January 17–20, 145–156

Munk, W., 1966: Abyssal recipes, *Deep–Sea Res.*. **13**, 707–730.

Pacanowsky, R. C. and S.G.H. Philander,1981: Parameterization of vertical mixing numerical models of tropical oceans, *J. Phys. Ocean.*, **11**, 1443–1451.

Polzin, K,L., J.M. Toole, J.R. Ledwell and R.W. Schmitt, 1997: Spatial variability of turbulent mixing in abyssal ocean, *Science*, **276**, 93–96

Rosati, A. and K. Miyakoda, 1988: A general circulation model for upper ocean simulation, *J. Phys. Oceanogr.*, **18**, 1601–1626

Schumann, U. 1991: Subgrid length scales for large eddy simulation of stratified turbulence, *Theor. Comput. Fluid Dyn.* **2**, 279–290

Semtner, A. J. Jr., 1995, Modeling ocean circulation, *Science,* **269**, 1379–1385

Semtner, A. J. Jr. and R.M. Chervin, 1992, Ocean general circulation from a global eddy resolving model, *J. Geophys. Res.* **97**, **C4**, 5493–5550

Smart, 1998: Comparison of modelled and observed dependence of shear on stratification in the upper ocean, *Dyn. Atmos. and Oceans,* **12**, 127–142

Toole, J. M., K. L. Polzin and R. W. Schmitt, 1994: Estimates of diapycnal mixing in the abyssal ocean, *Science*, **264**, 1120–1123

Wang, D., W.G. Large and J.C. McWilliams, 1996: Large Eddy simualtion of equatorial boundary layer: diurnal cycle, eddy voscsity and horizotal rotation, *J. Geophys. Res.* **101**, 3649–3662

Webster, C. A. G. 1964: An experimental study of turbulence in a density stratified shear flow, *J. Fluid Mech.*, **19**, 221–245

Wyld, H.W, 1961: Formulation of the theory of turbulence in an incompressible fluid, *Ann.of Phys.*, **14**, 143–

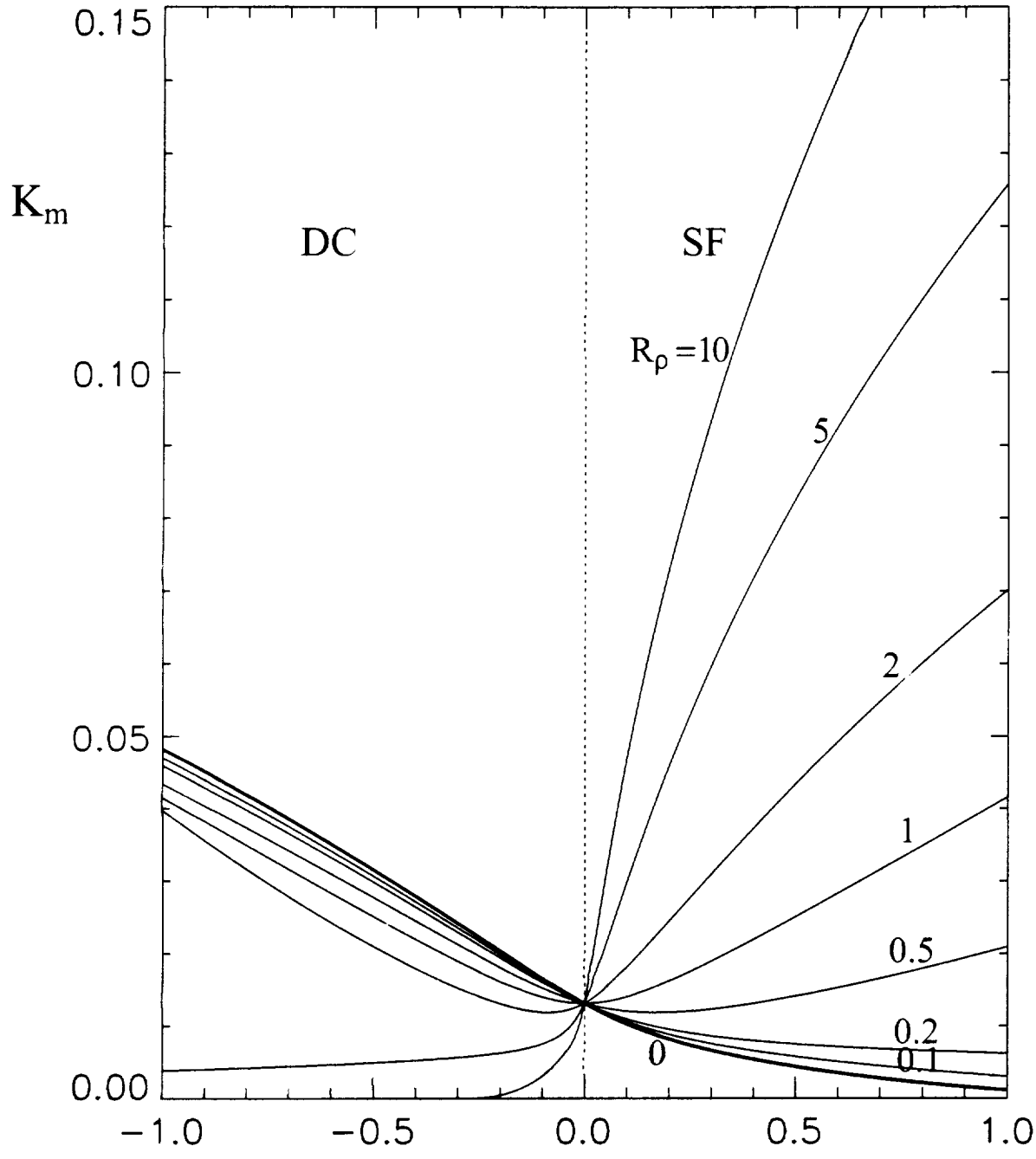

Fig.1

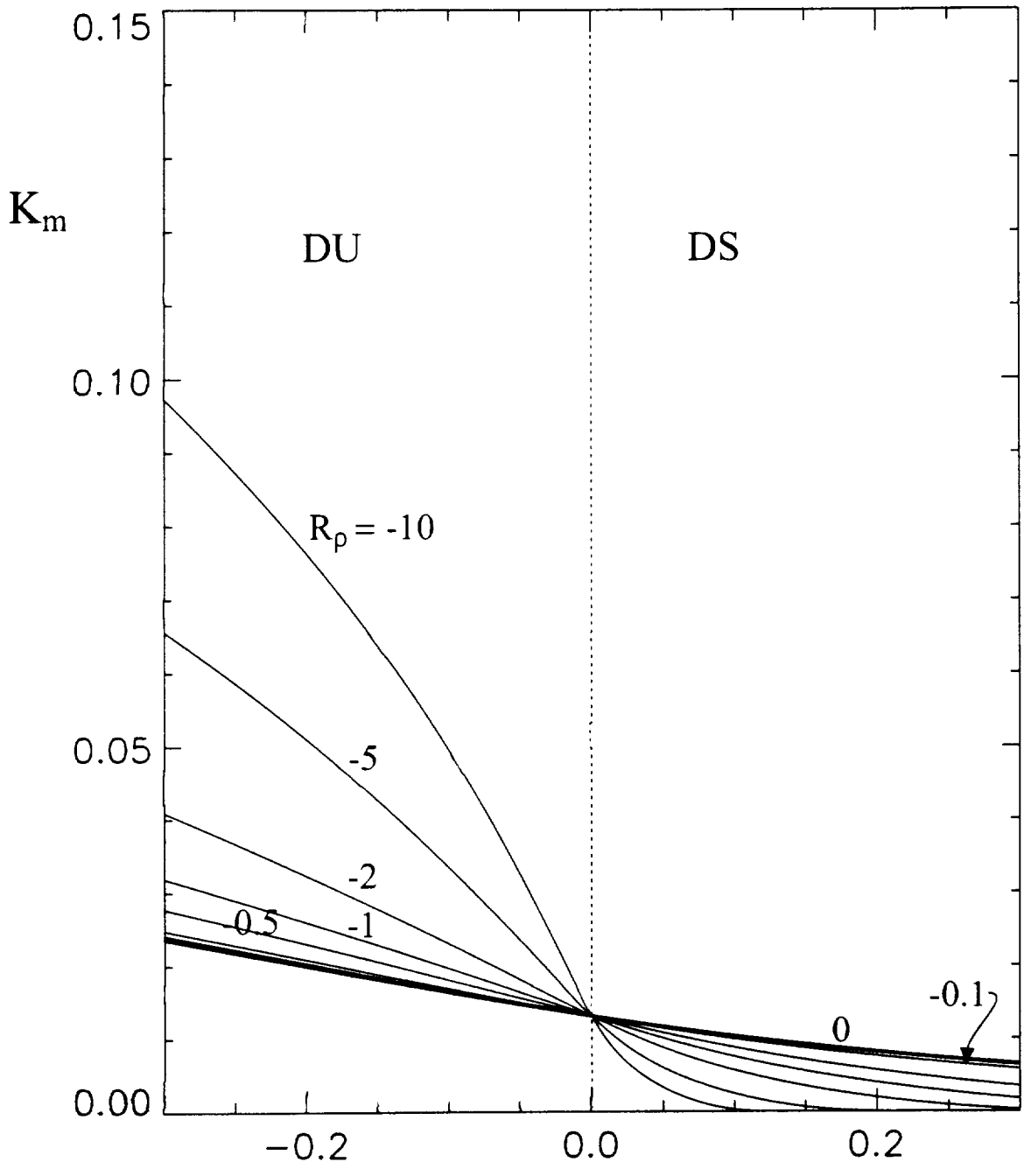

Fig.2

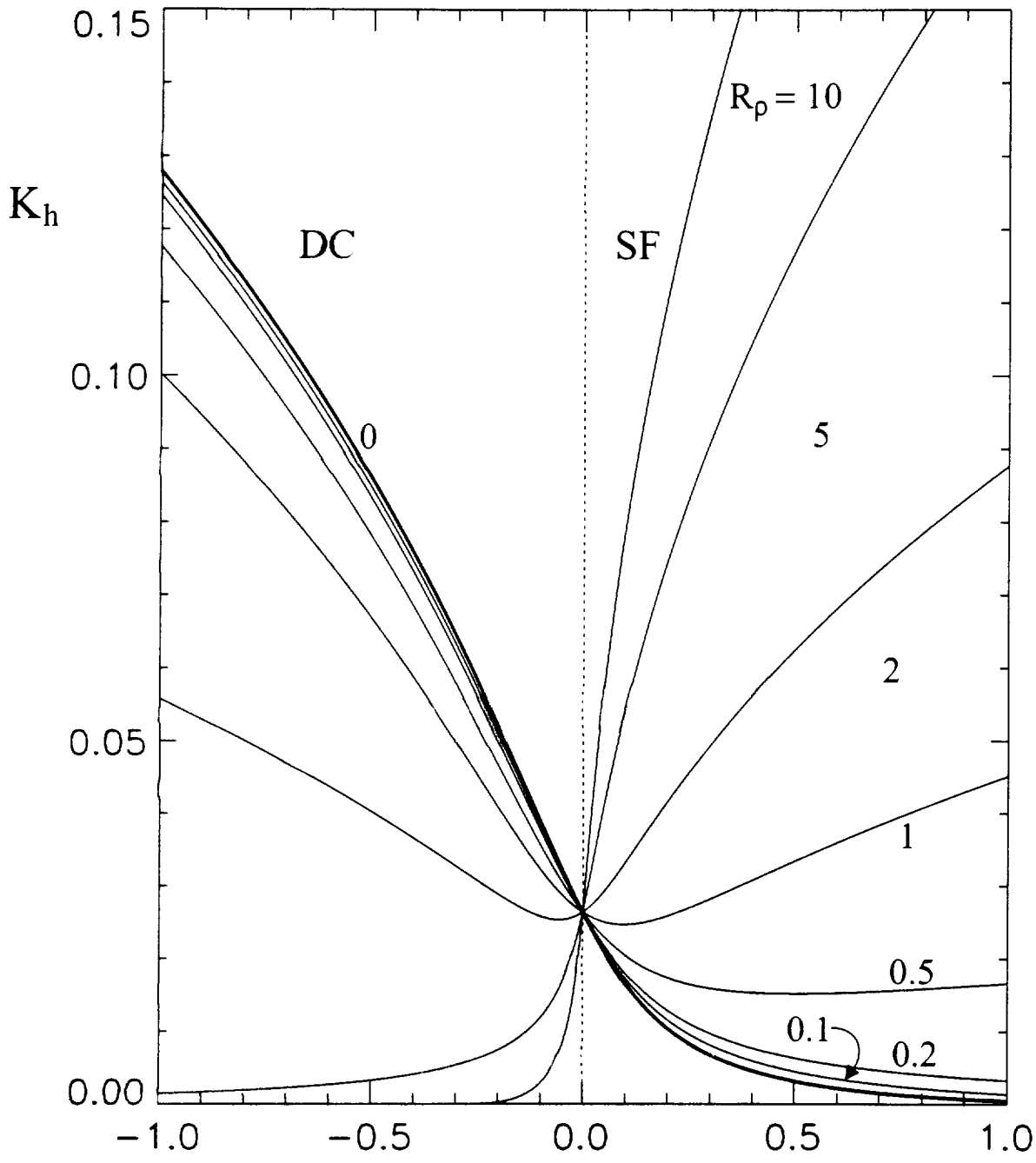

Fig.3

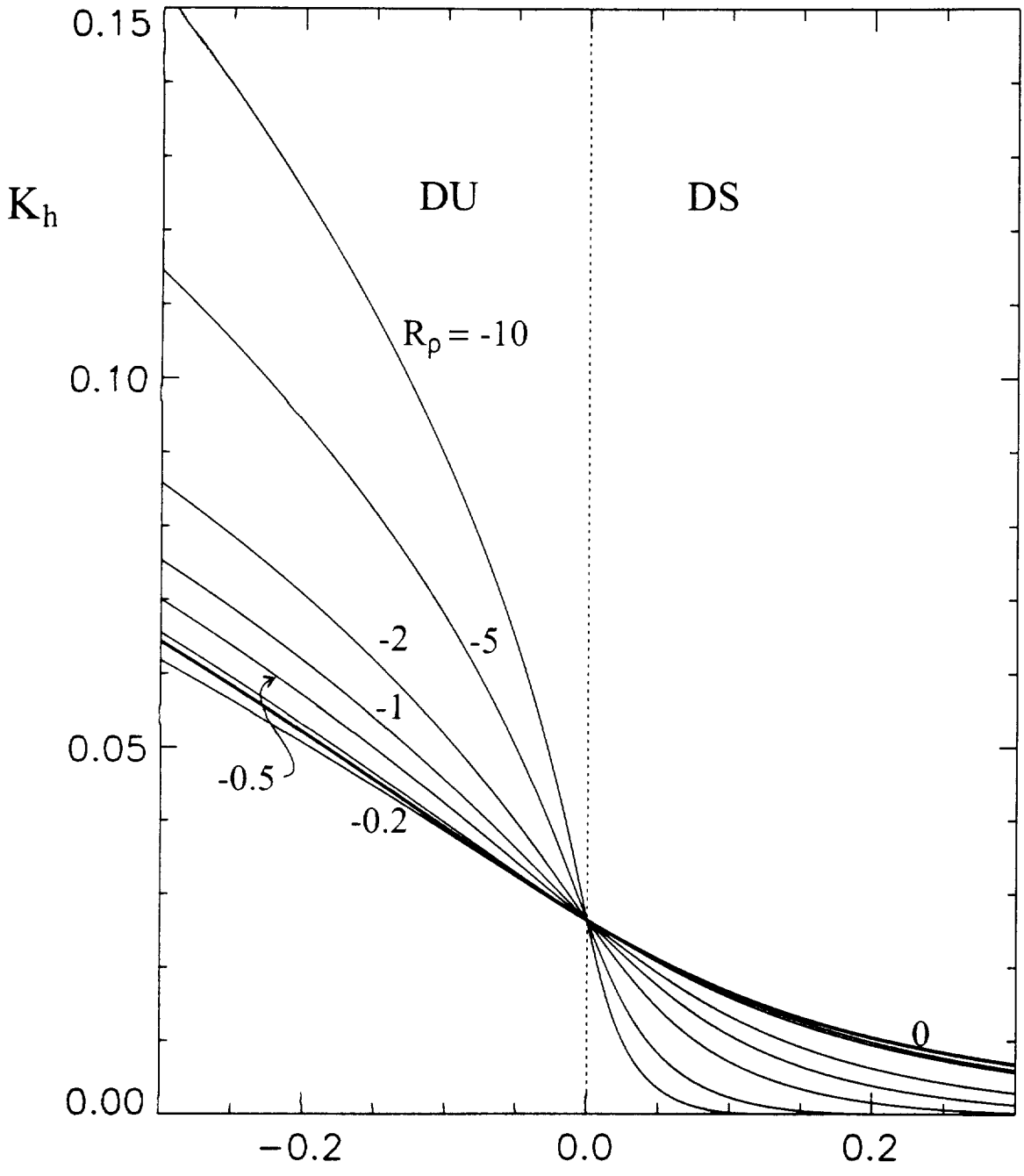

Fig.4

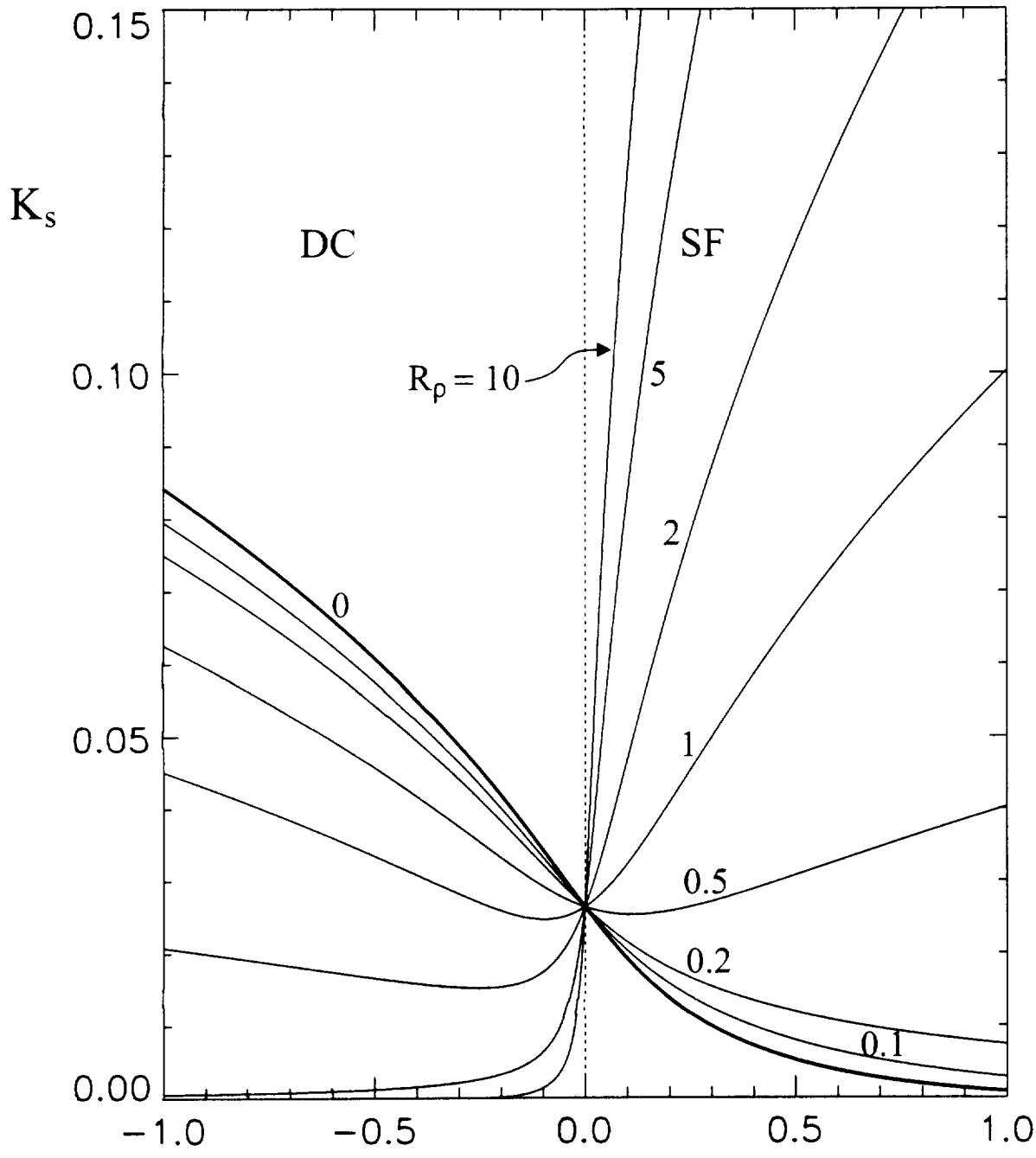

Fig.5

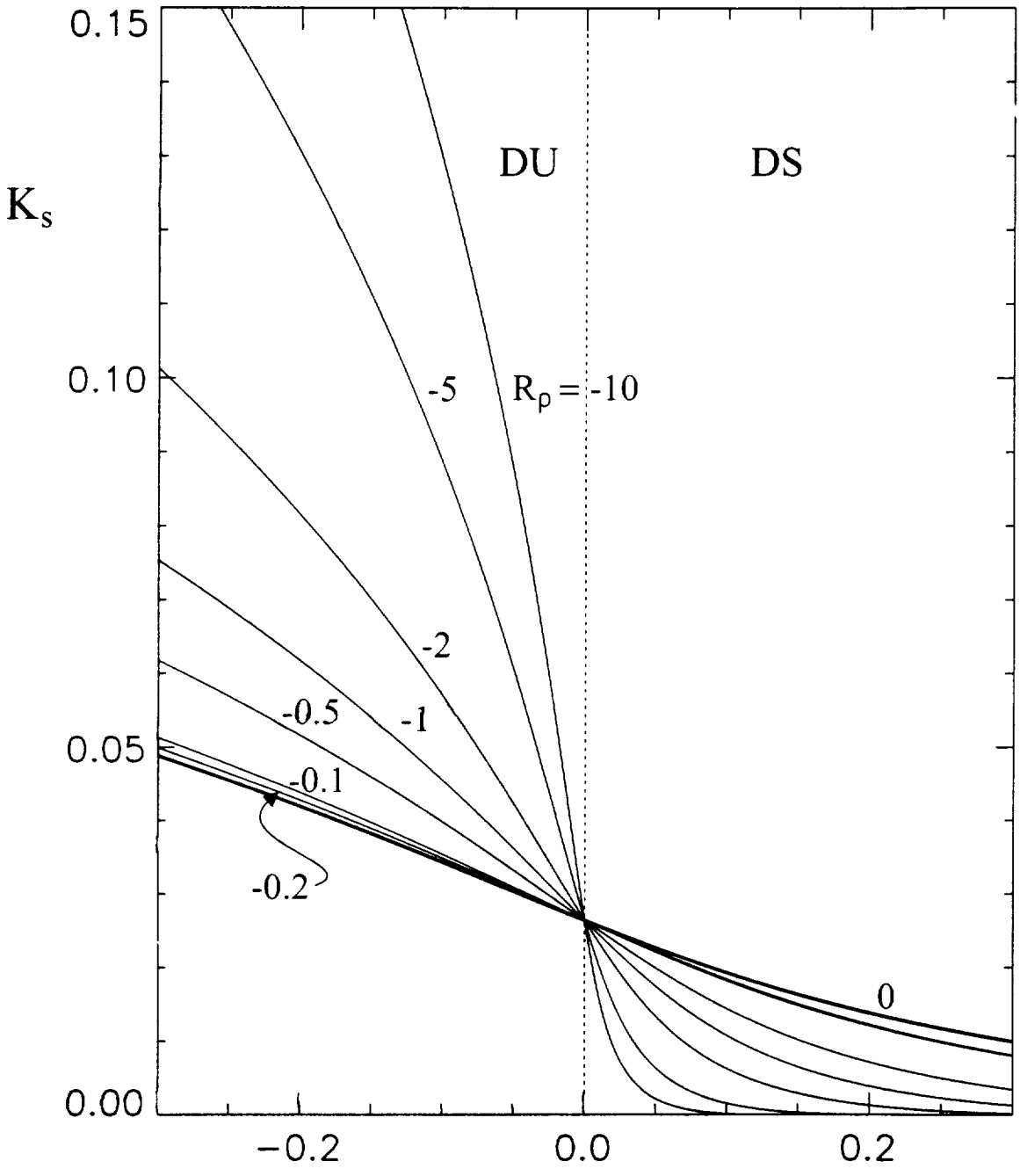

Fig.6

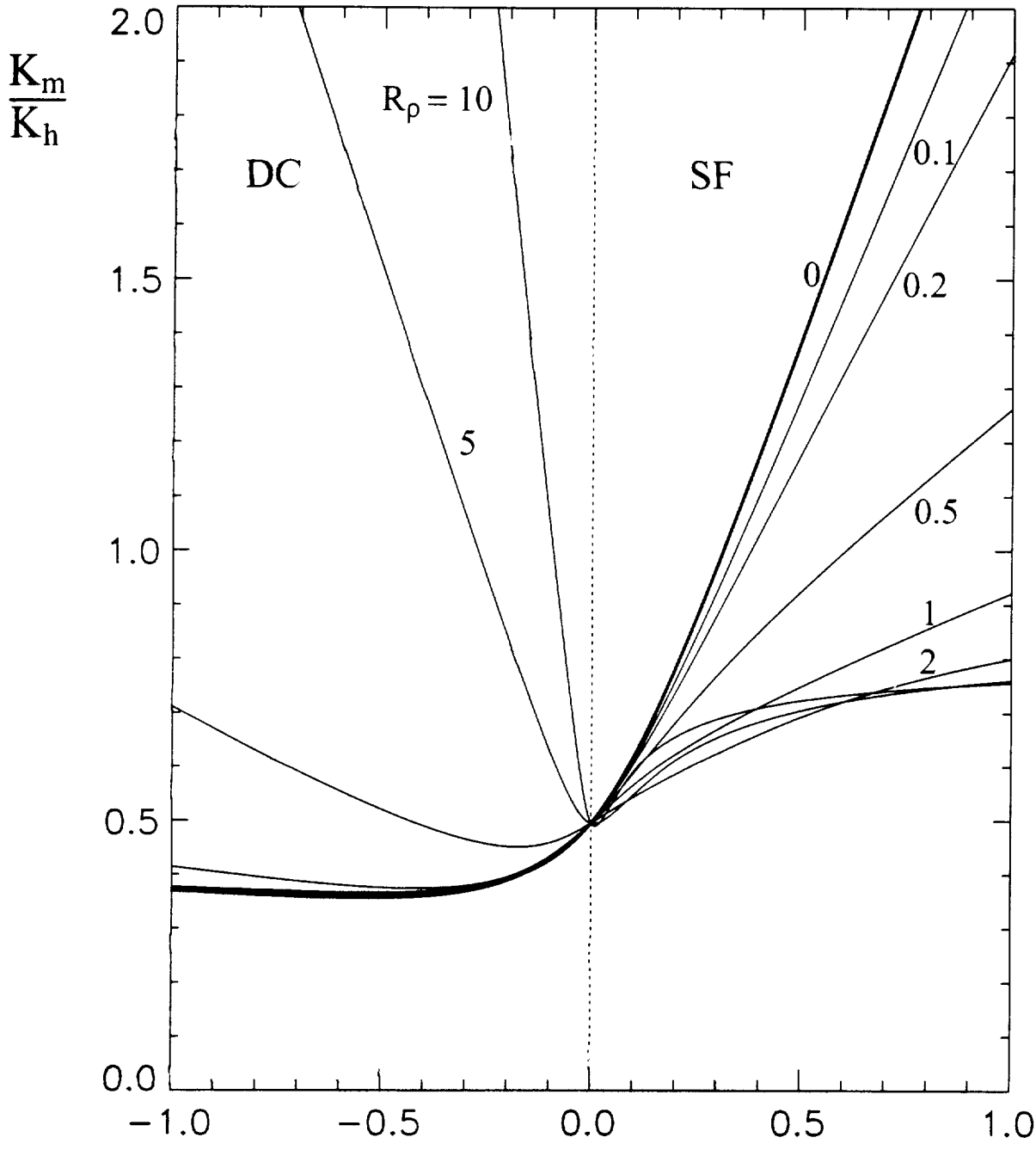
$\frac{K_m}{K_h}$
2.0
1.5
1.0
0.5
0.0
−1.0
−0.5
0.0
0.5
1.0
Ri
$R_\rho = 10$
DC
SF
5
0
0.1
0.2
0.5
1
2

Fig.7

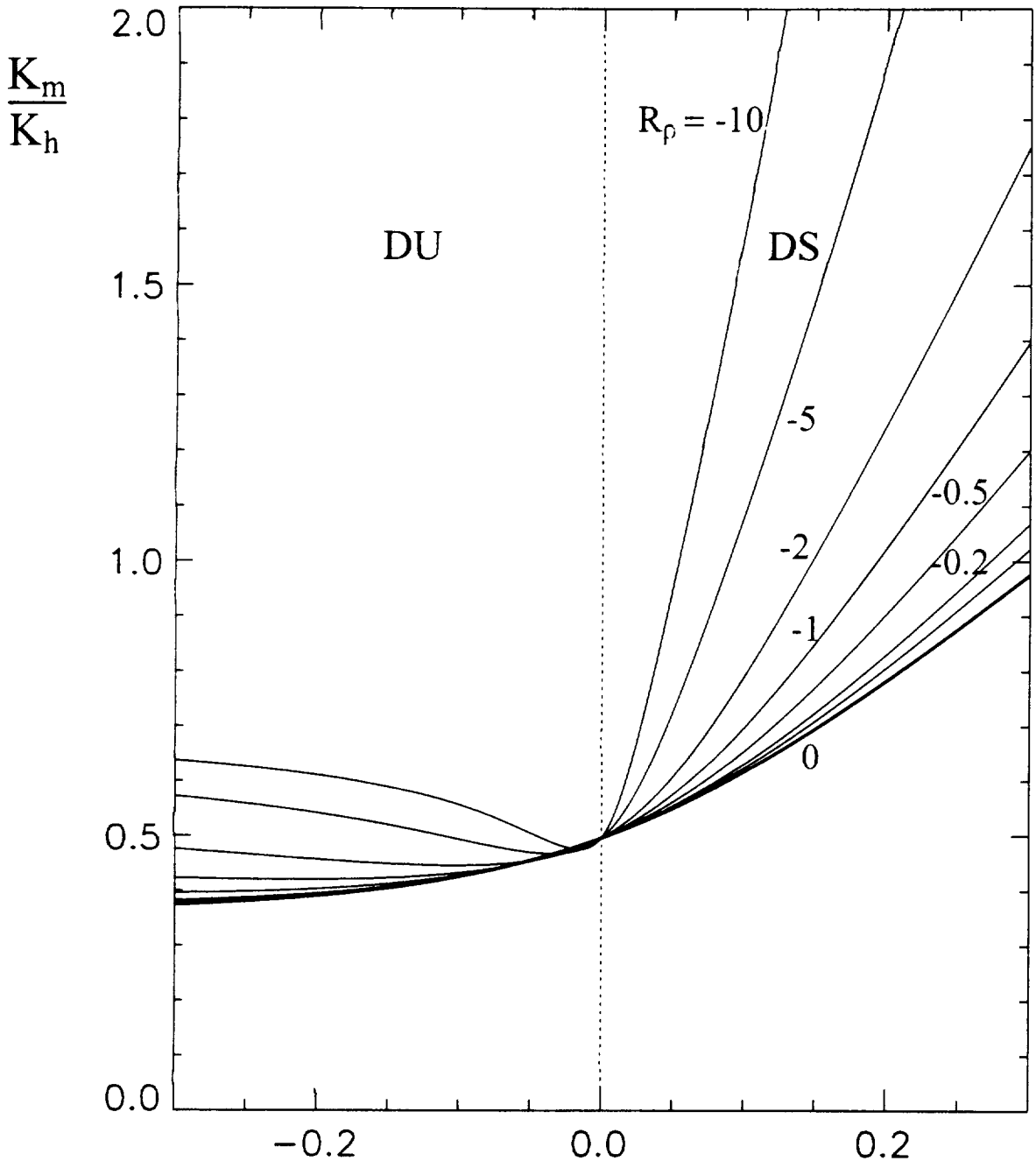

Fig.8

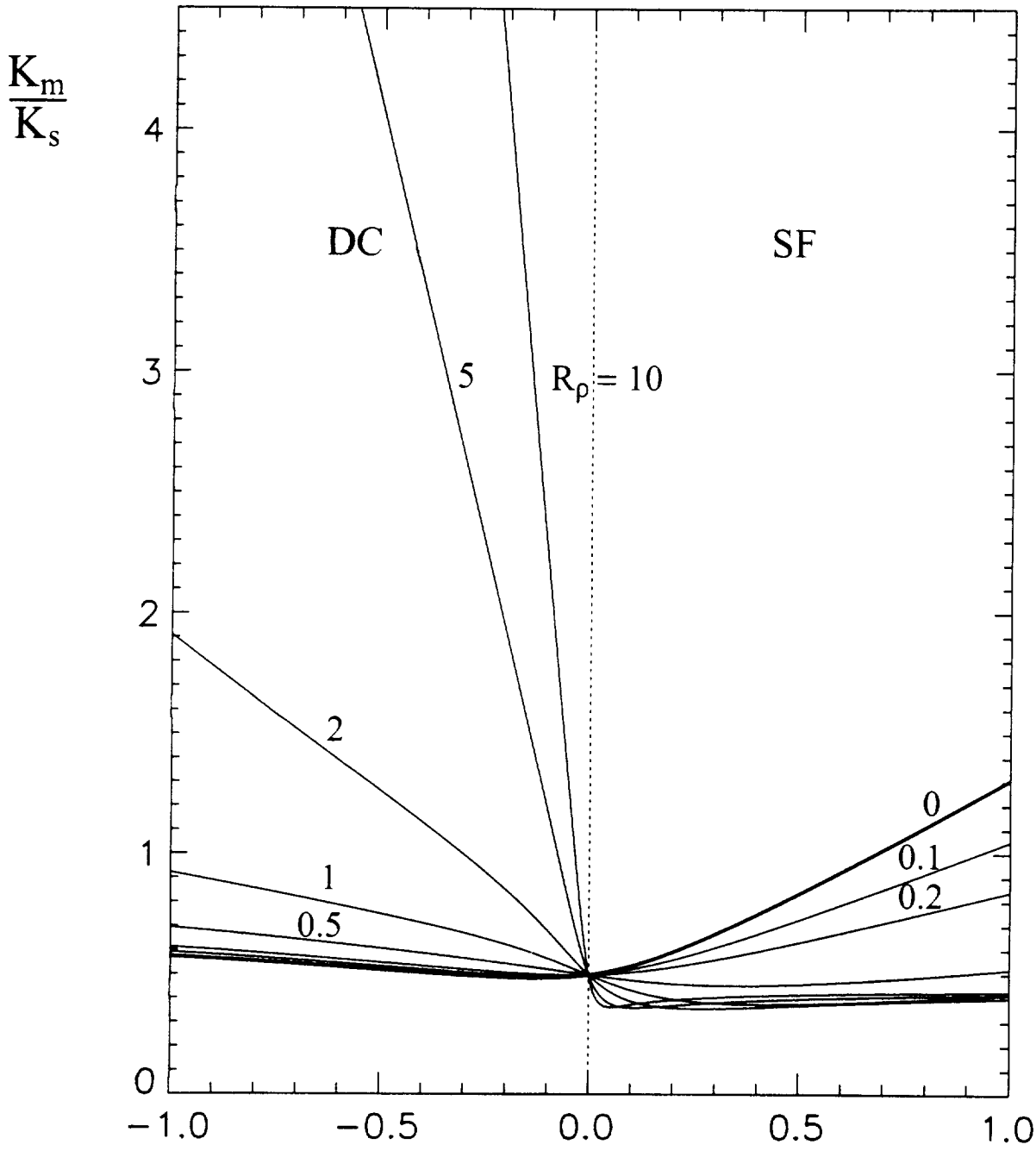

Fig.9

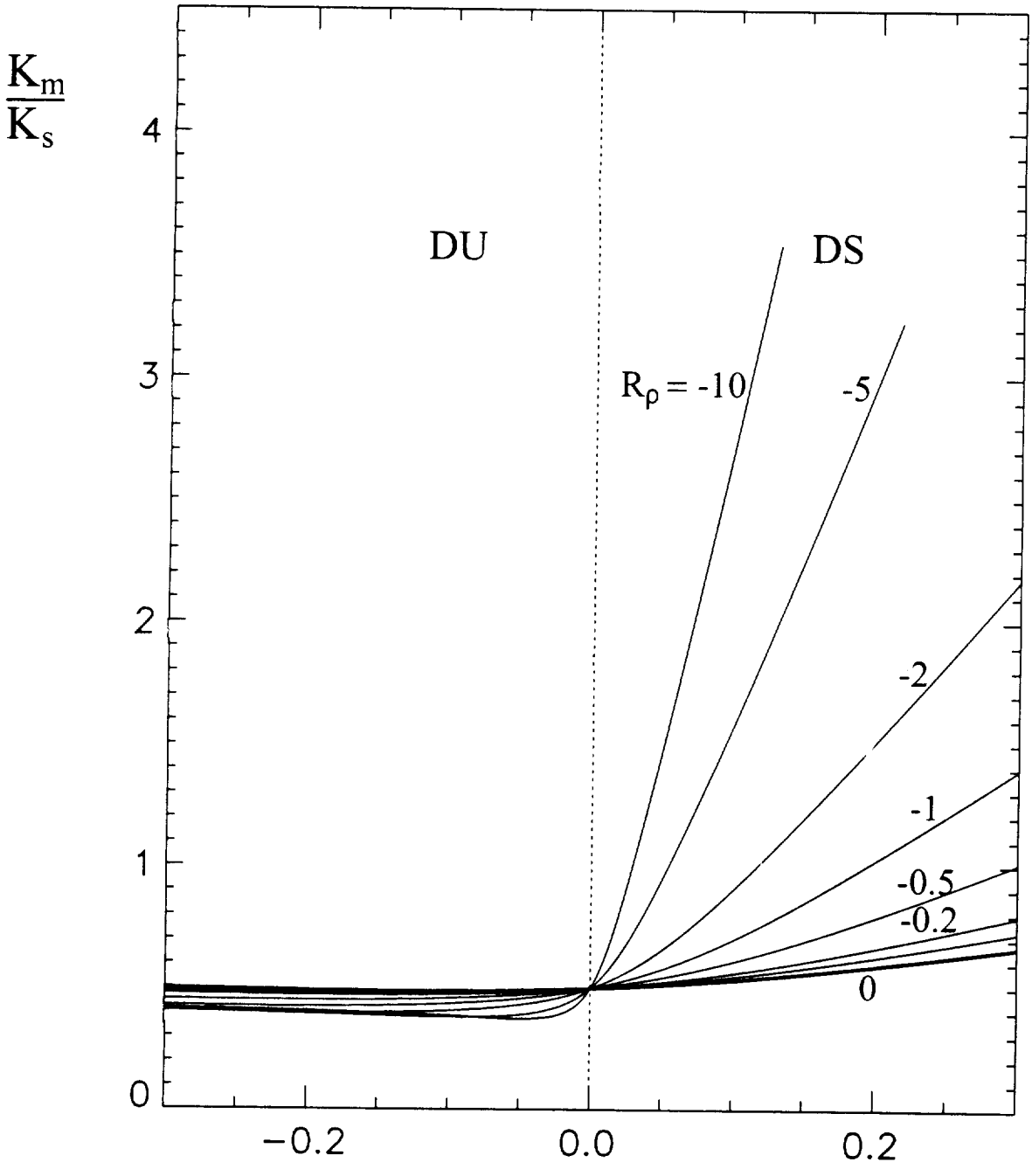

Fig.10

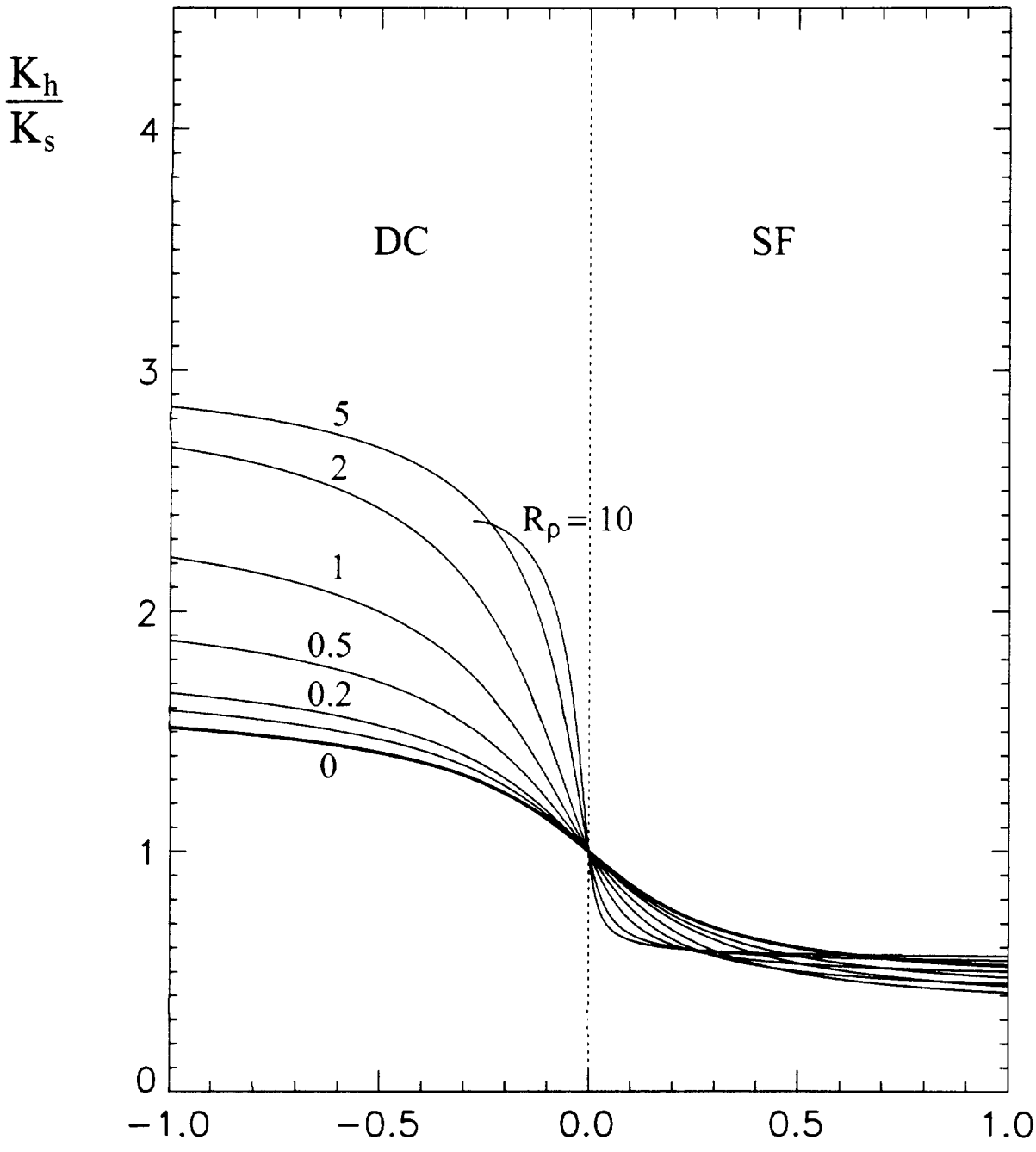

Fig.11

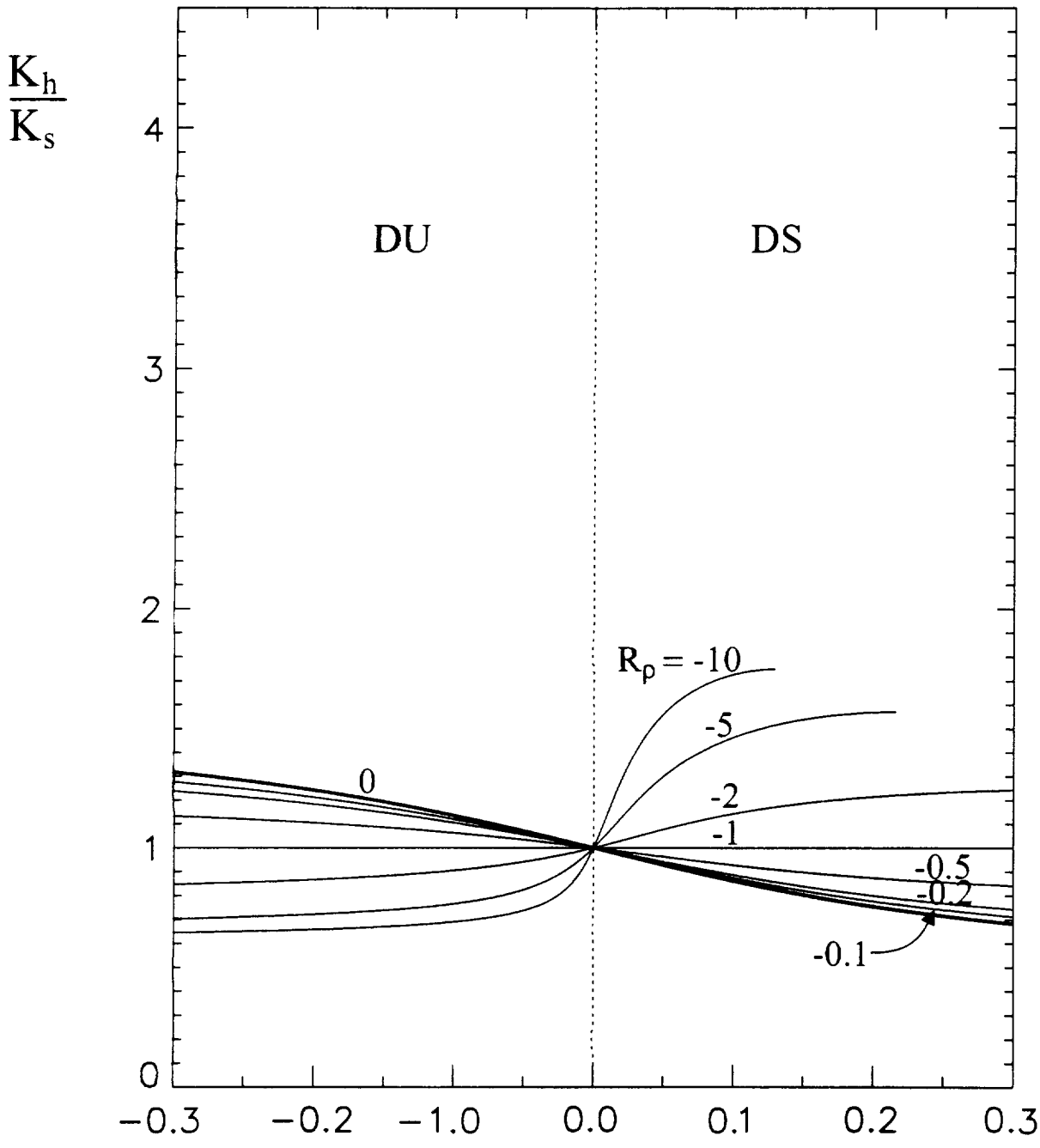

Fig.12

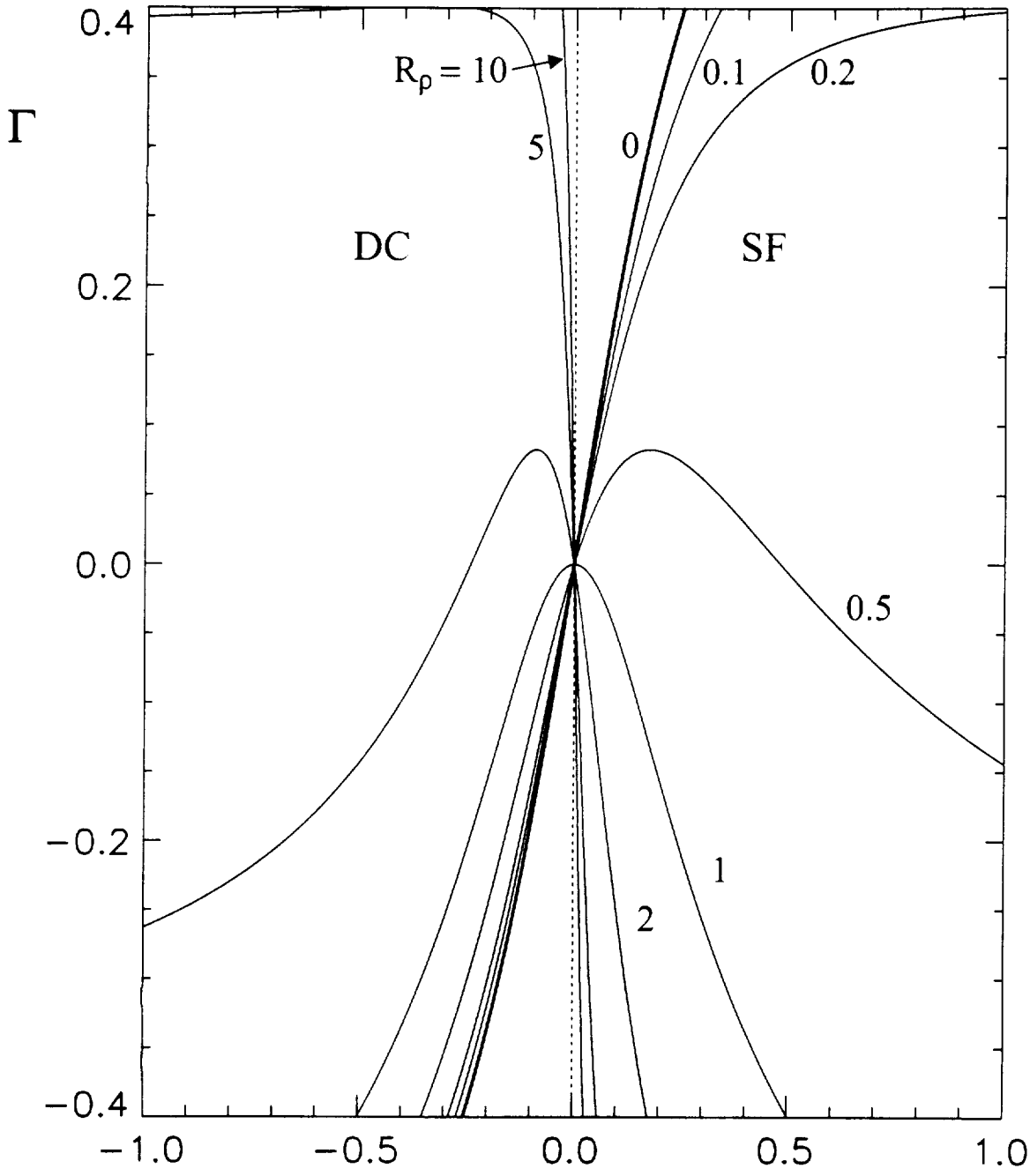

Fig.13

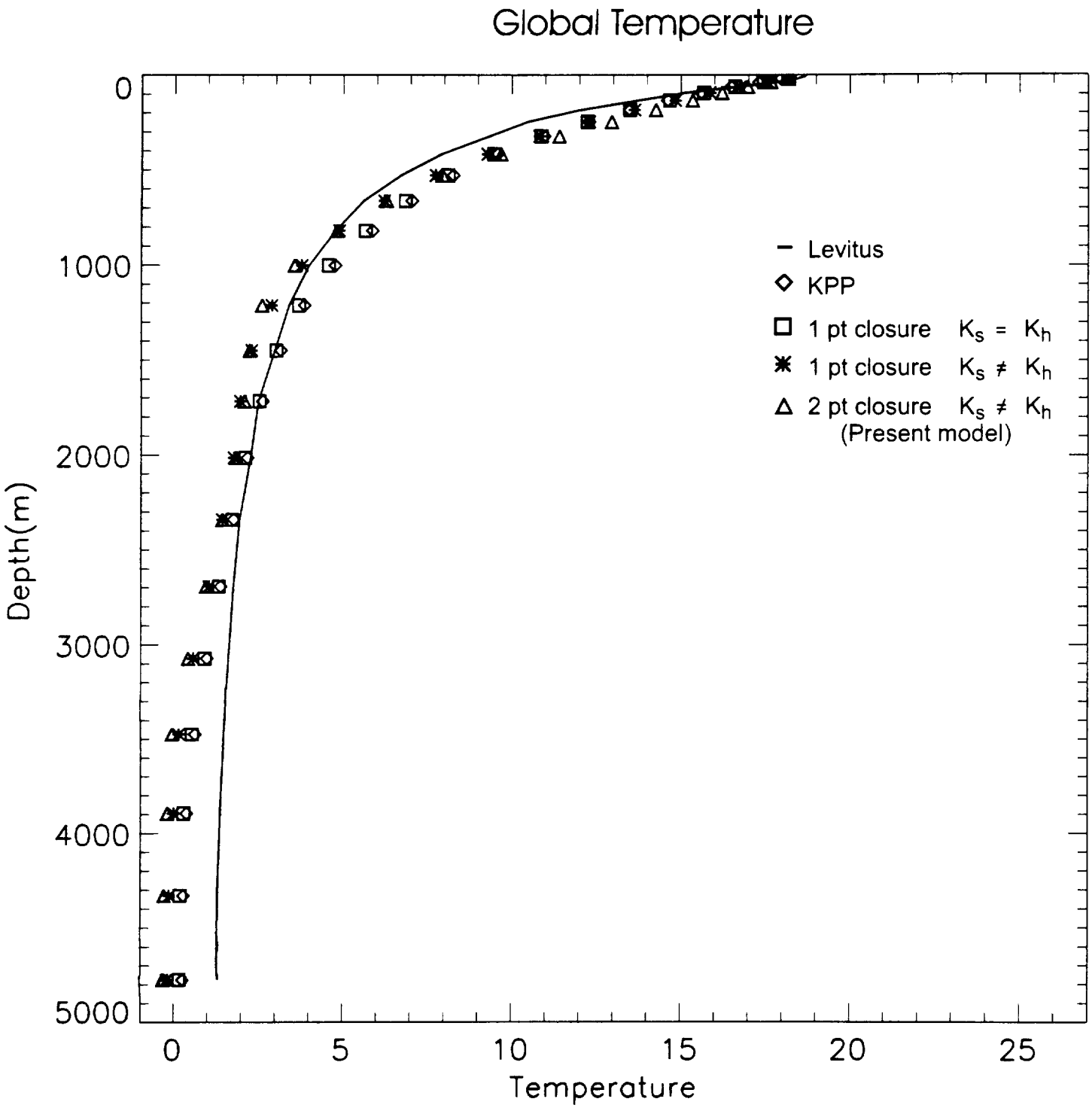
Global Temperature
0
1000
2000
3000
4000
5000
Depth(m)
0
5
10
15
20
25
Temperature
Levitus
KPP
1 pt closure $K_s = K_h$
1 pt closure $K_s \neq K_h$
2 pt closure $K_s \neq K_h$
(Present model)

Fig.14

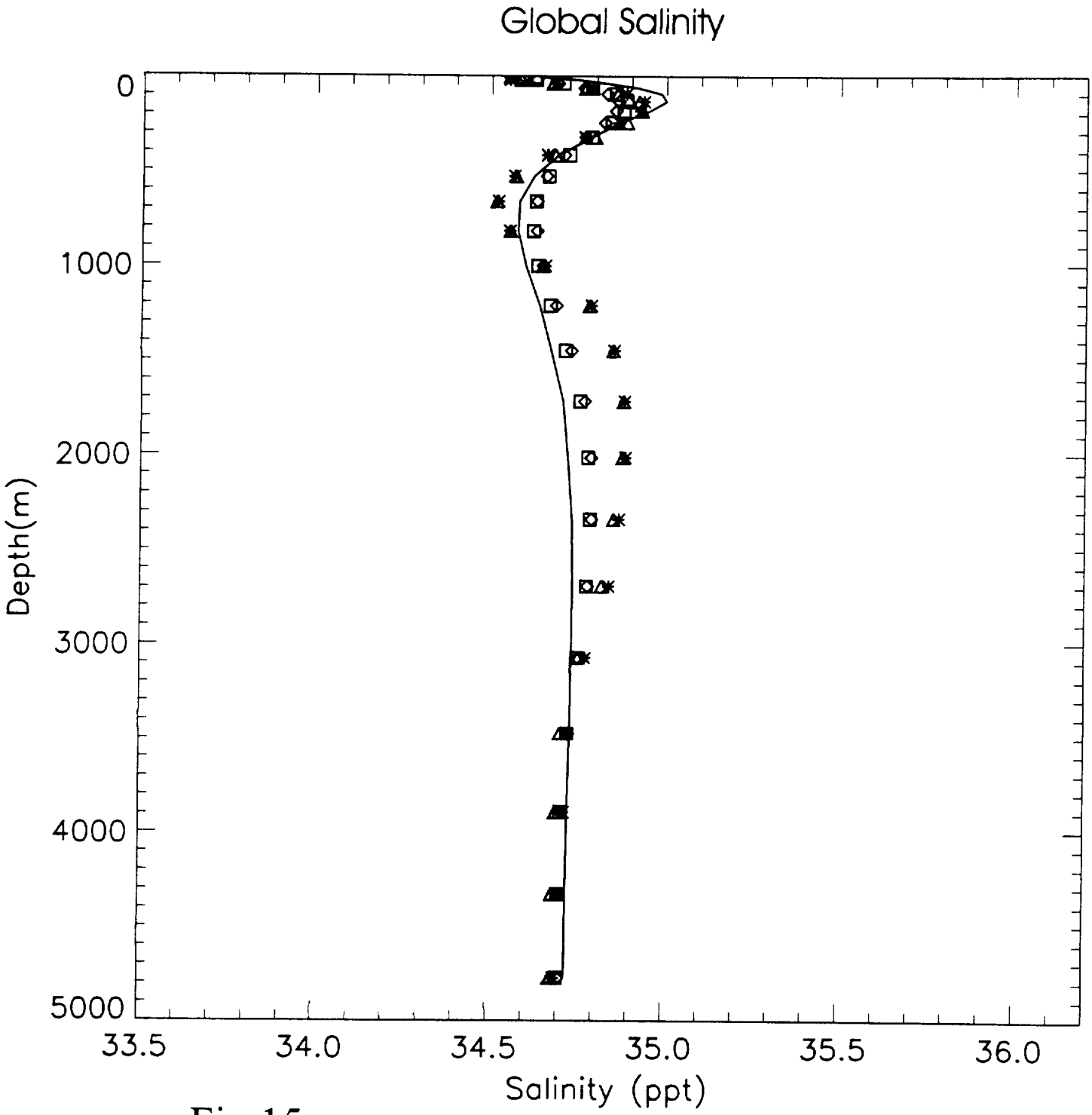
Global Salinity
0
1000
2000
3000
4000
5000
Depth(m)
33.5
34.0
34.5
35.0
35.5
36.0
Salinity (ppt)

Fig.15

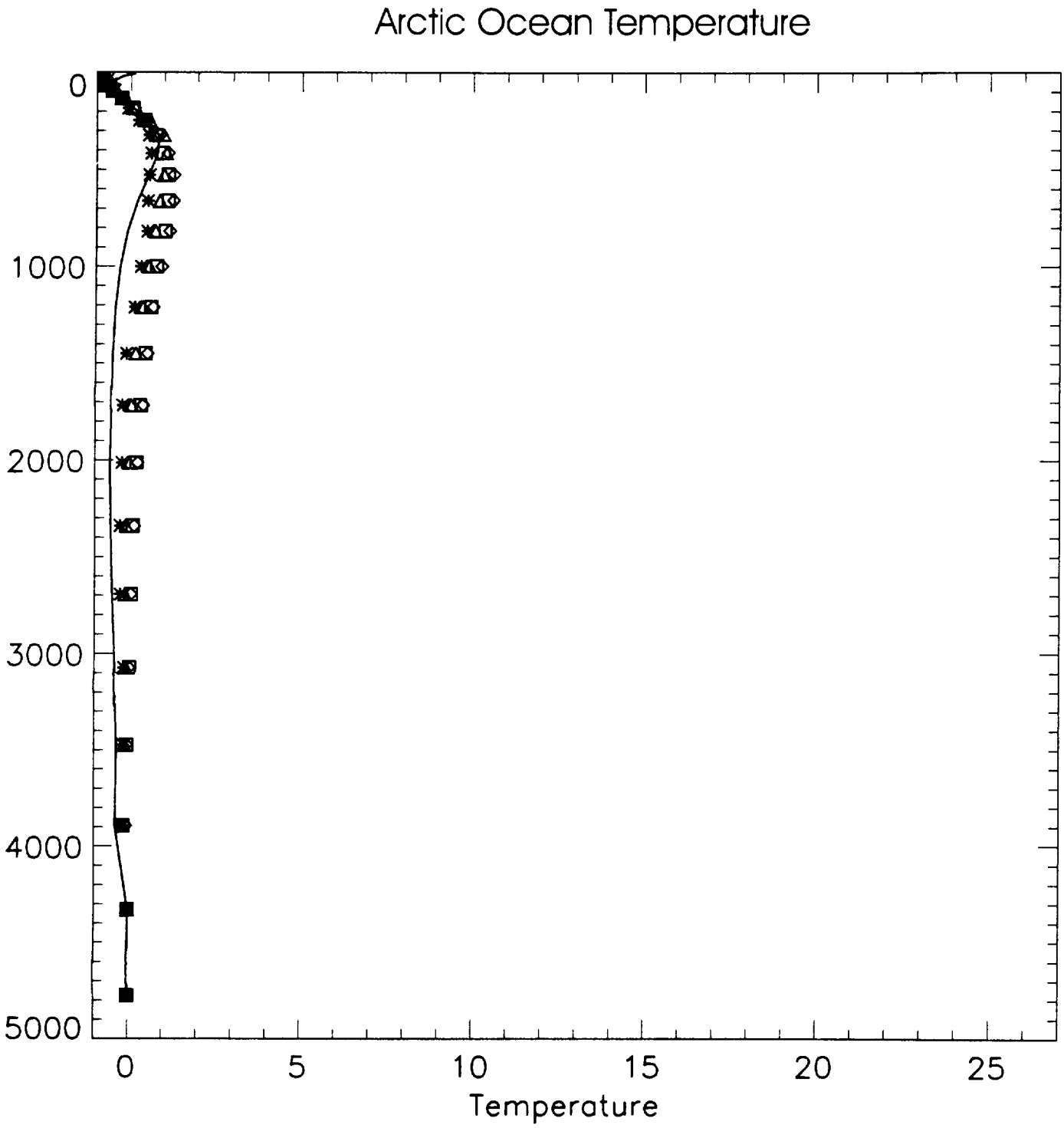
Arctic Ocean Temperature
0
1000
2000
3000
4000
5000
0
5
10
15
20
25
Temperature

Fig.16

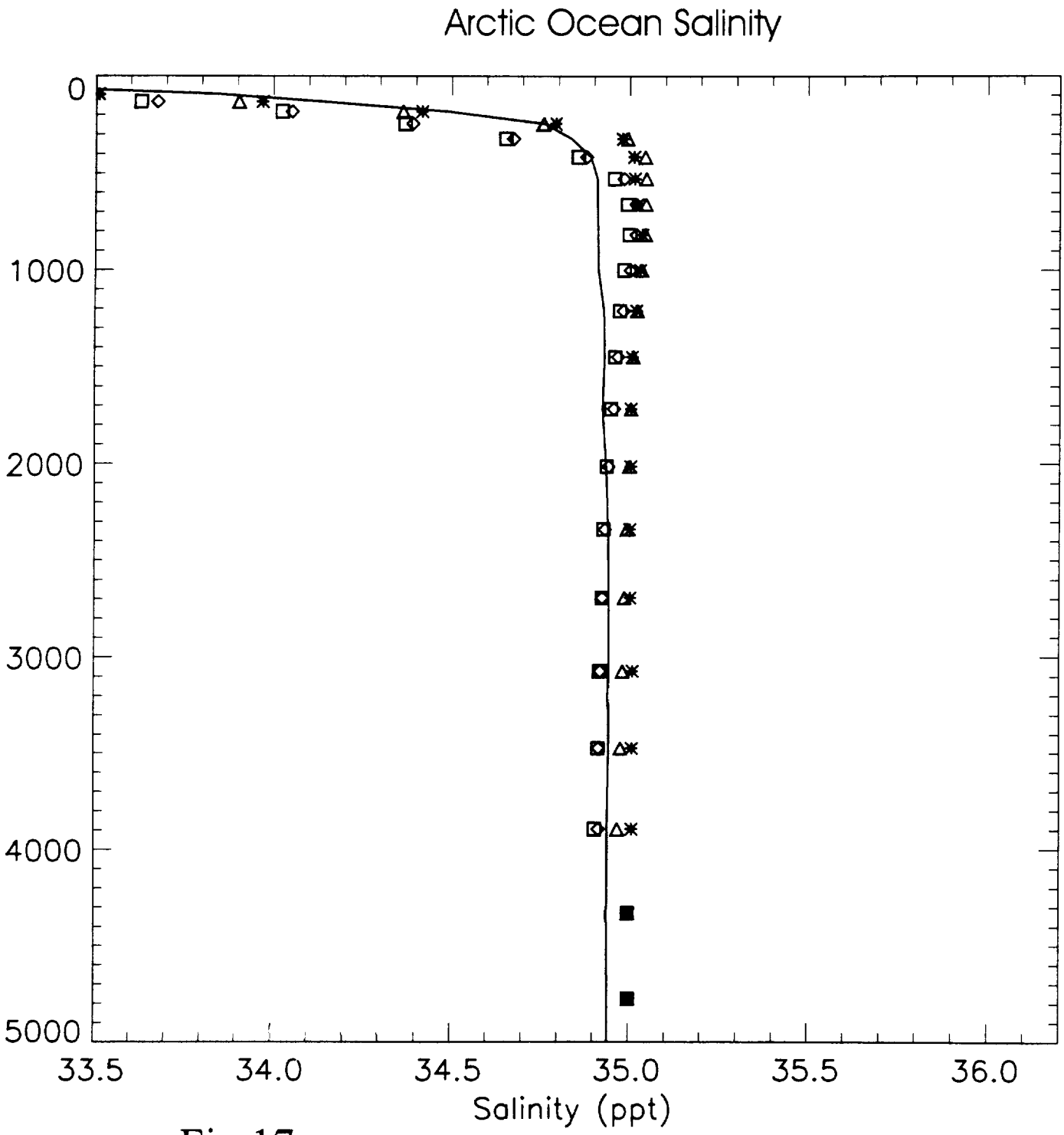
Arctic Ocean Salinity
0
1000
2000
3000
4000
5000
33.5
34.0
34.5
35.0
35.5
36.0
Salinity (ppt)

Fig.17

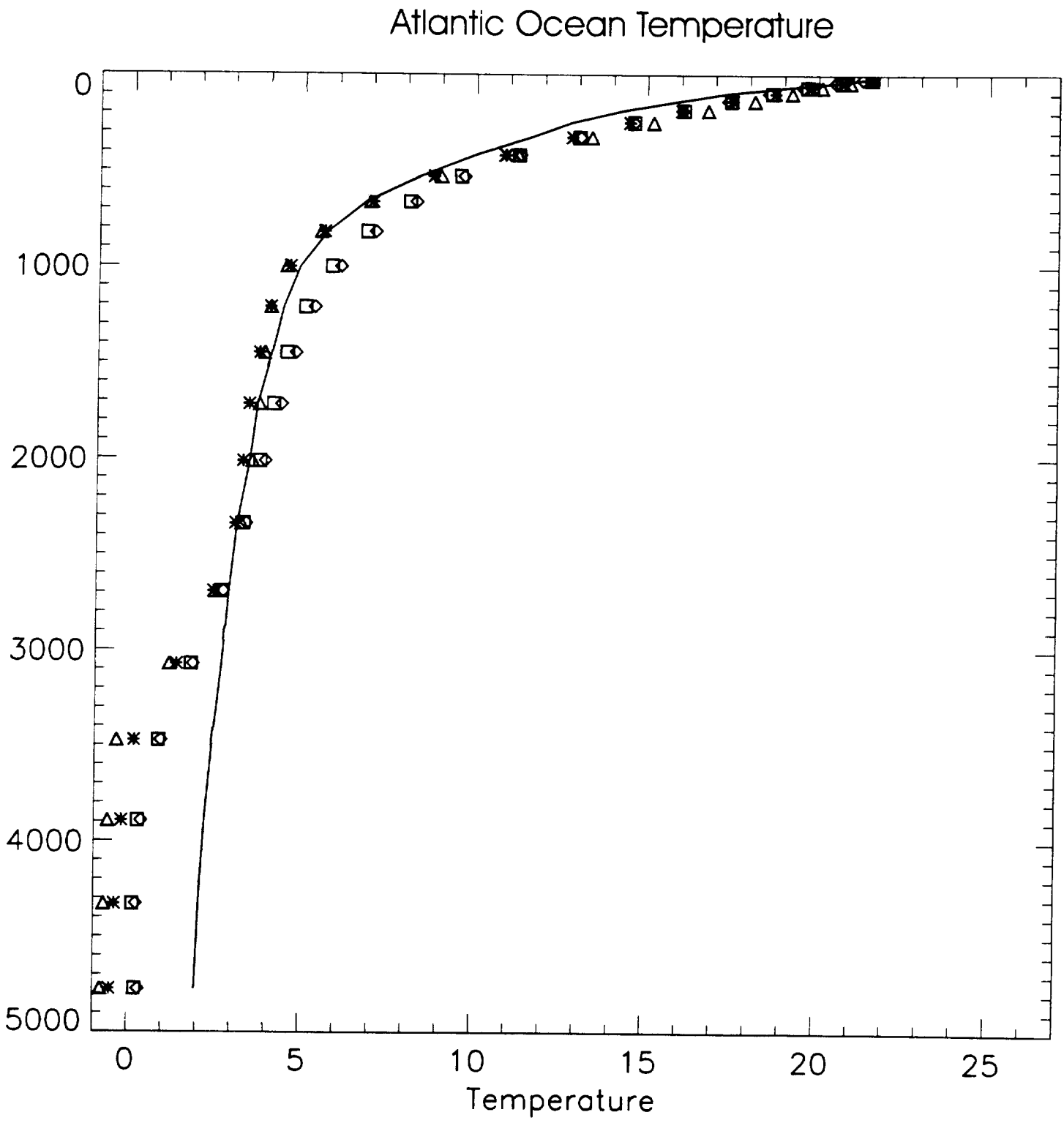
Atlantic Ocean Temperature
0
1000
2000
3000
4000
5000
0
5
10
15
20
25
Temperature

Fig.18

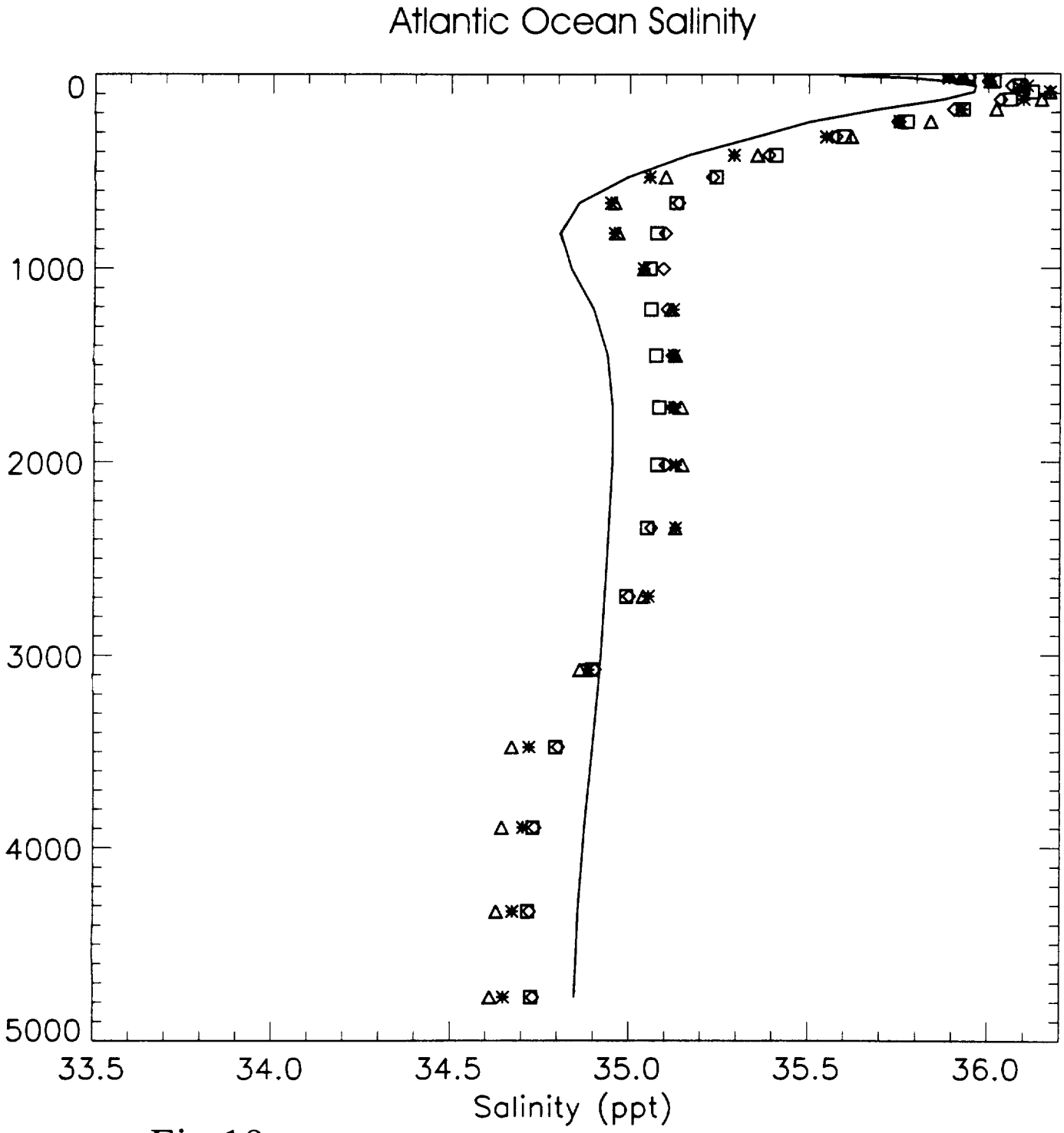
Atlantic Ocean Salinity
0
1000
2000
3000
4000
5000
33.5
34.0
34.5
35.0
35.5
36.0
Salinity (ppt)

Fig.19

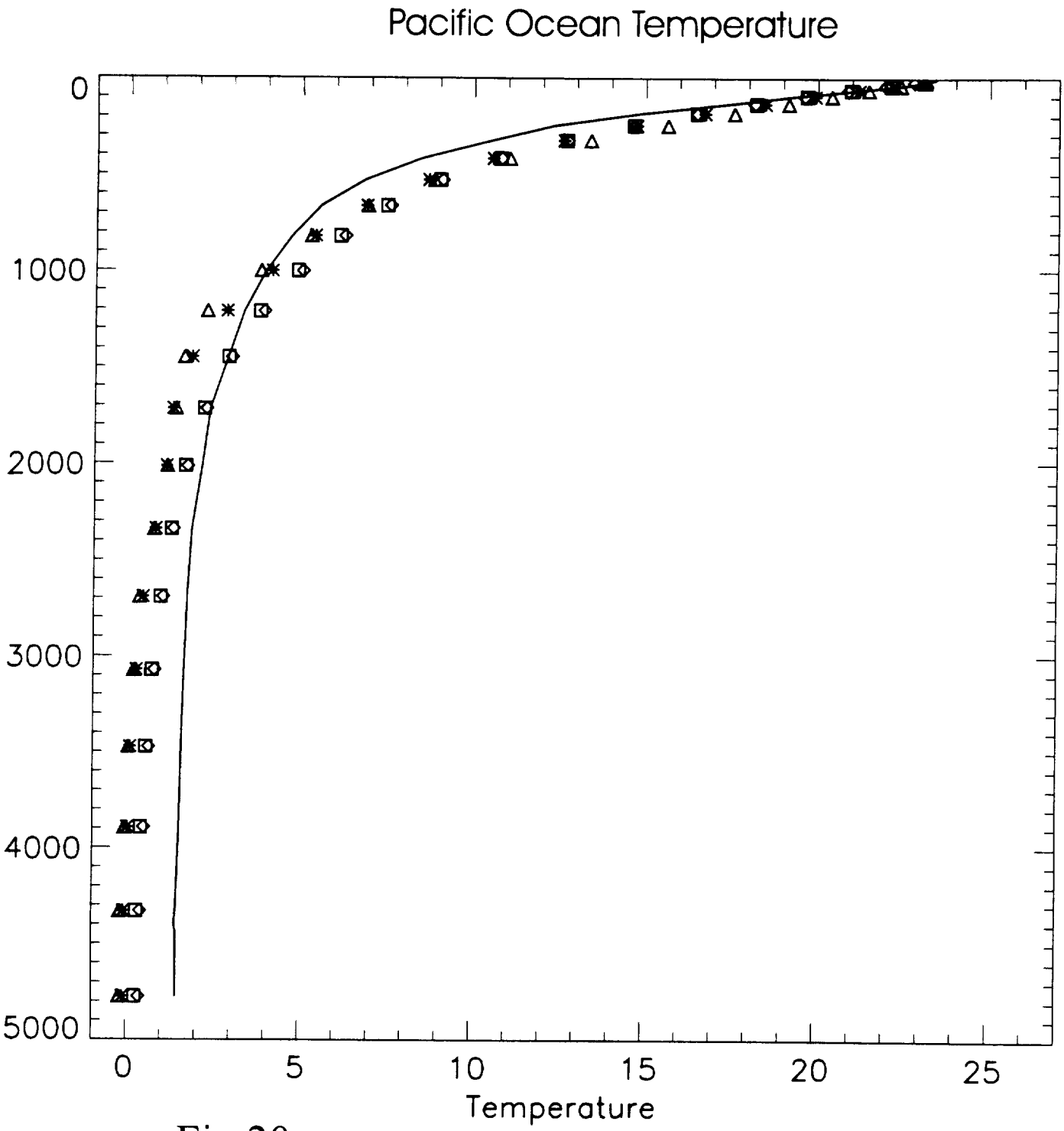
Pacific Ocean Temperature
0
1000
2000
3000
4000
5000
0
5
10
15
20
25
Temperature

Fig.20

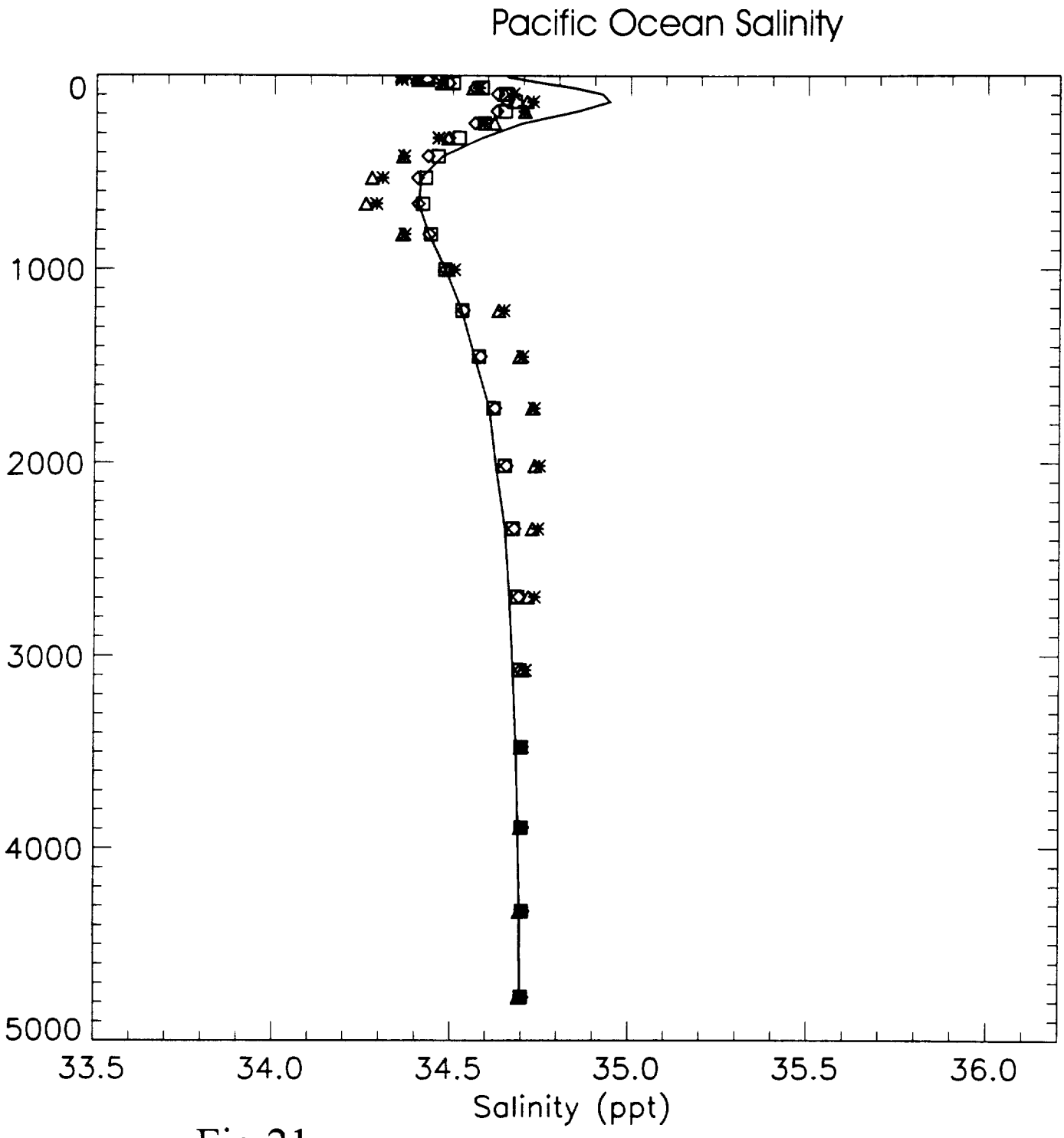
Pacific Ocean Salinity
0
1000
2000
3000
4000
5000
33.5
34.0
34.5
35.0
35.5
36.0
Salinity (ppt)

Fig.21

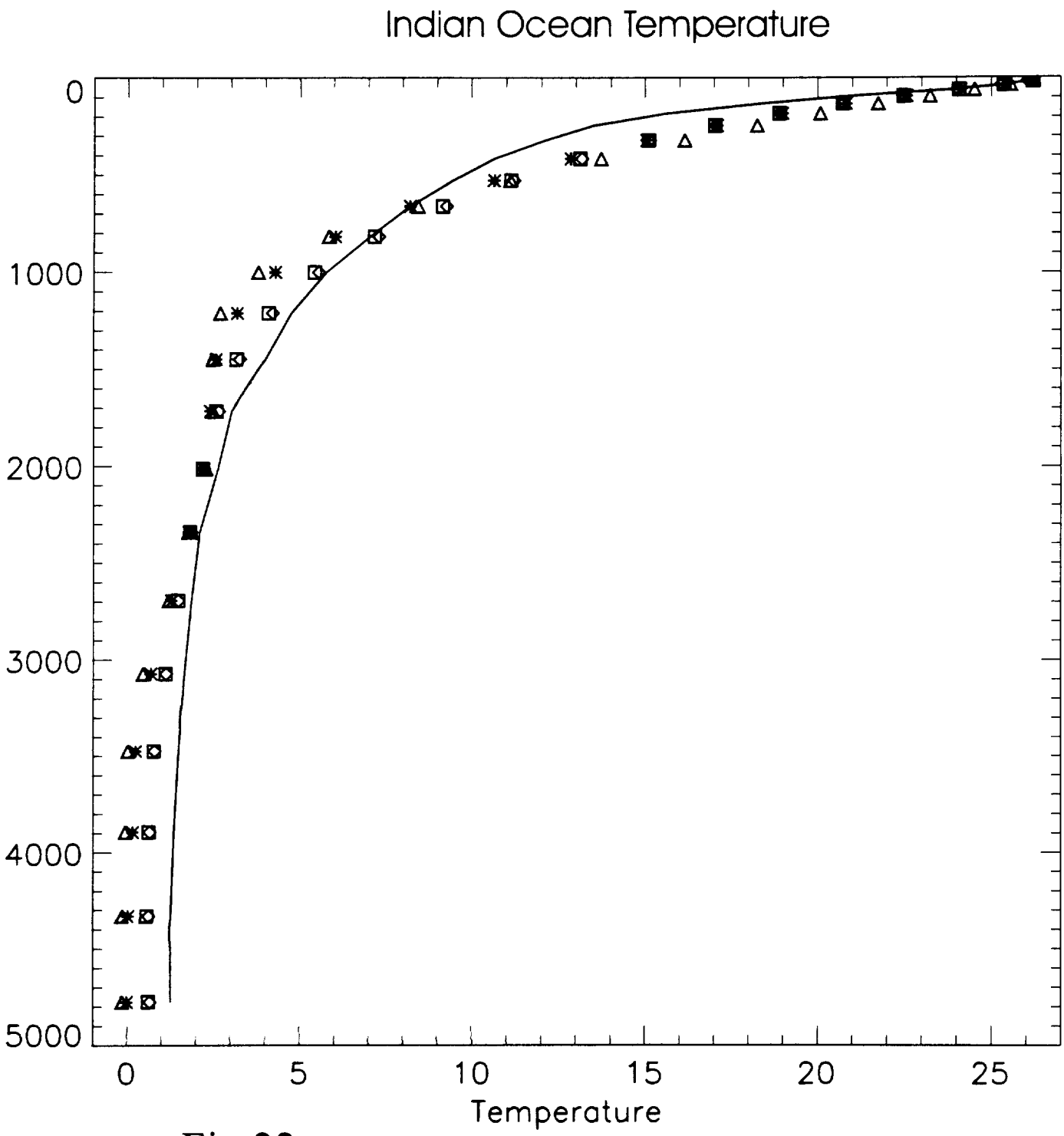
Indian Ocean Temperature
0
1000
2000
3000
4000
5000
0
5
10
15
20
25
Temperature

Fig.22

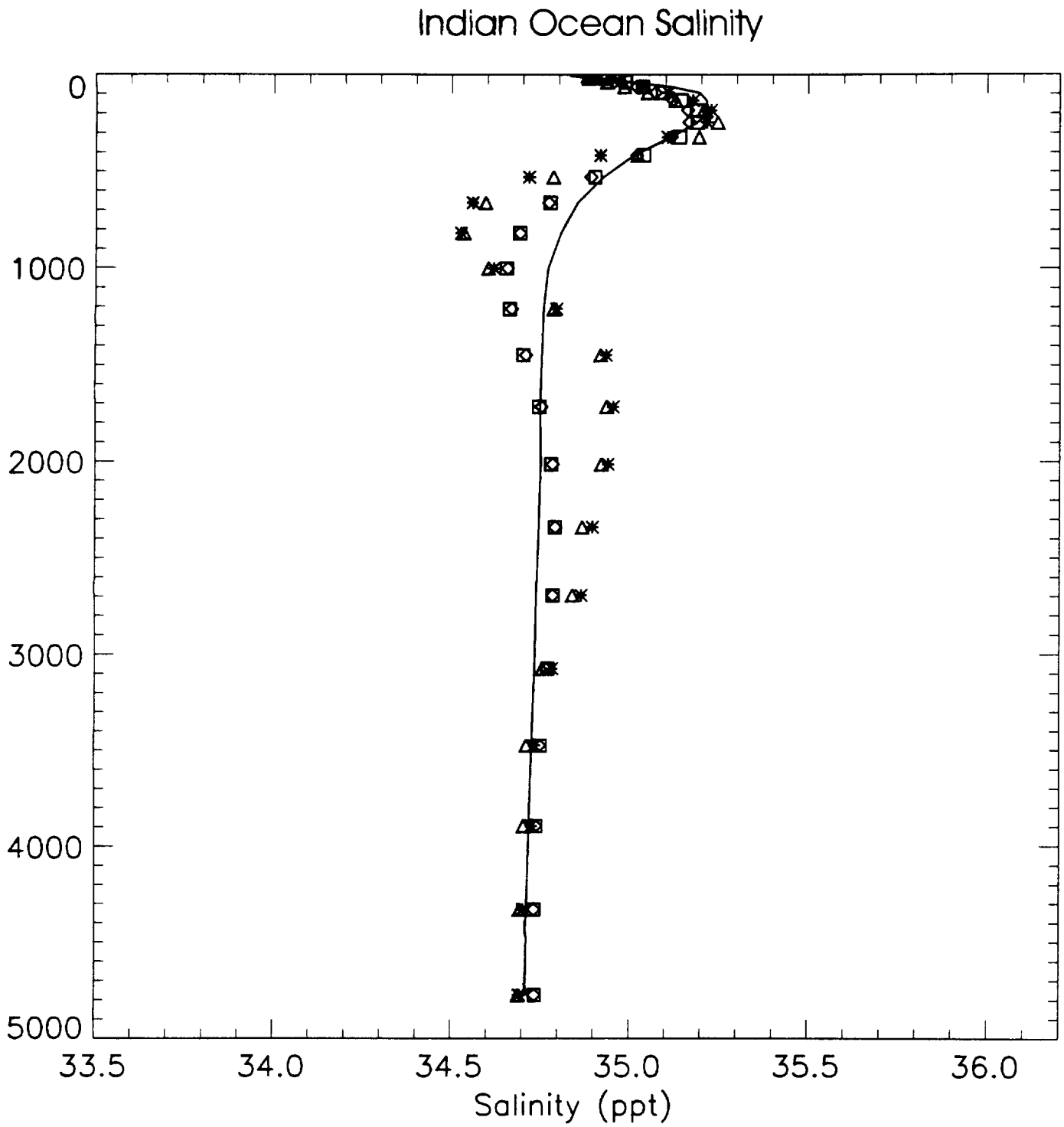
Indian Ocean Salinity
0
1000
2000
3000
4000
5000
33.5
34.0
34.5
35.0
35.5
36.0
Salinity (ppt)

Fig.23

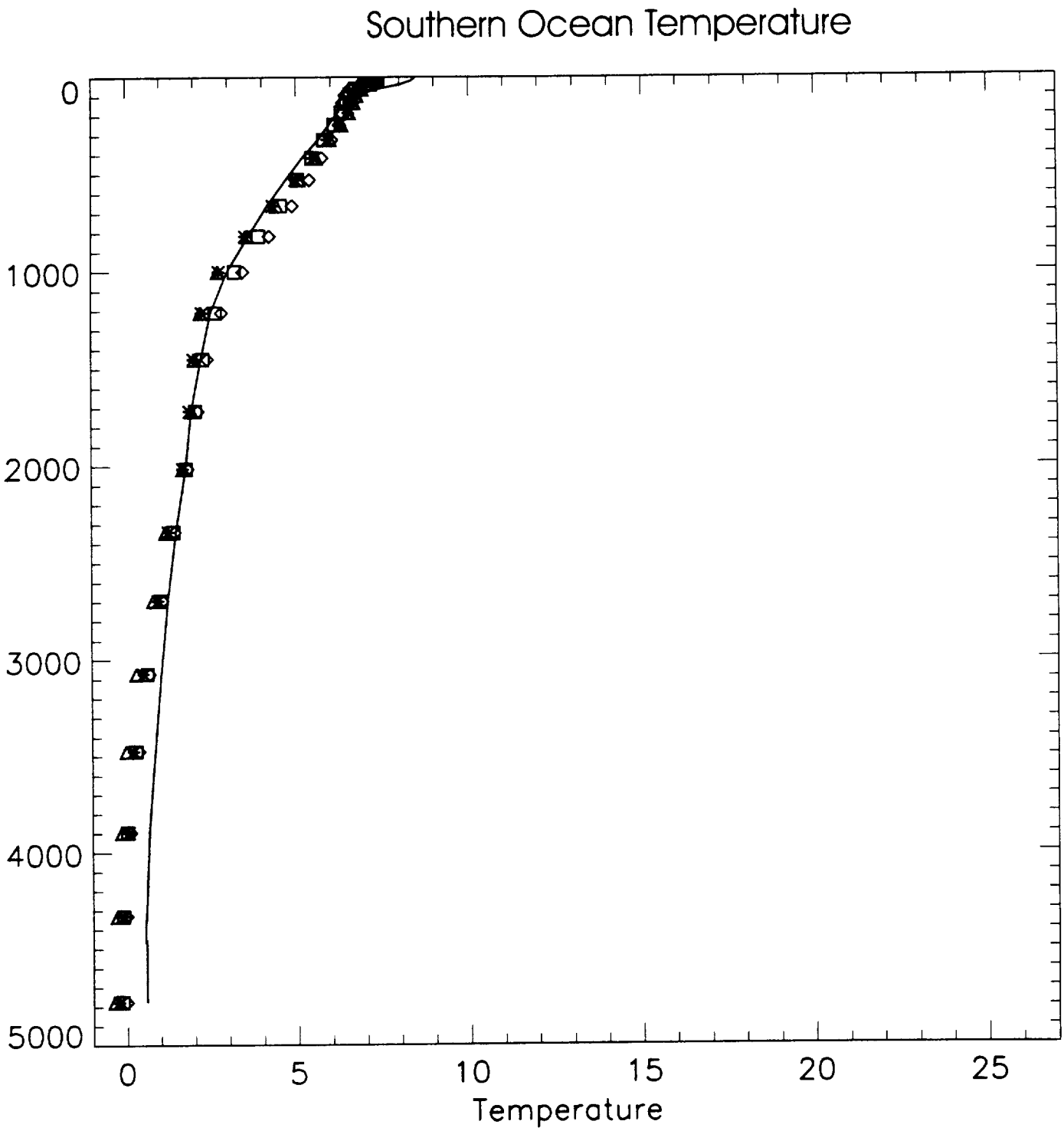
Southern Ocean Temperature
0
1000
2000
3000
4000
5000
0
5
10
15
20
25
Temperature

Fig.24

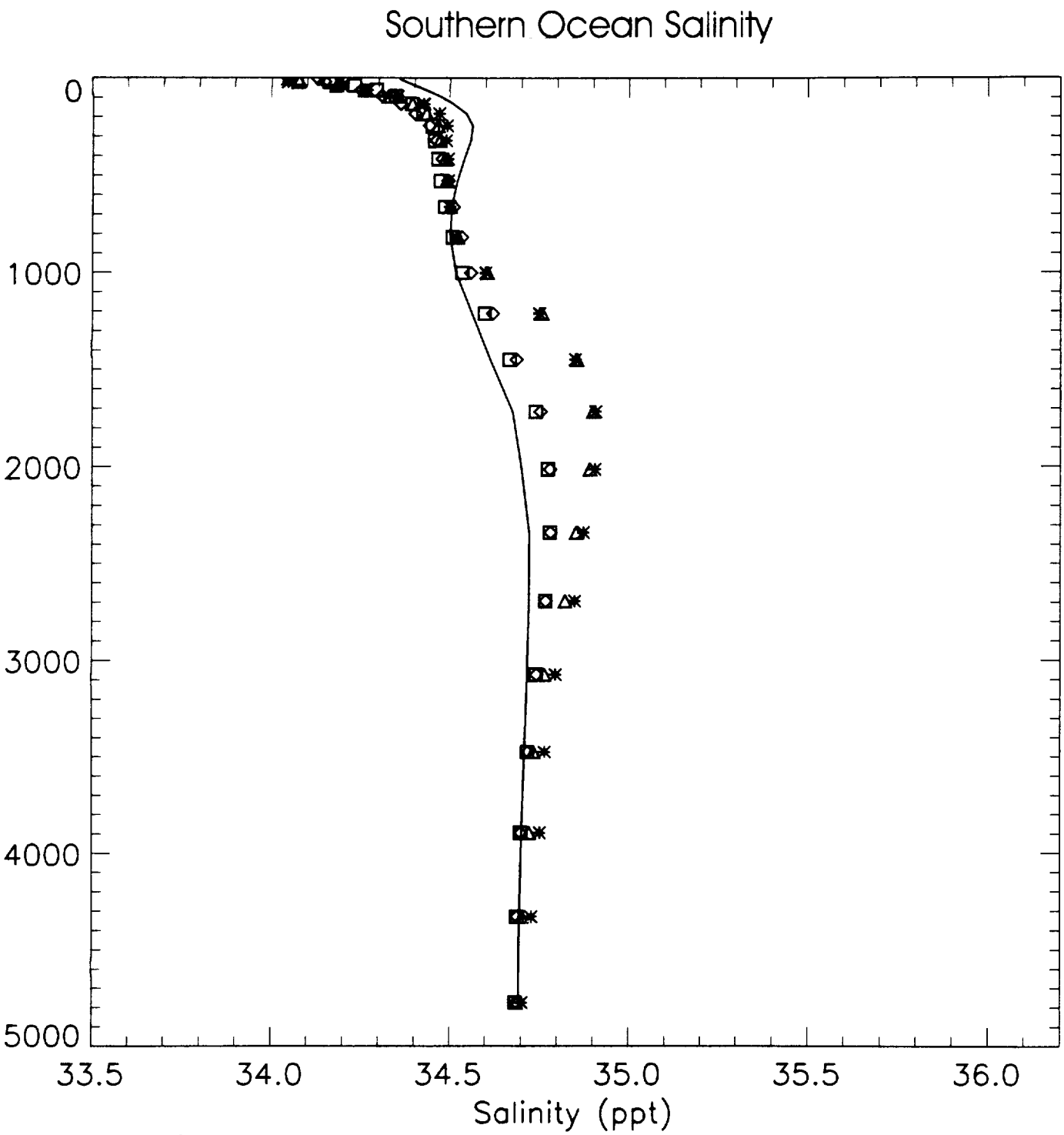
Southern Ocean Salinity
0
1000
2000
3000
4000
5000
33.5
34.0
34.5
35.0
35.5
36.0
Salinity (ppt)

Fig.25

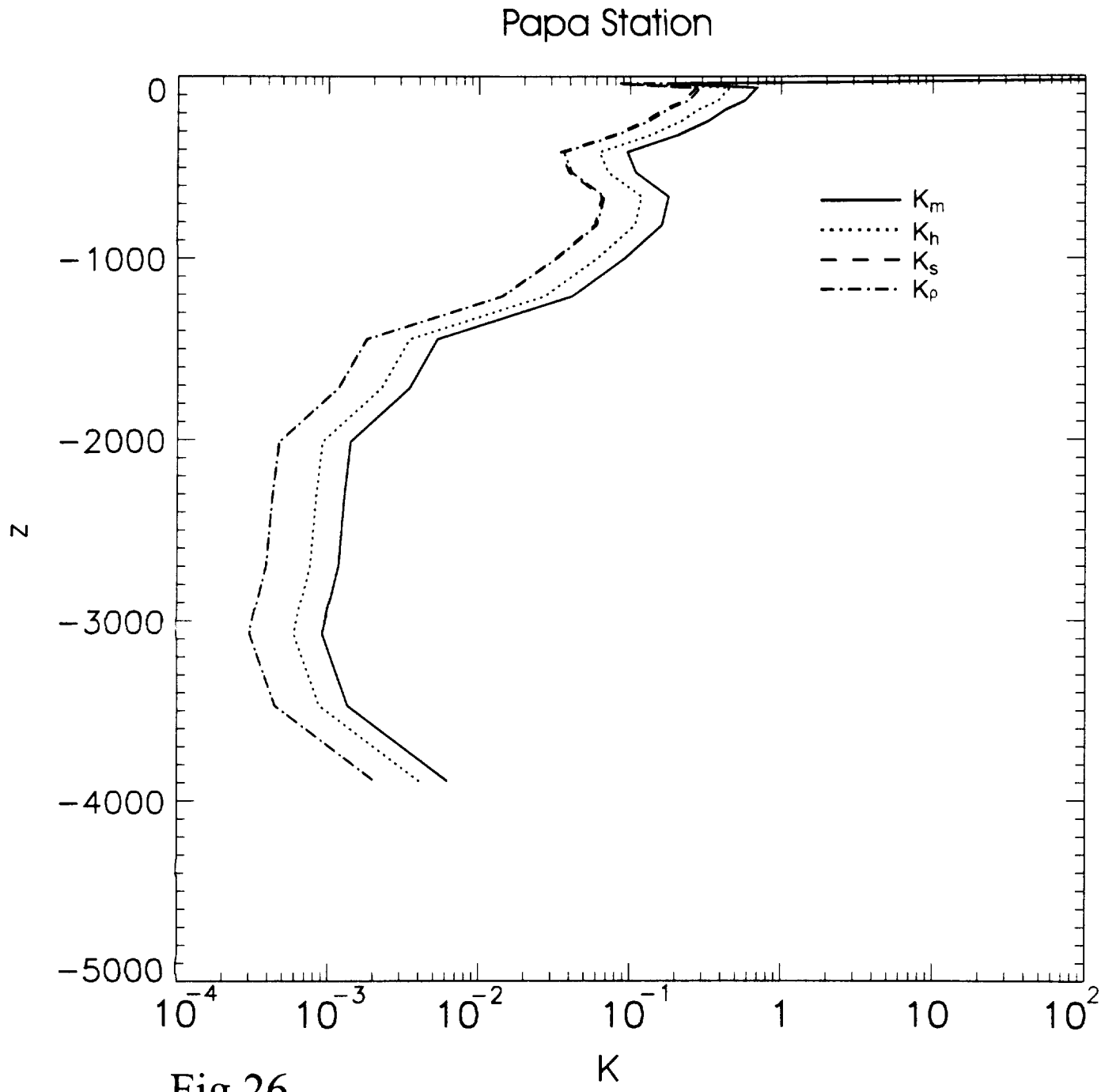
Papa Station
0
−1000
−2000
−3000
−4000
−5000
z
10^{-4}
10^{-3}
10^{-2}
10^{-1}
1
10
10^{2}
K
K_m
K_h
K_s
K_ρ

Fig.26

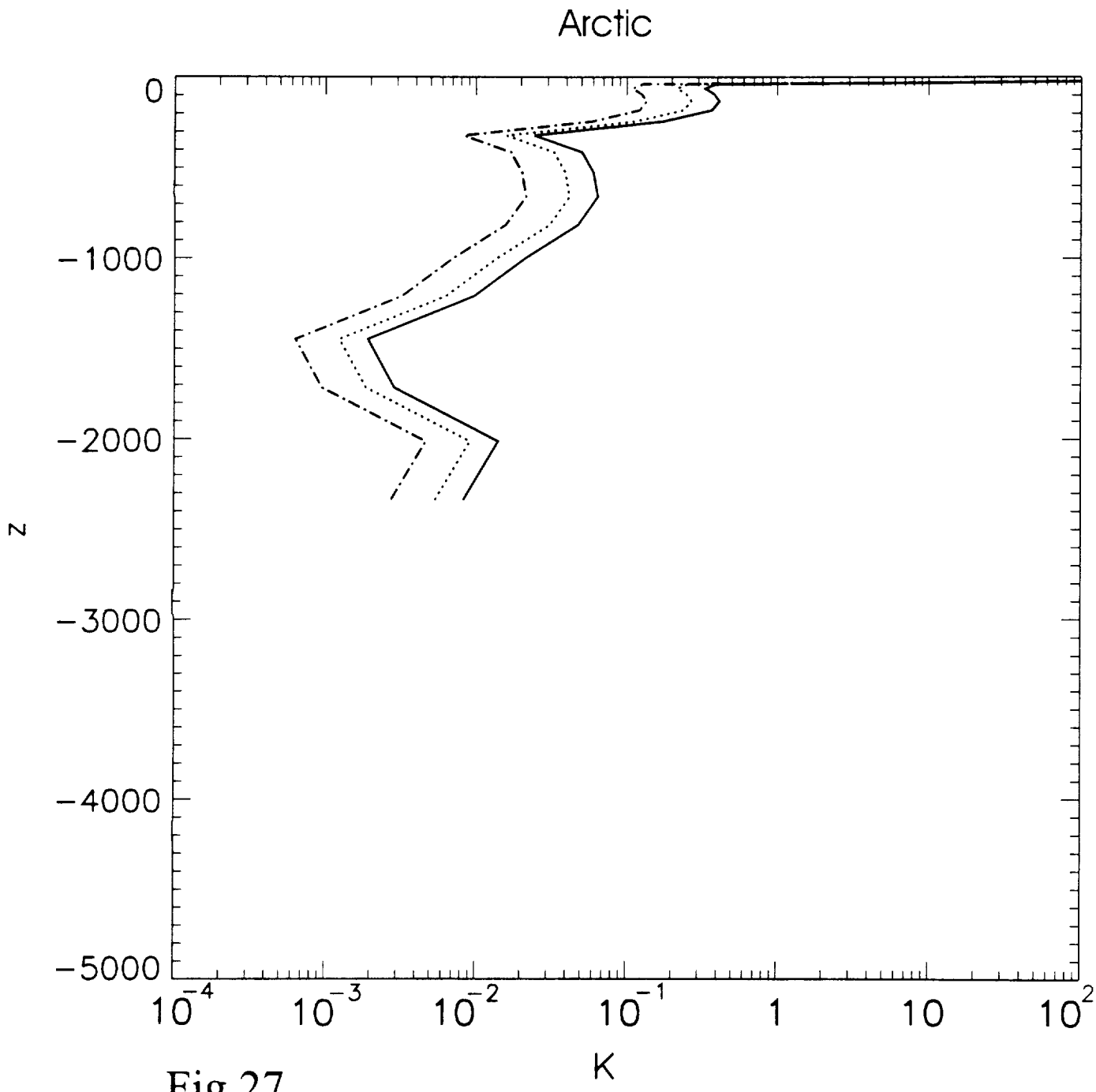

Fig.27

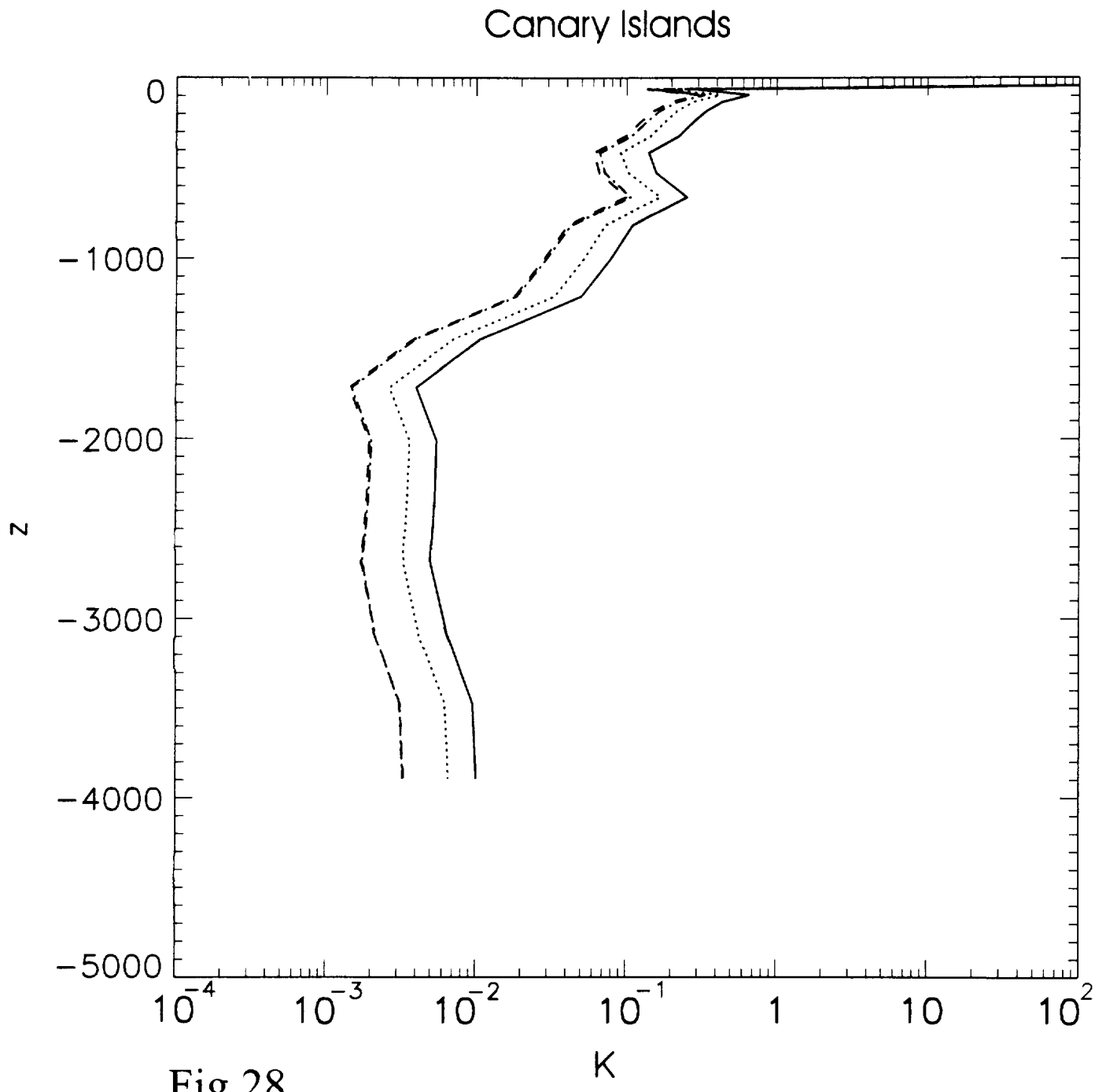
Canary Islands
0
−1000
−2000
−3000
−4000
−5000
z
10^{-4}
10^{-3}
10^{-2}
10^{-1}
1
10
10^{2}
K

Fig.28

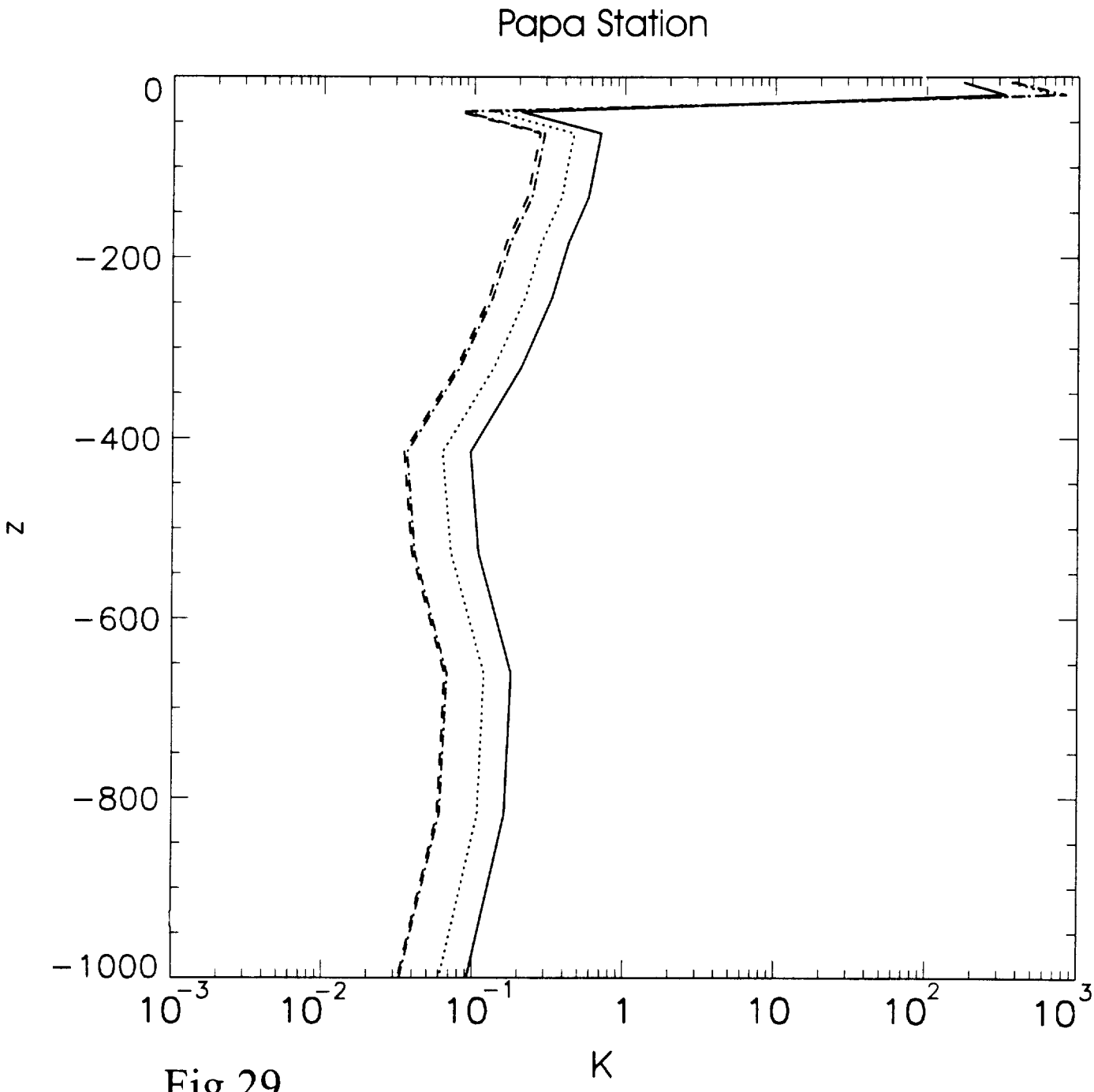

Fig.29

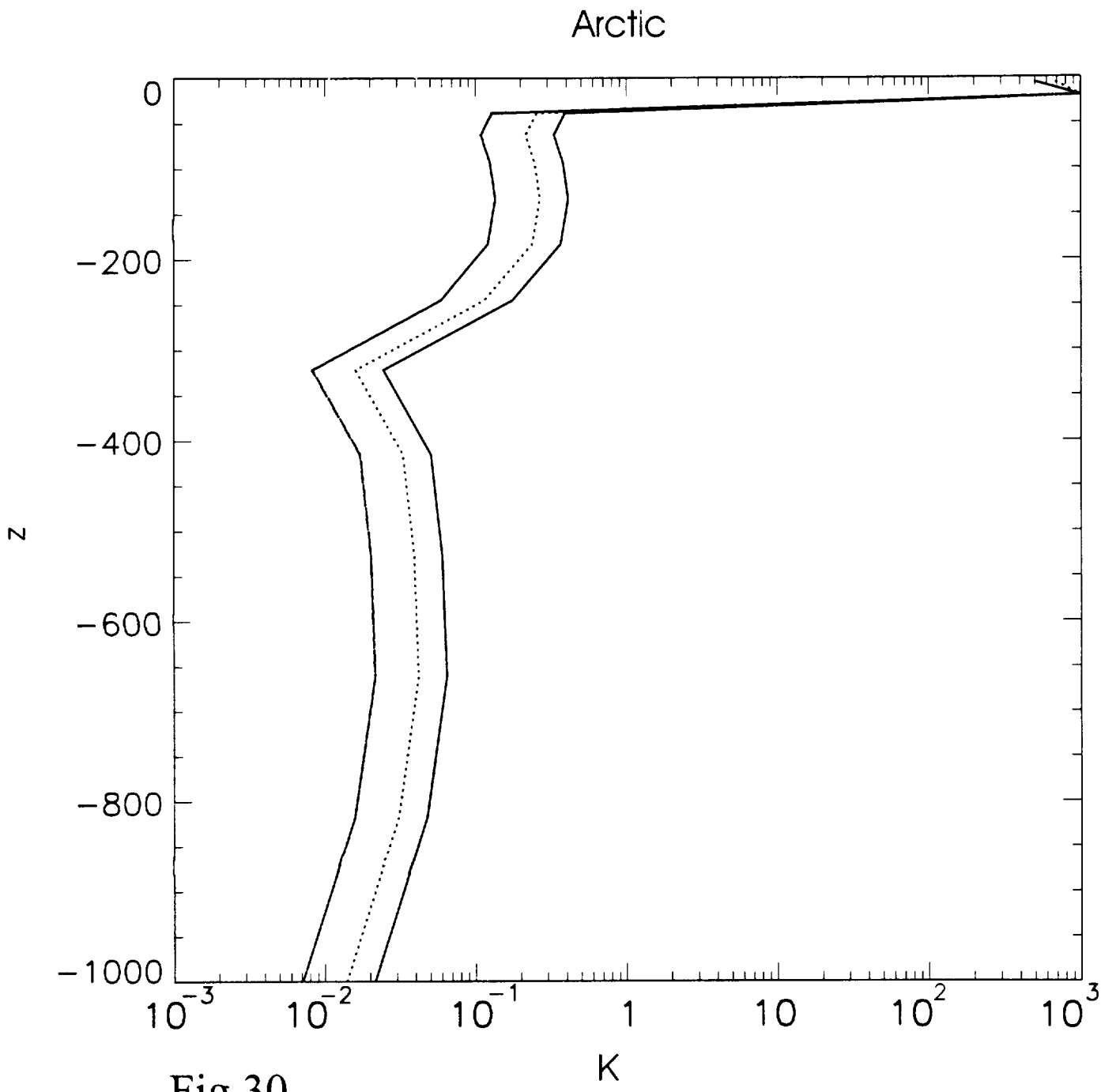

Fig.30

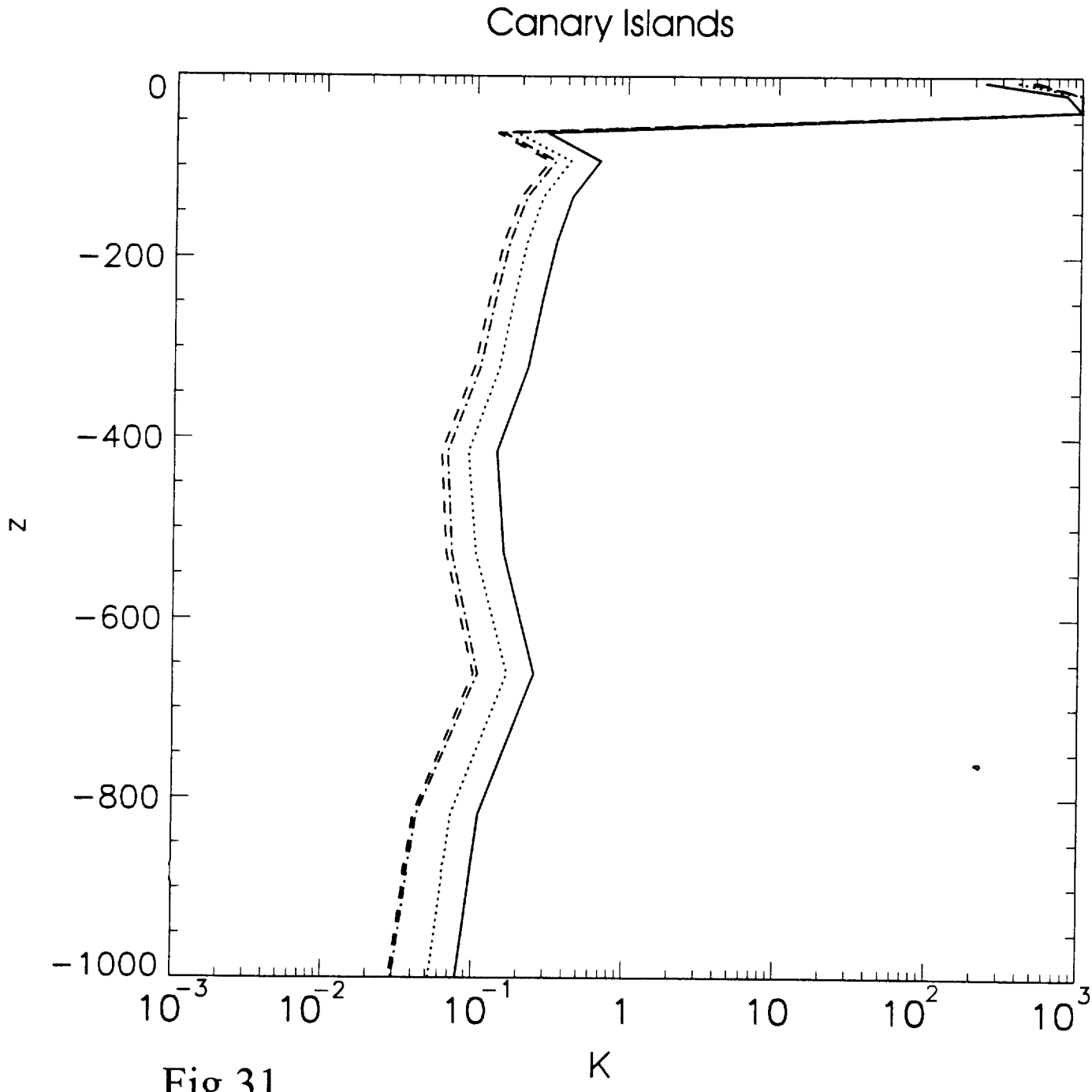
Canary Islands
0
−200
−400
−600
−800
−1000
z
10^{-3}
10^{-2}
10^{-1}
1
10
10^{2}
10^{3}
K

Fig.31

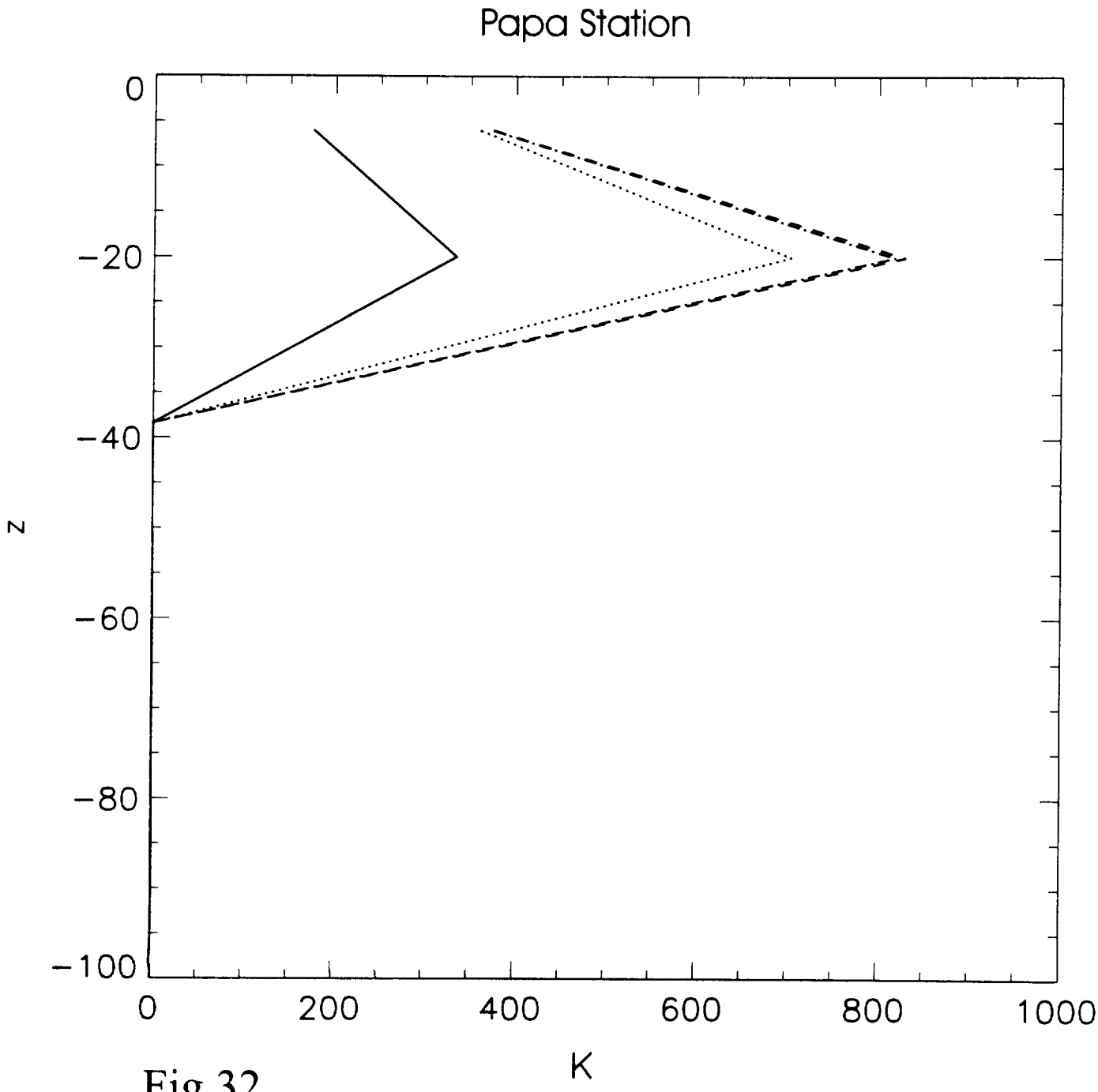

Fig.32

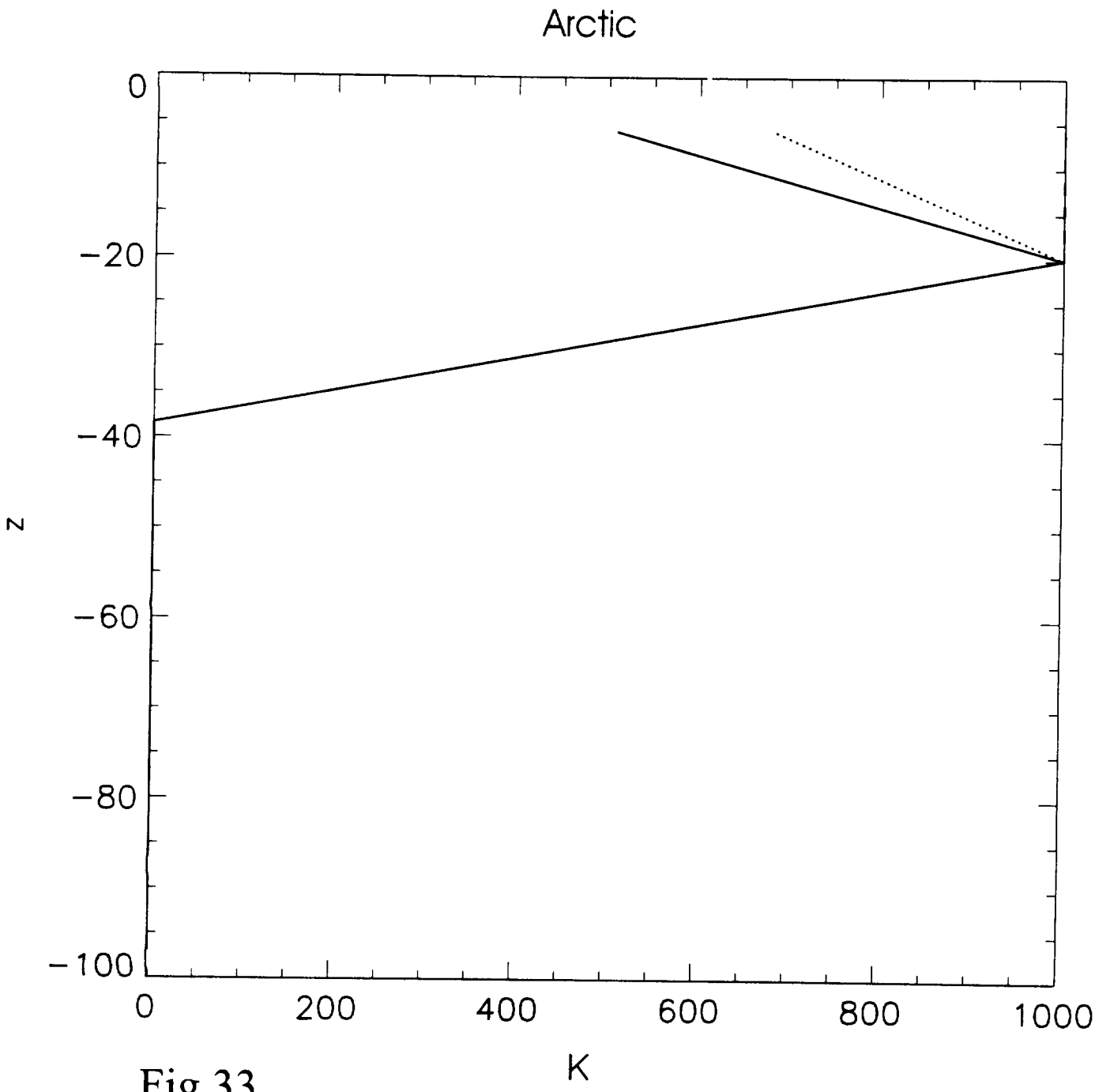

Fig.33

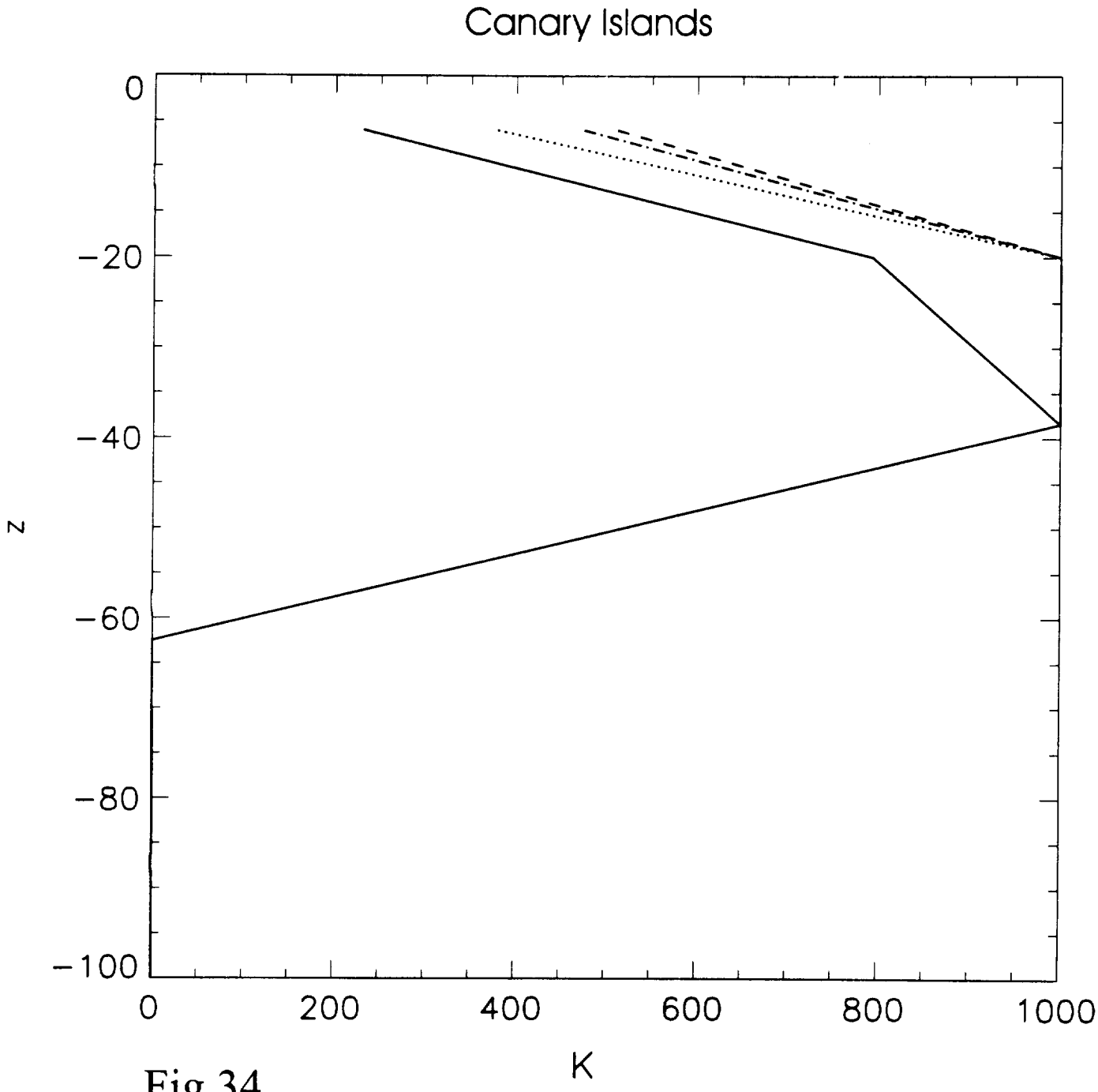

Fig.34

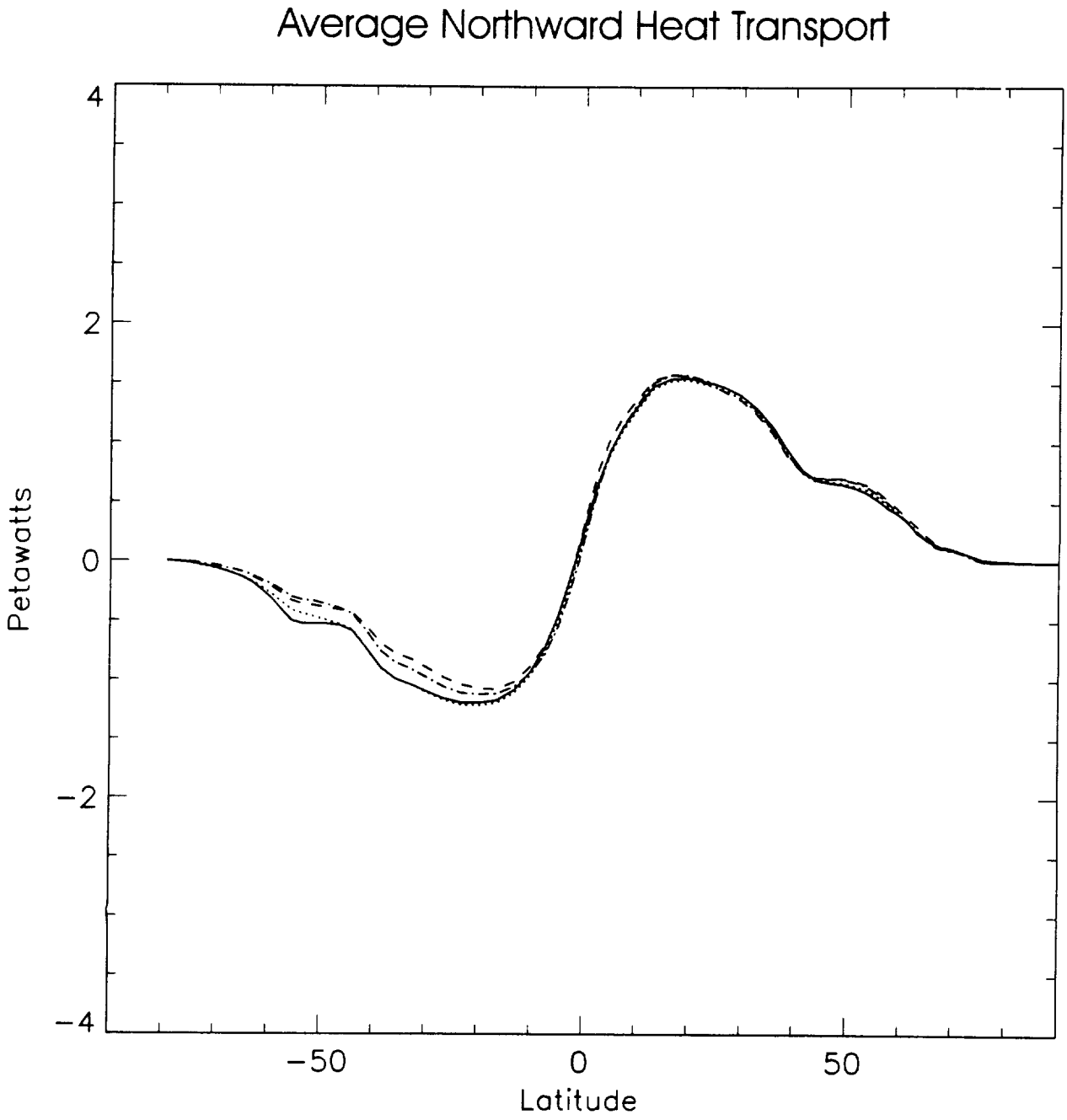
Average Northward Heat Transport
4
2
0
−2
−4
Petawatts
−50
0
50
Latitude

Fig.35